ABSTRACT

Title of Document: HOT AND COLD WATER AS A SUPERCRITICAL SOLVENT

Daphne Anne Fuentevilla, Doctor of Philosophy, 2012

Directed By: Professor Mikhail Anisimov, Department of Chemical and Biomolecular Engineering and Institute for Physical Science & Technology

This dissertation addresses the anomalous properties of water at high temperatures near the vapor-liquid critical point and at low temperatures in the supercooled liquid region. The first part of the dissertation is concerned with the concentration dependence of the critical temperature, density, and pressure of an aqueous sodium chloride solution. Because of the practical importance of an accurate knowledge of critical parameters for industrial, geochemical, and biological applications, an empirical equation for the critical locus of aqueous sodium chloride solutions was adopted in 1999 by the International Association for the Properties of Water and Steam (IAPWS) as a guideline. However, since this original *Guideline on the Critical Locus of Aqueous Solutions of Sodium Chloride* was developed, two new theoretical developments occurred, motivating the first part of this dissertation. Here, I present a theory-based formulation for the critical parameters of aqueous sodium chloride solutions as a proposed replacement for the empirical formulation currently

in use. This formulation has been published in the International Journal of Thermophysics and recommended by the Executive Committee of IAPWS for adoption as a *Revised Guideline on the Critical Locus of Aqueous Solutions of Sodium Chloride*. The second part of the dissertation addresses a new concept, considering cold water as a supercritical solvent. Based on the idea of a second, liquid-liquid, critical point in supercooled water, we explore the possibility of supercooled water as a novel supercooled solvent through the thermodynamics of critical phenomena. In 2006, I published a Physical Review letter presenting a parametric scaled equation of state for supercooled-water. Further developments based on this work led to a phenomenological mean-field "two-state" model, clarifying the nature of the phase separation in a polyamorphic single-component liquid. In this dissertation, I modify this two-state model to incorporate solutes. Critical lines emanating from the pure-water critical point show how even small additions of solute may significantly affect the thermodynamic properties and phase behavior of supercooled aqueous solutions. Some solutes, such as glycerol, can prevent spontaneous crystallization, thus making liquid-liquid separation in supercooled water experimentally accessible. This work will help in resolving the question on liquid polyamorphism in supercooled water.

HOT AND COLD WATER AS A SUPERCRITICAL SOLVENT

By

Daphne Anne Fuentevilla

Dissertation submitted to the Faculty of the Graduate School of the
University of Maryland, College Park, in partial fulfillment
of the requirements for the degree of
Doctor of Philosophy
2012

Advisory Committee:
Professor Mikhail Anisimov, Committee Chair
Professor Sheryl Ehrman
Professor Jeffrey Klauda
Professor Gregory Jackson
Professor John Weeks, Dean's Representative

Acknowledgements

I would like to thank my advisor, Professor Mikhail A. Anisimov, as well as Professor Emeritus Jan V. Sengers, who have kind hearts and abundant patience.

I would also like to acknowledge my family, especially my husband, Christopher R. Dewey, and my grandfather, Manuel E. Fuentevilla, who followed every step of my research.

For the work on $NaCl+H_2O$ solutions, I would like to acknowledge stimulating discussions with Professor M.E. Fisher.

For the work on supercooled water, I would like to acknowledge valuable discussions with Professors C. A. Angell, P. G. Debenedetti, O. Mishima, H. E. Stanley, and B. Widom.

The work on supercooled aqueous solutions would not have been possible without the support of Dr. V. Holten, assistant research scientist in Professor Anisimov's research group.

I thank the research group of Professor Anisimov and Professor Sengers, in particular the former Ph.D. student Jana Kalová from the Czech Republic.

The research of Professor Anisimov's group is supported by the Division of Chemistry of the National Science Foundation (Grant No. CHE-1012052), the Petroleum Research Fund of the American Chemical Society (Grant No. 52666-ND6), and by the International Association for the Properties of Water and Steam.

Finally, I would like to thank the U.S. Navy, the Naval Surface Warfare Center, Carderock Division, and the U.S. Department of Defense SMART Scholarship program for their support.

Table of Contents

List of Tables

List of Figures

Chapter 1. Introduction

Water pervades our lives. We are made of it, we drink it, we use it in manufacturing and for travel. We gauge the weather by it, we wash with it, we fight political battles over it and we look for it on other planets as a sign of possible habitability. Yet we do not fully understand it. The seeming simplicity of this odorless, tasteless, nearly colorless substance, a molecule of one oxygen and two hydrogen atoms, belies its complexity. Anomalies in the thermodynamic properties of water, such as those seen in the heat capacity, density, compressibility and thermal expansivity, among other properties, imply the existence of two critical points in liquid water, one hot and one cold.

This dissertation explores the implications of these two critical points of liquid water: the typical vapor-liquid critical point and a hypothesized liquid-liquid critical point. The first part of the dissertation is concerned with the concentration dependence of the critical temperature, density, and pressure of an aqueous salt solution, namely sodium chloride in water. Because of the practical importance of an accurate knowledge of the critical parameters for industrial, geochemical, and biological applications, an empirical equation for the critical temperature, critical pressure, and critical density of aqueous solutions of sodium chloride was adopted in 1999 by the International Association for the Properties of Water and Steam (IAPWS) as a guideline. However, since this original *Guideline on the Critical Locus of Aqueous Solutions of Sodium Chloride* was developed, two new theoretical developments occurred, motivating the first part of this dissertation. Here, I present a

theory-based formulation for the critical parameters of aqueous sodium chloride solutions as a proposed replacement for the empirical formulation currently in use. This formulation has been published in the International Journal of Thermophysics [1] and recommended by the Executive Committee of IAPWS for adoption as a *Revised Guideline on the Critical Locus of Aqueous Solutions of Sodium Chloride*.

The second part of the dissertation addresses a new concept, considering cold water as a supercritical solvent, based on the idea of a second, liquid-liquid, critical point in supercooled water. We apply the thermodynamics of critical phenomena to explore the possibility of supercooled water as a novel supercritical solvent. I present my work, published in Physical Review Letters [2], and further developed by Christopher Bertrand [3] and Vincent Holten [4], developing a scaled equation of state for supercooled water and demonstrating the thermodynamic consistency of the second-critical-point scenario using the physics of critical phenomena. This work was a starting point for further development in this field and our research group, using a phenomenological mean-field "two-state" model, recently clarified the nature of the phase separation in a polyamorphic single-component liquid. Assuming the existence of the water liquid-liquid critical point, I show that the "two-state" model can be modified to include the addition of a solute, which generates critical lines emanating from the pure-water critical point. Because of the anomalous large value of change in pressure with respect to temperature for almost incompressible liquid water near the liquid-liquid critical point, the value of the Krichevskiĭ parameter, which largely determines the high selectivity of supercritical fluid solvent to fine variations of temperature and pressure, may be anomalously large even if the critical temperature

weakly depends on the solute concentration. Physically, it means that even a very small addition of the solute may significantly affect the properties of cold water and aqueous solutions. Finally, I present different scenarios for phase behavior of supercooled aqueous solutions. Some solutes, such as glycerol, can prevent spontaneous crystallization, thus making liquid-liquid separation in supercooled water experimentally accessible. This work explores the potential for supercooled liquid water to behave as a supercooled supercritical solvent and will help in resolving the question on liquid polyamorphism in supercooled water.

Section 1. Supercritical fluids

Supercritical fluids are well known for their suitability as solvents due to the ease of tuning their properties close to the critical point. Above the vapor-liquid critical point, distinct liquid and gas phases do not exist, and the supercritical fluid will remain one phase while retaining properties of both, allowing it to disperse through solids like a gas but also act as a liquid solute. Near the critical point, these supercritical fluids exhibit large changes in thermodynamic properties, such as density, heat capacity, expansivity and compressibility, with small changes in pressure or temperature. These properties are linked to the critical-point anomalies, in particular, very large compressibility and very low interfacial tension [5]. Upon addition of a solute, the resulting supercritical fluid mixture has extraordinary properties, which can be tuned by temperature and pressure, thus establishing the basis for innovative technologies.

At high temperatures, the peculiar properties of fluid mixtures in the vicinity of the critical point of the pure solvent are commonly utilized in supercritical-fluid technologies, such as fluid extraction and separation [6,7], enhanced oil recovery [8,9], supercritical chromatography [10,11], and micronization [12,13]. At low temperatures, supercritical carbon dioxide is an example of a common supercritical fluid and is used in place of an organic solvent for decaffeination of coffee and the extraction of hops for beer production [14]. The high density of the supercritical fluid state speeds up the extraction process, and when the mixture is returned to standard temperature and pressure, the fluid evaporates leaving behind only the product [15].

The supercritical state describes a fluid above its critical point, where phase boundaries between fluid phases disappear and it is possible to transition from liquid like properties to gas like properties without passing through a phase transition. The pressure-temperature phase diagram for ordinary water, Fig. 1, shows a critical point, defined by the critical parameters temperature, T_c, pressure, P_c, and density, ρ_c, terminating the vapor-liquid coexistence line at $T_c = 647.096\ \mathrm{K}$, $P_c = 22.064\ \mathrm{MPa}$, and $\rho_c = 322\ \mathrm{kg \cdot m^{-3}}$ [16] and a second, hypothesized critical point for liquid water terminating a supercooled liquid-liquid coexistence line at 224 K and 27.5 MPa [4] at temperatures below that of stable liquid water. The dotted lines in the diagram indicate an area beyond which the fluid exceeds the critical pressure and temperature. In Chapter 2, I focus on the supercritical state defined by the established high-temperature, high-pressure vapor-liquid critical point. In Chapter 3, I will revisit this diagram to discuss the implications of the hypothesized second critical point of supercooled liquid water.

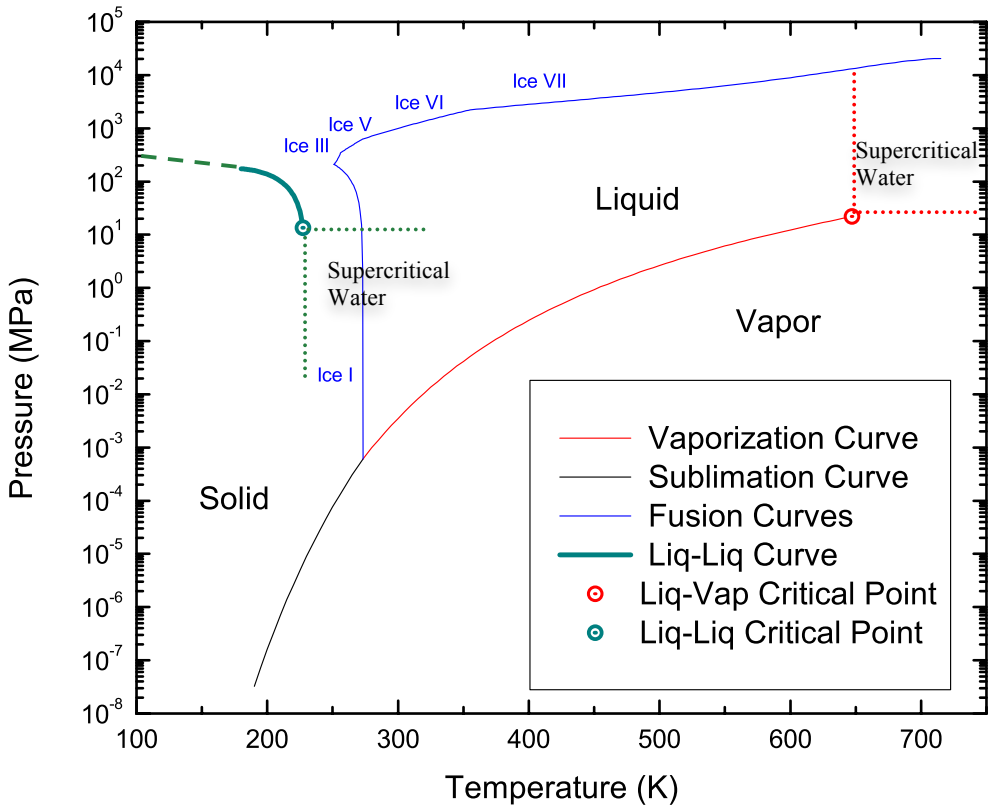

Figure 1. Pressure-temperature phase diagram for ordinary water showing the hypothesized liquid-liquid coexistence curve in the metastable liquid region. Dotted lines denote an area where the fluid is above the critical temperature and critical pressure of the liquid-liquid critical point or vapor-liquid critical point of pure water.

Subsection 1. Promising applications and implications for the study of supercritical water solutions

Near the vapor-liquid critical point and the hypothesized liquid-liquid critical

point, the thermodynamic properties of water exhibit large changes in thermodynamic properties, such as density and heat capacity shown in Fig. 2, with small changes in pressure or temperature. The divergence of these properties is attributed to proximity to the vapor-liquid critical point in hot water and the hypothesized liquid-liquid critical point in cold water. At high temperatures, the ability to tune the properties of water with small changes in temperature or pressure makes it suitable for use as a supercritical fluid. Indeed, water is a common supercritical fluid and high-temperature, high-pressure water, near its vapor-liquid critical point, as a supercritical-fluid solvent, is well studied [17].

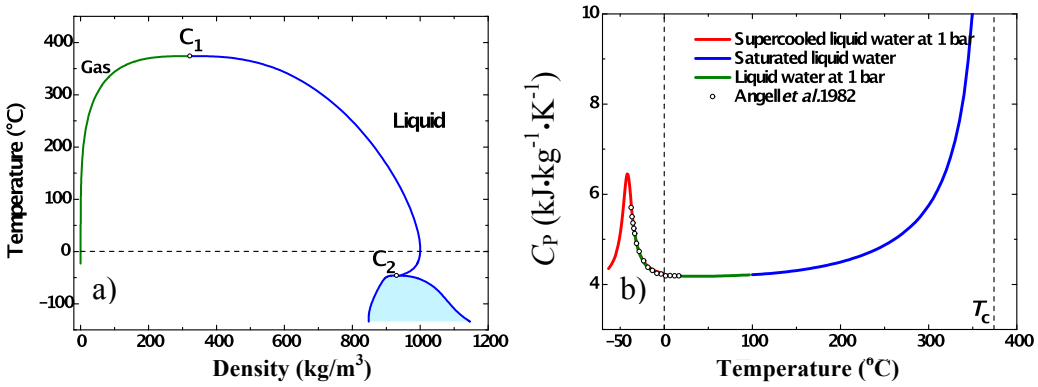

Figure 2. Density (a) and heat capacity (b) of liquid water shown over a temperature range encompassing the vapor-liquid critical point and the hypothesized liquid-liquid critical point. In (a), C_1 and C_2 represent the location of the critical points, the solid blue line represents the density of liquid water, and the green line represents the density of water vapor. In (b), T_c indicates the temperature of the vapor-liquid critical

point and the dashed line at 0 °C indicates the boundary between stable and metastable liquid water.

Supercritical water oxidation for hazardous waste [18,19], supercritical water reactors [20,21], and supercritical water decomposition for biomass gasification [22,23] are a few of the recent uses of high temperature, high pressure supercritical water. However, these processes present engineering challenges since supercritical fluids are excellent solvents and the ease of tuning the properties of a fluid near its critical point can also equate to significant variability in properties with the addition of small amounts of contaminant. The study of aqueous solutions near the critical point is required to overcome these challenges.

High-temperature, high-pressure supercritical water is also found in nature in deep hydrothermal vents [24]. Furthering our understanding of supercritical saltwater solutions has implications for geothermal processes, such as the role of supercritical water solutions in the leaching of mineral and nutrients from the seabed into the ocean, or for the study of the microorganisms that inhabit these hydrothermal vents.

Supercooled water has not previously been considered as a supercritical fluid. However, certain cloud formations are composed of supercooled water droplets at temperatures approaching the hypothesized critical temperature [25]. Airplane icing is a safety concern attributed to the freezing of these supercooled water droplets on impact with control surface of the wing. Understanding the thermodynamic behavior of supercooled water has implications for practical issues such as airplane icing and weather prediction, but also for furthering the science of climate change [26]. The

study of supercooled water as a supercritical solvent could help describe the effects of pollutants on these supercooled water cloud formations. More directly, however, the study of supercooled aqueous solutions has the potential to offer further insight into the second-critical-point hypothesis for liquid water, and to result in suggestions for experimentalists in the field.

Chapter 2: Hot Water as a Supercritical-Fluid Solvent

One of the simplest and most well studied of aqueous solutions is that of sodium chloride and water. Upon addition of a solute, the phase diagram of water will shift, creating a critical locus defined by the concentration dependence of the critical parameters temperature, density, and pressure. In its simplest form, this critical locus bridges between critical points of the two substances in Type I critical phenomena [27], as defined by Scott and van Konynenburg. Projecting onto the pressure-temperature plane, the line of increasing solute concentration is shown as a schematic of typical Type I critical behavior (Fig. 3a). Binary fluids exhibit a variety of phase behavior, however, and the specific classification of NaCl-H_2O solutions (Fig. 3b) is not known. Experimental data for the critical locus of aqueous sodium chloride is only available up to twelve mole percent (thirty mass percent) sodium chloride and the temperature and pressures required to explore the critical locus up to the critical point terminating the vapor-liquid coexistence curve for pure sodium chloride are prohibitively high.

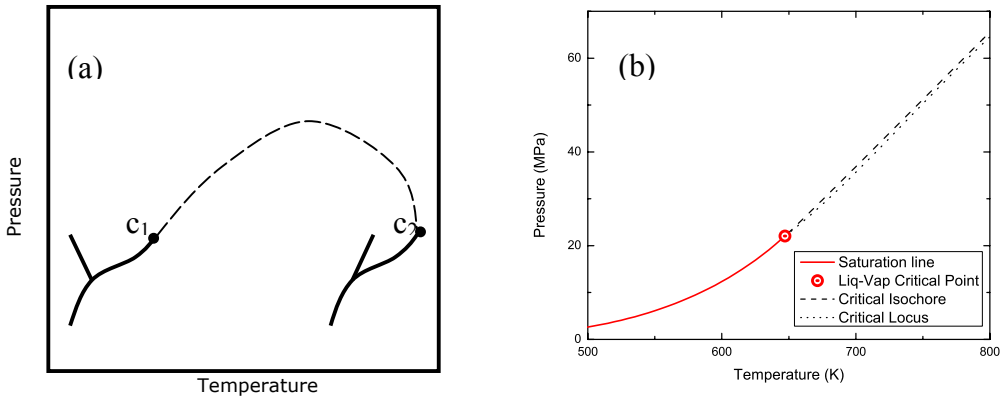

Figure 3. Projection of concentration onto a pressure-temperature phase diagram, showing the vapor-liquid critical line of a simple binary mixture. (a) Typical Type I critical behavior showing the critical point following the dashed line from c_1 to c_2 with increasing solute concentration [28]. (b) Additions of small amounts of sodium chloride shift the critical point of water to higher temperatures and pressures that closely follow the critical isochore [16].

The study of aqueous solutions of sodium chloride provides a basis for studying supercritical solutions in general, but is also important in its own right. Near-critical conditions have been measured in the ocean [29] suggesting that understanding the behavior of near-critical NaCl-H_2O solutions may play a role in underwater navigation, marine biology and discussions on the conditions for the origin of life. In addition, some of the most promising applications for supercritical water, such as supercritical water oxidation, which recovers energy and reclaims water for wet waste streams by utilizing the high reaction rate between oxygen and contaminants of the supercritical state, results in salt precipitates that can affect the efficiency of the process [30].

Section 1. Critical locus of sodium chloride aqueous solutions

The critical behavior of water with dilute amounts of NaCl has been documented experimentally [31-33]. The vapor-liquid critical locus of aqueous electrolytes exhibits an initial, sharp dependence on the critical temperature with increases of electrolyte in dilute solutions. This behavior, shown in Fig. 4, presents challenges for theory-based descriptions. Povodyrev *et al*. [34] and Kim and Fisher [35] have produced reports summarizing the experimental evidence of this behavior and proposing a theoretical basis for the results.

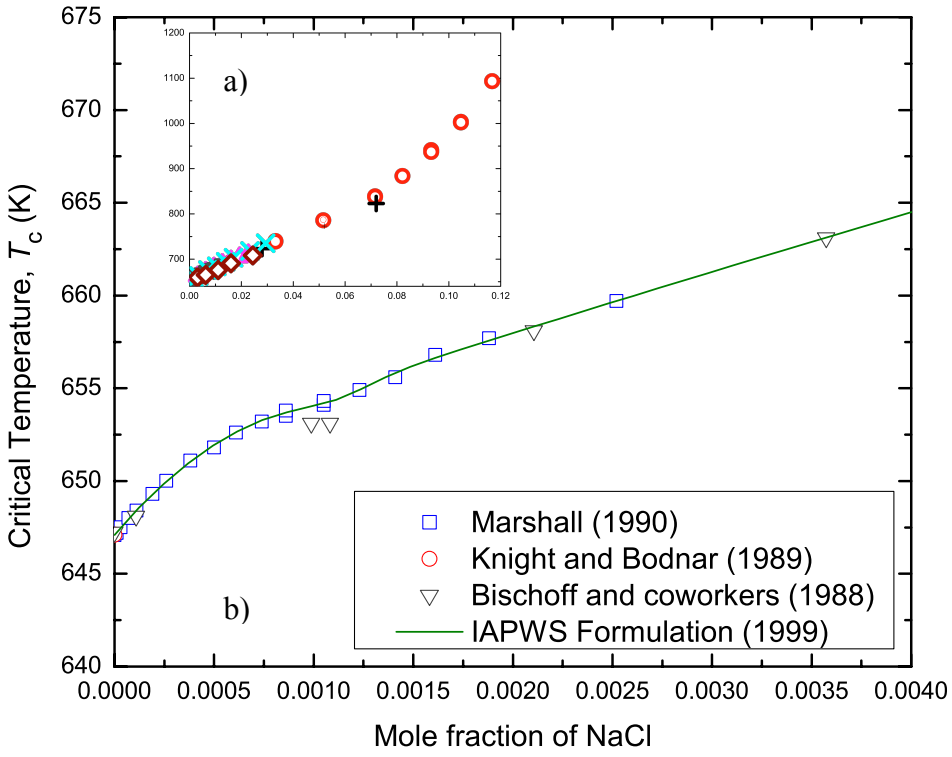

Figure 4. Critical locus of salty water at various concentrations. The symbols represent the experimental data of Marshall [31], Knight and Bodnar [32], and Bischoff and coworkers [33]. The solid green line is the empirical Povodyrev equation, adopted by IAPWS [34]. (a) Inset graph shows the behavior of the critical locus over the entire range of available data, from $0 \le x \le 0.12$, where x is mole fraction of NaCl. (b) Highlights the sharp initial curve of the critical locus in the dilute region $x \le 0.001$.

The International Association for the Properties of Water and Steam (IAPWS) is an international non-profit association of national organizations concerned with the properties of water and steam, particularly thermophysical properties and other

aspects of high-temperature steam, water and aqueous mixtures that are relevant to thermal power cycles and other industrial applications. IAPWS stated purpose is to "provide internationally accepted formulations for the properties of light and heavy steam, water and selected aqueous solutions for scientific and industrial applications", and to serve as "an international forum for the exchange of experiences, ideas and results of research on high-temperature aqueous media" [36]. Due to the practical importance of the critical parameters of high-temperature saltwater solutions for industrial applications, IAPWS adopted the 1999 equation of Povodyrev as the standard for the critical locus of NaCl-H_2O solutions [37]. This empirical equation used an analytic function to separately describe the sharp increase in slope of the dilute region of the phase diagram and the non-dilute region, and using a crossover equation to unite the two curves with a hyperbolic tangent function.

Since that time, two new theoretical developments have occurred, motivating the formulation of a theory-based equation to describe the critical parameters of aqueous sodium chloride solutions. First, just as for molecular fluid mixtures, the critical temperature, pressure and density were assumed by Povodyrev et al. [34] to be analytic functions of the concentration. However, Kim and Fisher [35] have subsequently shown that a classical theory for the non-ionic solvent+ion mixture combined with a Debye-Hückel theory for the ionic interactions yields a non-analytic dependence of T_c, P_c, and ρ_c on the concentration in salt solutions. They also presented evidence for such a non-analytic concentration dependence based on the experimental data of Marshall [31] for the critical temperature of sodium-chloride solutions.

Second, there is considerable evidence that molecular, as well as ionic fluids, belong to the critical universality class of Ising-like systems [38,39]. For Ising-like systems, the critical behavior is characterized by two independent scaling fields, h_1 and h_2, and one dependent scaling field, h_3, which are analytic functions of the physical fields. Originally it was thought that for fluid mixtures with N thermodynamic degrees of freedom, the two independent scaling fields should be analytic functions of the N independent physical fields [40,41]. However, more recently, Fisher and co-workers [42-44] have pointed out that for a proper description of critical phase transitions in fluids, all three Ising scaling fields should be taken as analytic functions of all $N + 1$ physical fields, thus also including the dependent physical field. This improved principle of scaling behavior is now referred to as complete scaling. And indeed, complete scaling has turned out to give a proper account of the observed asymmetric critical phase behavior in fluids [45-49]. Here, I show that complete scaling implies an analytic relationship between the critical pressure and the critical temperature, even though P_c and T_c individually exhibit a non-analytic dependence on the concentration as predicted by Kim and Fisher [35].

In this chapter, I present a modified formulation for the critical locus of aqueous sodium-chloride solutions, but one which is fully consistent with these new theoretical developments. I proceed as follows. In Section 1.1 of Chapter 2, I review the available experimental information for the critical parameters of aqueous sodium chloride solutions. In Section 2 of Chapter 2, I discuss the theoretical predictions for the concentration dependence of the critical parameters of salt solutions, a possible theoretical basis for a crossover equation uniting separate dilute and non-dilute

regions, and the relationship between the critical pressure and the critical temperature. In Section 3 of Chapter 2, I then develop a set of equations for the critical parameters of aqueous solutions of sodium chloride consistent with these theoretical predictions. The results of this work, including range of validity and adoption of a revised guideline by IAPWS, as well as the corresponding value of the Krichevskiĭ parameter for the aqueous NaCl solution, I discuss in Sections 4, 5 and 6 of Chapter 2 respectively.

Subsection 1. Experimental data overview

A comprehensive review of the available experimental data for the critical parameters of aqueous sodium chloride solutions has been presented by Povodyrev et al. [34]. To my knowledge no new experimental data have been published since 1999. The available information for the critical temperature, pressure, and density is summarized in Figs. 5, 6, and 7, respectively. The experimental data cover a concentration range up to a NaCl mole fraction x of about 0.12, or thirty mass percent. I have not considered some earlier determinations which seem to be less accurate [57,58]. Measurements of Bochkov have also not been included, due to inaccessibility of the Ph.D. thesis with the original data [59] and an apparent deviation in the data from more recent experiments, which can be seen in the figures presented in the Povodryev review [34].

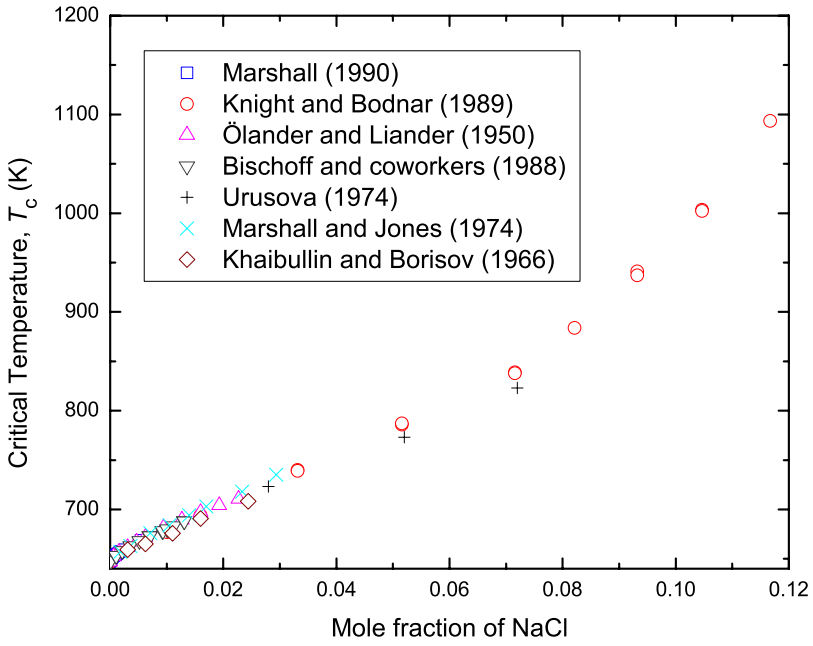

Figure 5. Experimental values for the critical temperature of salty water as a function of the mole fraction, x, of NaCl. Symbols represent the experimental data of Marshall [31], Knight and Bodnar [32], Ölander and Liander [50], Bischoff and coworkers [33,51-52], Urusova [53], Marshall and Jones [54], and Khaibullin and Borisov [55].

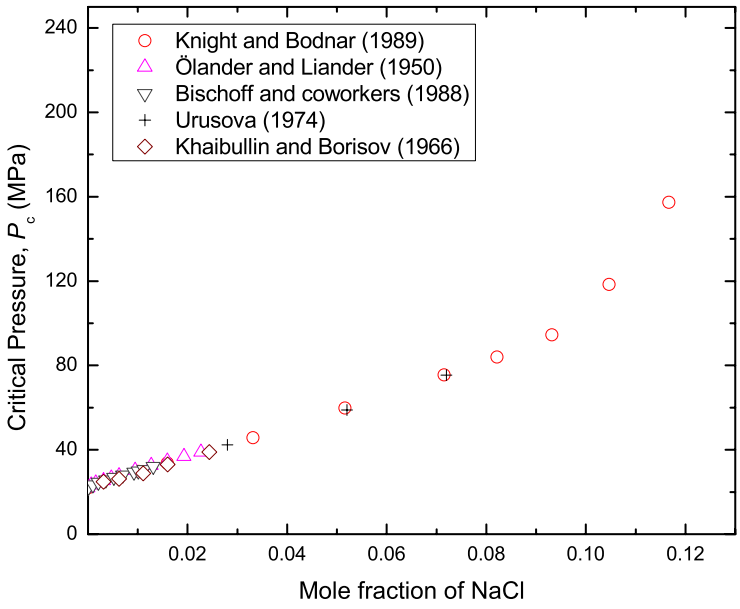

Figure 6. Experimental values for the critical pressure of salty water as a function of the mole fraction, x, of NaCl. Symbols represent the experimental data of Knight and Bodnar [32], Ölander and Liander [50], Bischoff and coworkers [33,51-52], Urusova [53], and Khaibullin and Borisov [55].

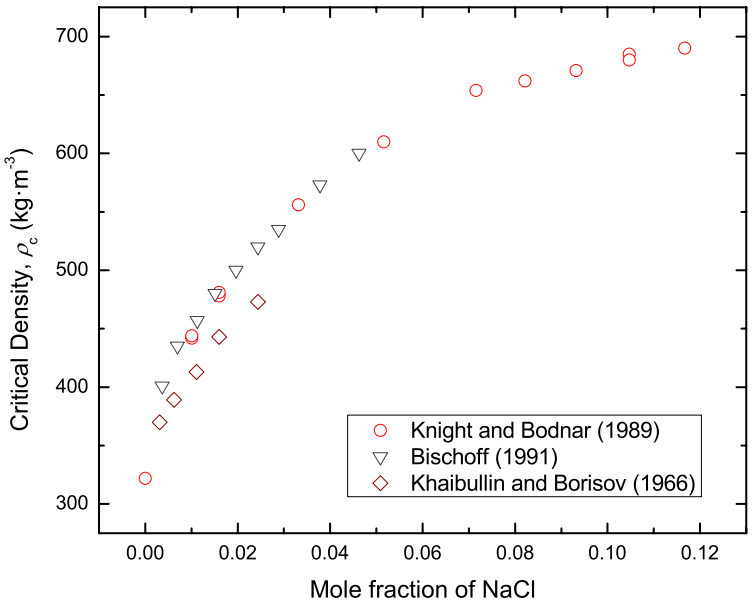

Figure 7. Experimental values for the critical density of salty water as a function of the mole fraction, x, of NaCl. Symbols represent the experimental data of Knight and Bodnar [32], Bischoff [56], and Khaibullin and Borisov [55].

In developing equations for the critical temperature and the critical pressure, I adopted the measurements of Marshall [31], of Bischoff and coworkers [33,51-52,56], and of Knight and Bodnar [32] as the primary data set, because of the range of concentrations covered, the experimental method used, and the documentation of method and error. For the critical density, I used the data of Knight and Bodnar [32] and the compilation of Bischoff [56]. As can be seen from Figs. 5 and 7, the data of Khaibullin and Borisov [55] are inconsistent with the other experimental information. Table 1 summarizes the available experimental data and highlights the primary data set. For additional discussion of the experimental information and of previous

attempts to develop equations for the critical parameters of aqueous sodium chloride solutions, beyond what is summarized below, please refer to the article of Povodyrev et al. [34]. The values currently accepted for the critical parameters of pure H_2O are [16,60-62]:

$$T_c^0 = 647.096 \text{ K}, \; P_c^0 = 22.064, \; \rho_c^0 = 322 \text{ kg} \cdot \text{m}^{-3}. \qquad (1)$$

Table 1. Summary of available experimental data on the NaCl-H_2O critical locus. Shading indicates inclusion in the primary data set.

Authors	T_c	P_c	ρ_c	Mole fraction range	Error (Y/N)	Year
Bischoff [56]	✓	✓	✓	0 - 0.05	N	1991
Bischoff and coworkers [32,51-52]	✓	✓		0 – 0.013	Y	1988,1989
Marshall [31]	✓			0 – 0.0053	Y	1990
Marshall and Jones [54]	✓			0.03	Y	1974
Knight and Bodnar [32]	✓	✓	✓	0 – 0.12	Y	1989
Urusova [53]	✓	✓		0.028 – 0.072	N	1974
Khaibullin and Borisov [55]	✓	✓	✓	0 – 0.025	Y	1966
Ölander and Liander [50]	✓	✓		0 – 0.022	Y	1950

ITS-90 and a note about temperature scales.

Available experimental data for the critical locus of sodium chloride was published between 1950 and 1991 [31-33,51-56]. During this time, the International

Committee on Weights and Measures went through two revisions to the International Temperature Scale, an equipment calibration standard [63]. Although most papers did not report their equipment calibration standard, measurements taken prior to 1968 were assumed to adhere to ITS-48, and measurements taken prior to 1990 were assumed to adhere to ITS-68. All temperatures have been converted into the International Temperature Scale of 1990 (ITS-90) wherever needed [64,65] but this correction was, generally, within the experimental uncertainty.

Experimental data of Ölander and Liander, 1950

Of the data considered, Ölander and Liander [50] provided the earliest measurements of dilute NaCl solutions at the critical temperature. Their experiment, published in 1950, was conducted using a copper lined steel bomb. The sample was pumped into the bomb, allowed thirty minutes to equalize, and then sampled from the bomb top and bottom through 1mm inner diameter copper capillaries wound through cooling mantles. The NaCl sample concentration was determined by titrating the chloride ion with silver nitrate using chromate as an indicator. Four thermocouples differed by 1^{o}C or less during the experiment and pressure was read to 1 $kg \cdot cm^2$. Error in concentration was not provided but possible sources were discussed. It was reported that the steel pump and valves rusted, although the author states the iron hydroxide formation would not affect measurements. The copper lining was also compromised and yielded cuprous chloride and oxide in small amounts. The critical temperature for pure water was measured at 374 ^{o}C (647 K), which matches the current accepted critical temperature of 647.096 K [62].

Experimental data of Khaibullin and Borisov, 1966

Khaibullin and Borisov [55] published data on the critical locus of NaCl and water in 1966. The work was published in Russian and translated into English. The test solution was transferred to an autoclave under partial vacuum, and electromagnetically stirred during heating in an apparatus constructed by the authors. Temperature, pressure and gamma quanta were measured and samples of the vapor phase were periodically withdrawn. Gamma quanta, measured using a scintillation counter, were converted into the corresponding densities of each phase. Khaibullin and Borisov conducted control experiments with distilled water to show the specific gravities of liquid and vapor phases were measured within $\pm$ 0.002 $g \cdot cm^3$. No other error estimates were provided. Khaibullin and Borisov's experimental data suggest lower critical temperatures than those published by Ölander et al. [50], Marshall et al. [31,54], and Bischoff et al. [33,51-52,56] and the measured critical density deviates from that found from the later measurements of Knight and Bodnar in 1989 [32] as well as Bischoff in 1991 [56].

Experimental data of Urusova, 1974

M.A. Urusova [53] published his critical locus of NaCl and water in 1974. His work, like Khaibullin and Borisov's, was translated from Russian to English. Vapor pressures were measured for solutions of NaCl and water in an autoclave with mercury seals using *P-V* curves. The vapor pressure was not determined at the moment of appearance of the vapor phase due to a small loss of gas at 350 ^oC and

corrections were made to the pressure after the measurement. Error in mole percent of sodium chloride was given as 0.3. Urusova's experimental data deviates further from other experimental results with increasing salt concentration.

Experimental data of Marshall and Jones, 1974

In 1974, Marshall and Jones [54] published experimental results obtained from sealing known compositions of NaCl-H_2O solution in fused silica capillary tubes with a 0.8 mm inner diameter. The volume ratio of liquid to vapor was determined by measuring the relative lengths in the tube. Inserting the tube into a stirred molten salt bath and vibrating it constantly, the molten salt bath temperature was raised. The temperature at which the meniscus between liquid and vapor apparently disappeared was recorded with the volume fraction of liquid just prior to the point of apparent criticality. Since the true critical temperature is the temperature at which the two phases are in equal volume when the meniscus disappears, this value represents the temperature at which the meniscus separating the phases becomes undetectable to the eye, and several volumes of each solution composition were tested to obtain the apparent critical temperatures and their volume fraction. The critical temperatures published were obtained from plotting the apparent critical temperature from experiment versus the volume fraction of the liquid phase and reading from a best-fit line a value of the critical temperature at 50% volume fraction liquid. Marhsall and Jones estimate their critical temperatures are valid within 0.5 ^{o}C.

Experimental data of Marshall, 1990

In 1990, Marshall [31] published a detailed look at the curve of the critical locus in the dilute solution limit. Using the same experimental methods as his earlier 1974 work, he obtained temperature measurements that were reproducible to $\pm 0.1-0.2\ ^{\circ}\mathrm{C}$, with better precision at the lower temperatures. The overall experimental accuracy of each measurement was estimated to be within $\pm 0.2-0.5\ ^{\circ}\mathrm{C}$. As seen in Fig. 3, the Marshall 1990 data provides the clearest picture of the initial curve of the critical locus at dilute concentrations of sodium chloride. However it also raises some questions. At concentrations of sodium chloride between about 0.1 and 0.15 mole percent (or 0.3 to 0.45 mass percent), the Marshall 1990 data exhibit a slight dip in the curvature of the critical locus. Additionally, this apparent dip appears to serve as a divide between the curvature of the critical locus in the dilute limit and the curvature of the critical locus in the non-dilute limit. The presence of this apparent dip is specifically addressed in some later attempts to empirically and theoretically describe the data, and plays an important role in our proposed formulation for the critical locus.

Experimental data of Rosenbauer and Bischoff 1988, Bischoff and Pitzer 1989 and Bischoff, 1991

Rosenbauer and Bischoff [33,51-52] explored some of the discrepancies from previously published experiments and published their own experimental results in 1988. These experiments were conducted in a fixed-volume pressure vessel of passivated titanium or a small Rene pressure vessel of similar design, held vertical in

a fluidized particle bath furnace. Openings at the top and bottom of the vessel were connected via capillary tubing to allow for sampling and pressure measurements. The vessel was filled, sealed and heated to temperature while maintaining sufficient pressure to keep the sample liquid. After equilibrium, samples were taken from the top of the vessel and the pressure was allowed to drop in response. Pressure drop as a result of sampling became increasingly small as the phase boundary was approached and it was apparent a liquid and vapor were present. Samples from the bottom of the vessel defined the liquid composition. Samples were taken via a gas-tight glass syringe and the chloride concentration analyzed by ion chromatography. The level of background contamination in the experiments was reported as approximately 0.5 ppm. Constant measuring of hydrogen gas was used to monitor for possible contamination. Temperature calibration was noted as particularly important due to changes in thermocouple response time after repeated temperature cycles. Temperatures are reported as accurate to $\pm 0.5\ ^{\circ}C$ and precise to $\pm 0.4\ ^{\circ}C$. Pressure is reported as accurate to ± 0.5 bar.

Bischoff and Pitzer published a compilation of available experimental data in 1989 [66] and Bischoff published additional experimental data in 1991 [56]. Bischoff's estimates of critical parameters were based on a combination of experimental data and the use of empirical curve fitting.

Experimental data of Knight and Bodnar, 1989

Knight and Bodnar [32] published results on the critical locus of NaCl and water in 1989 obtained from synthetic fluid inclusion experiments. In these

experiments thermally fractured quartz was placed in platinum capsules with amorphous silica powder and known compositions of NaCl-water solution. The capsules were sealed and the quartz fractures were healed in the presence of the NaCl-H_2O solution at controlled pressures and temperatures. Temperatures were estimated to be accurate to $\pm 0.2\ ^{\circ}C$ at the critical point of pure water ($373.946\ ^{\circ}C$), $\pm 2.0\ ^{\circ}C$ at $573\ ^{\circ}C$, and $\pm 5.0\ ^{\circ}C$ at $660\ ^{\circ}C$. Pressures were read to the nearest 5 bar increment with an estimated accuracy of ± 10 bar . Samples were frozen after the run to verify the salinity.

Section 2. Theory

Although an empirical formulation, like the Povodryev equation adopted by IAPWS [37], can accurately represent available experimental data, a theory-based equation is generally preferred. Theory-based equations offer a more physical representation of the experimental data and are more likely to offer flexibility if parameters of the studied system change. For example, a theory-based equation for the critical locus of aqueous sodium chloride would provide a logical starting place for the evaluation of the critical locus for other aqueous salt solutions if sufficient experimental data on these systems became available in the future.

In this section, I discuss the theoretical predictions for the concentration dependence of the critical parameters of salt solutions, speculate on the theoretical basis for treating dilute and non-dilute sections separately, and discuss the relationship between the critical pressure and the critical temperature.

Subsection 1. Concentration dependence on the critical parameters

A theory of the concentration dependence of the critical locus of salt solutions has been developed by Kim and Fisher [35]. For this purpose they considered the dependence of T_c, P_c, and ρ_c on a salt concentration ϕ which they identified with the mole ratio of ions and molecules. For a fully dissociated salt solution, ϕ is related to the mole fraction x as

$$\phi = \frac{2x}{1-x}. \tag{2}$$

They found that the ionic interactions cause the presence of non-analytic terms when the critical parameters of the dilute salt solution are expanded as a function of ϕ:

$$T_c(\phi) = T_c^0\left[1 + s_1\phi + s_{3/2}\phi^{3/2} + s_2\phi^2 + ...\right] \tag{3}$$

and similar expansions for $P_c(\phi)$ and $\rho_c(\phi)$:

$$P_c(\phi) = P_c^0\left[1 + p_1\phi + p_{3/2}\phi^{3/2} + ...\right], \tag{4}$$

$$\rho_c(\phi) = \rho_c^0\left[1 + r_1\phi + r_{3/2}\phi^{3/2} + ...\right]. \tag{5}$$

In this dissertation, I adopt the convention that T_c^0, P_c^0, and ρ_c^0 designate the critical parameters of the pure solvent, H_2O in our case as given by Eq. 1.

To elucidate the non-analytic concentration dependence in the dilute solution limit, Kim and Fisher defined a function [35]

$$G(y) \equiv \frac{T_c(\phi) - T_c^0}{T_c^0 y^2} \tag{6}$$

for a dilute aqueous sodium chloride solution. When plotted as a function of $y \equiv \sqrt{\phi}$ for comparison with the experimental data of Marshall [27], $G(y)$ highlights the 3/2 power dependence, which appears linear when plotted in this manner. This plot is reproduced in Fig. 8. As documented in Ref. [31,67], the reproducibility of these temperatures was about ± 0.1 to 0.2 K, with the better precision at the lower concentrations. The error bars in the values for $G(y)$ displayed in Fig. 8 correspond to an assumed error of ± 0.1 K in $T_c(\phi)$. Although one cannot rule out a possible analytic concentration dependence of the critical temperature within the accuracy of the experimental data, the non-analytic Eq. 3 of Kim and Fisher does yield a more physical representation of the concentration dependence of the critical temperature in the dilute solution limit.

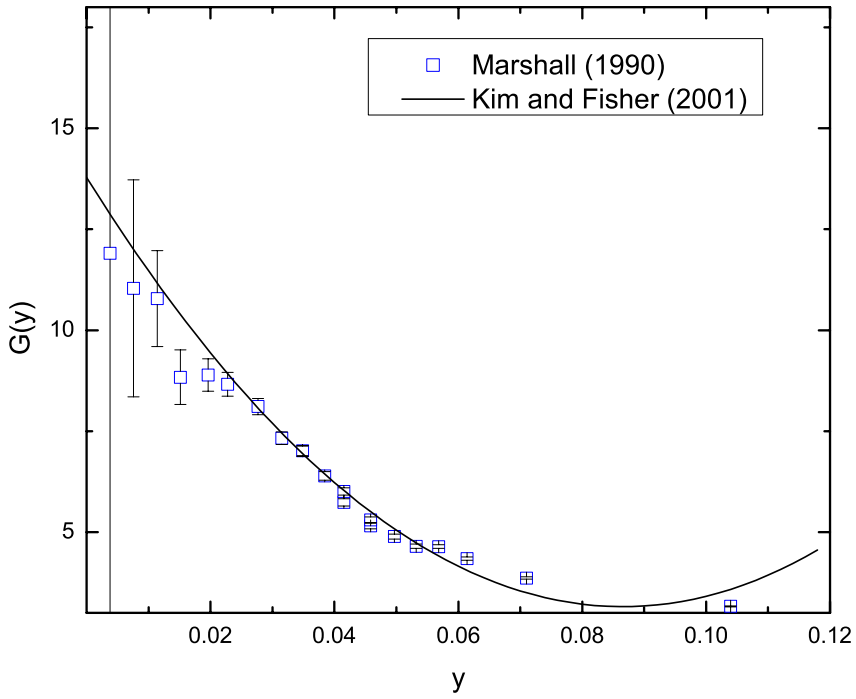

Figure 8. A plot of $G(y)$ vs. y for dilute NaCl+H_2O solutions. The plot, with $G(y)=\left[T_c(\phi)-T_c^{H_2O}\right]/T_c^{H_2O}y^2$ and $y=\sqrt{\phi}=\sqrt{2x/(1-x)}$, highlights the theory-based non-analytic dependence proposed by Kim and Fisher [35].

Although the Kim and Fisher equation represents the dilute solution behavior well, it does not extend to higher concentrations of salt without jeopardizing the fit in the dilute solution region, Fig. 9.

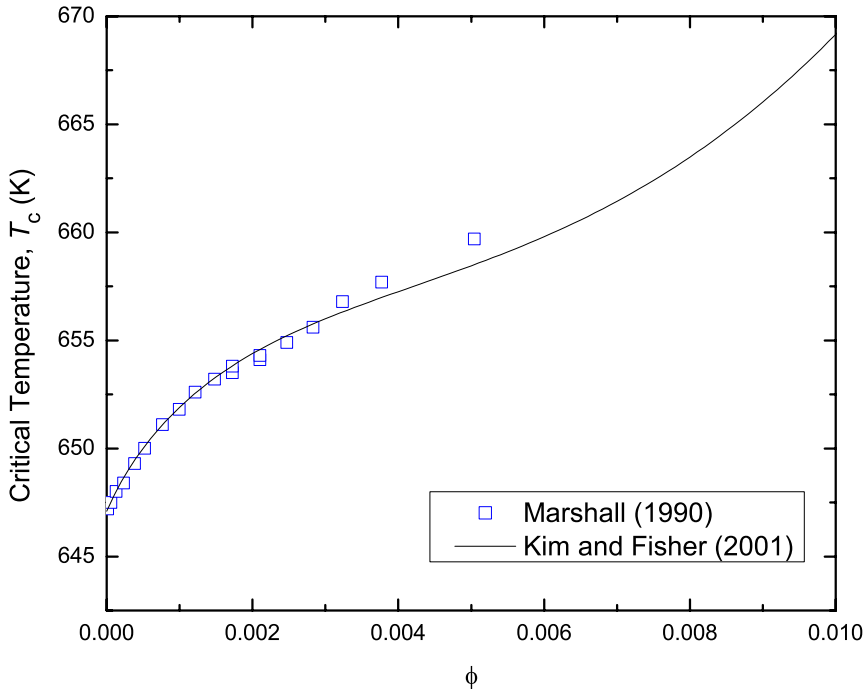

Figure 9. Critical temperature, T_c, as a function of salt concentration, ϕ, of NaCl+H_2O solutions. Blue squares are the experimental data of Marshall 1990 [31], and the solid black line is the theory-based fit using the equation $T_c = T_c^0\left[1 + s_1\phi + s_{3/2}\phi^{3/2} + s_2\phi^2\right]$, where the salt concentration ϕ is related to the mole fraction of NaCl through the equation $\phi = 2x/(1-x)$. Reproduced from Ref [35].

Subsection 2. Distinction between dilute and non-dilute behavior in the critical locus of sodium chloride

From Fig. 5 it appears that the critical temperature of H_2O is a continuous function of the NaCl concentration in the entire experimental range indicating that the

phase behavior of the NaCl+H_2O system exhibits type I phase behavior in the classification scheme of Van Konynenburg and Scott [27]. As discussed by several investigators [68-70], one would expect an interruption in the critical locus for an aqueous salt solution like NaCl+H_2O.

A careful examination of the experimental data for the dilute solution behavior of aqueous sodium chloride solutions relies primarily on the 1990 data of Marshall [31]. To date, it is the only experimental dataset with the resolution of data points to provide a detailed look at the sharp initial curve of the critical locus. From Figs. 4 and 8, we note that the experimental data of Marshall [31] show a little dip at $y \simeq 0.05$ or $x \simeq 0.001$ separating the initial sharp curve characterizing the dilute solution behavior, and the non-dilute behavior. Three data points available from Bischoff and co-workers from 1988 [33] in the dilute solution region suggest support for the apparent dip and the initial sharp curvature, as seen in Fig. 4.

The apparent dip in the experimental data of Marshall plays an important role in the development of our theory-based equation for the critical locus of sodium chloride. Although the Kim and Fisher equation does not extend to higher concentrations of salt without jeopardizing the fit in the dilute solution region, the apparent dip in experimental data, shown in Figs. 4 and 9, provides a possible justification for separate treatment of the dilute and non-dilute behavior of the critical locus.

Fluid mixtures exhibit a variety of phase behavior that has been classified by Scott and van Konynenburg [71,27] into six principle classes best differentiated by the *P-T* projections of their phase diagrams [28]. Chemically similar binary mixtures

typically exhibit Type I phase behavior characterized by a smooth shift of the critical point from one pure component to the other with increasing concentration. A schematic of Type I phase behavior was shown in Fig. 3, and an example of this type of system is the critical locus of an ethane + *n*-heptane solution, shown in Fig. 10 below.

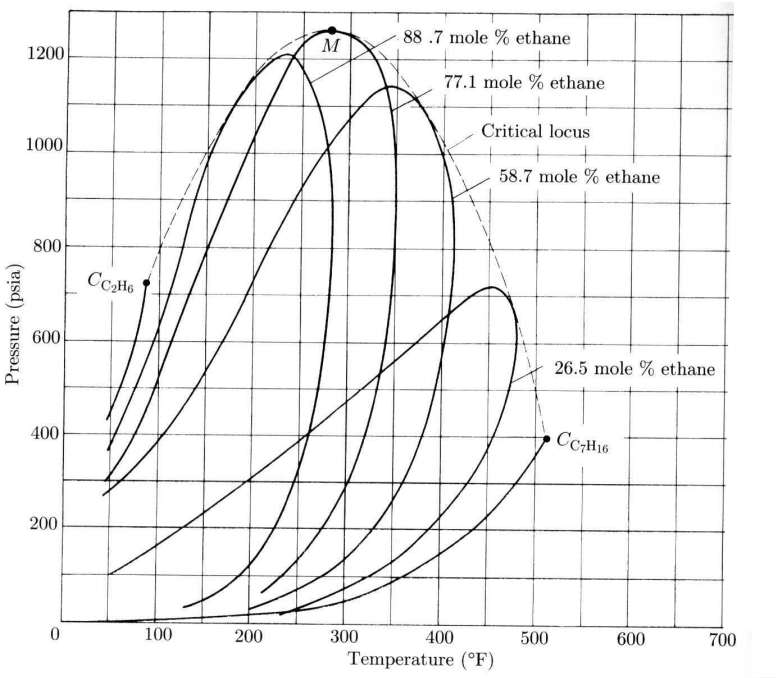

Figure 10. Critical locus (dashed) of ethane + *n*-heptane solutions. Solid lines represent the bubble-dew curves for various values of the mole fraction of ethane, reproduced from [72].

However, not all mixtures exhibit a continuous critical line [27,28,71]. Other types of phase behavior, such as a type IV or type V mixture, exhibit a critical line that begins at the vapor-liquid critical point of the less volatile component but ends in a Lower Critical End Point (LCEP) at a three-phase, liquid-liquid-gas line. This three-

phase line may be short, and end at higher temperatures and pressures with an Upper Critical End Point (UCEP) from which the critical line of the more volatile component connects [28]. A schematic of Type V phase behavior and the critical line of methane + *n*-hexane mixtures is shown in Fig. 11, below.

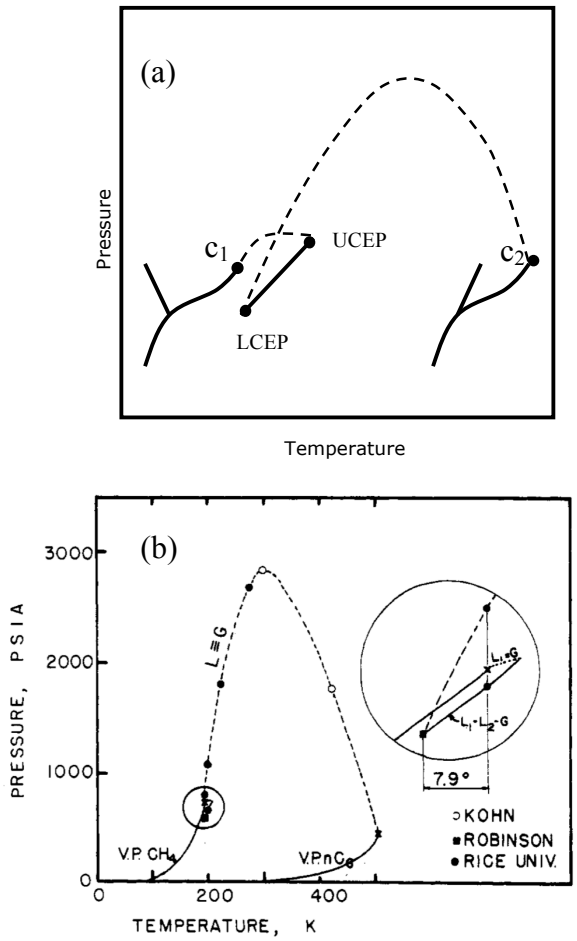

Figure 11. Type V phase behavior: (a) schematic [28], and (b) methane + *n*-hexane phase diagram, reproduced from [73]. The lower temperature vapor pressure curve for methane (V.P. CH_4) in (b) terminates in a vapor-liquid critical point, as does the vapor pressure curve for *n*-hexane (V.P.nC_6). A projection of the critical line for increasing concentrations of *n*-heptane connects the pure methane critical point to the UCEP of a three phase line, which ends in a LCEP connecting a critical line to the pure *n*-heptane critical point, as shown in the magnified inset circle.

The apparent dip in the experimental data of Marshall [31] cannot be conclusively confirmed without additional experimental data. However, such a dip could emerge in a binary system exhibiting near-Type V phase behavior and may indicate that the critical locus is about to be interrupted. In this scenario, the chemical miscibility of the species in the near-critical dilute solution region would exhibit near-tricritical behavior. The three phase line characteristic of Type V phase behavior would not appear, but the preference of the chemical species to form this tricritical solution would be strong enough to separate the curvature of the dilute and non-dilute region as well as create a dip in the critical line at the transition. A schematic summarizing the imagined scenario is shown as Fig. 12.

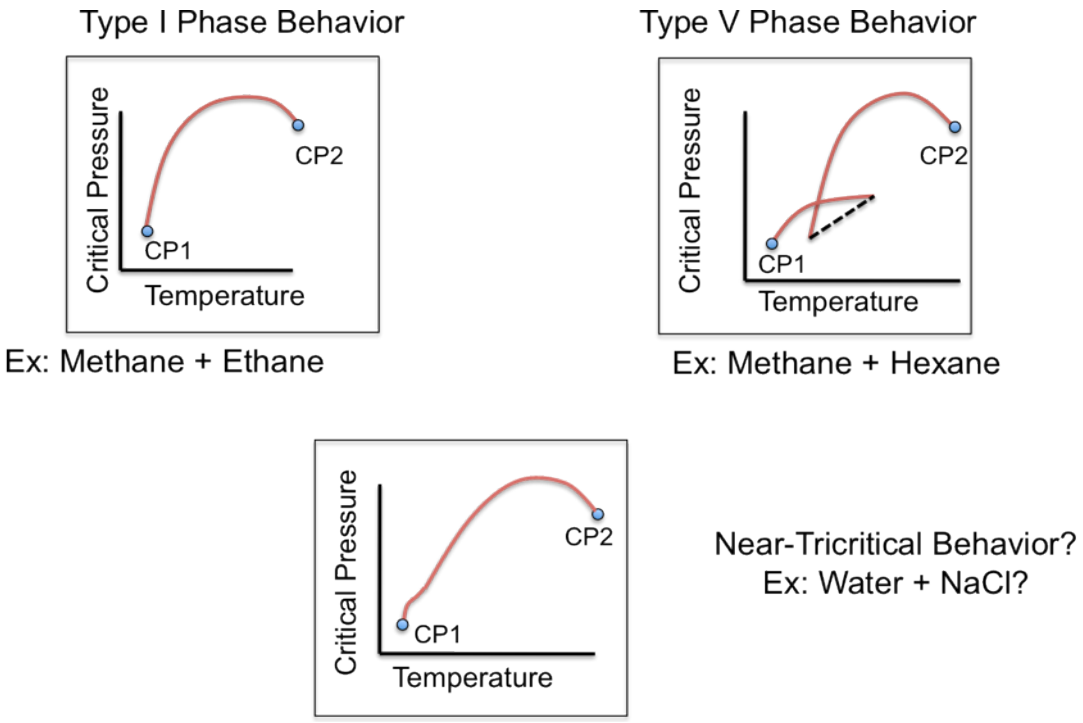

Figure 12. Schematic of possible phase behavior of NaCl+H_2O solutions. (a) Type I phase behavior as exhibited by methane + ethane solutions [28], (b) Type V phase behavior as exhibited by methane + hexane solutions [28], and (c) possible near-tricritical behavior exhibited by water and sodium chloride solutions.

In this near-Type V phase behavior scenario, the addition of some third component could change the phase behavior to Type V or IV [28]. Experimentally, this speculative near-Type V phase behavior could be confirmed with measurements of the aqueous sodium chloride critical locus in the presence of a third component. This third component has the potential to emphasize the tendency of the aqueous salt solution to separate and manifest the hypothesized tricritical point.

This possible theoretical basis for such a dip, while unconfirmed, also provides a theoretical basis for the separate treatment of the dilute and non-dilute

regions of the NaCl and water critical locus. The empirical approach of Povodreyev et al. [34] addressed difficulties in accurately describing all the experimental data with a single equation by using a crossover equation to unite two analytic curves. In contrast, my proposed theory-based formulation describing the critical locus of aqueous sodium chloride justifies the use a crossover equation to unite two non-analytic curves with an experimentally verifiable hypothesis based on known phase behavior, and the non-analytic concentration dependence of the critical locus developed by Kim and Fisher [35].

Subsection 3. Complete scaling and critical locus of solutions

Fluids belong to the universality class of Ising-like systems whose critical behavior is characterized by two independent scaling fields, h_1 and h_2, and one dependent scaling field, h_3, which is a generalized homogeneous function of h_1 and h_2 [74]. The scaling fields are defined such that at the critical point

$$h_1 = h_2 = h_3 = 0 \,. \tag{7}$$

These Ising scaling fields are analytic functions of the physical fields. That is, the anomalous singular critical behavior of various thermodynamic properties is solely caused by the non-analytic dependence of h_3 on h_1 and h_2 and not by any non-analyticities in the dependence of the scaling fields on the physical fields. According to the principle of complete scaling for binary solutions, the scaling fields will be analytic functions of four physical fields which can be identified with the temperature T, the pressure P, the chemical potential μ_1 of the solvent, and the chemical-

potential difference $\mu_{21} = \mu_2 - \mu_1$, where μ_2 is the chemical potential of the solute [46-48]. To satisfy Eq. 7 at the critical point, it is convenient to introduce difference functions defined by

$$\Delta T \equiv T - T_c, \Delta P \equiv P - P_c, \Delta\mu \equiv \mu_1 - \mu_{1,c}, \mu_{21} \equiv \mu_{21} - \mu_{21,c}, \tag{8}$$

where the subscript c refers to the value of a property at the critical point. Then in linear approximation, the relationships between the Ising scaling fields and the physical fields can be written as:

$$h_1 = a_1\Delta\mu_1 + a_2\Delta T + a_3\Delta P + a_4\Delta\mu_{21}, \tag{9}$$

$$h_2 = b_1\Delta T + b_2\Delta\mu_1 + b_3\Delta P + b_4\Delta\mu_{21}, \tag{10}$$

$$h_3 = c_1\Delta P + c_2\Delta\mu_1 + c_3\Delta T + c_4\Delta\mu_{21}, \tag{11}$$

where a_i, b_i, and c_i are system-dependent coefficients [38,75]. In applying complete scaling I consider the pure solvent as the reference state. That is, in Eqs. 9-11 I interpret ΔT, ΔP, $\Delta\mu_1$, and $\Delta\mu_{21}$ as

$$\Delta T \equiv T - T_c^0,\ \Delta P \equiv P - P_c^0,\ \Delta\mu \equiv \mu_1 - \mu_{1,c}^0,\ \Delta\mu_{21} \equiv \mu_{21} - \mu_{21,c}^0, \tag{12}$$

where the superscript 0 again refers to the critical parameters of the pure solvent. Because of Eq. 7, it follows from Eqs. 9-11 that at any point on the critical locus

$$h_1 = a_1\left(\mu_{1,c} - \mu_{1,c}^0\right) + a_2\left(T_c - T_c^0\right) + a_3\left(P_c - P_c^0\right) + a_4\left(\mu_{21,c} - \mu_{21,c}^0\right) = 0, \tag{13}$$

$$h_2 = b_1\left(T_c - T_c^0\right) + b_2\left(\mu_{1,c} - \mu_{1,c}^0\right) + b_3\left(P_c - P_c^0\right) + b_4\left(\mu_{21,c} - \mu_{21,c}^0\right) = 0, \tag{14}$$

$$h_3 = c_1\left(P_c - P_c^0\right) + c_2\left(\mu_{1,c} - \mu_{1,c}^0\right) + c_3\left(T_c - T_c^0\right) + c_4\left(\mu_{21,c} - \mu_{21,c}^0\right) = 0. \tag{15}$$

If we now eliminate $\mu_{1,c} - \mu_{1,c}^0$ and $\mu_{21,c} - \mu_{21,c}^0$ from these equations, we may conclude that $P_c - P_c^0$ must be an analytic function of $T_c - T_c^0$:

$$P_c = P_c^0\left[1 + p_1\Delta T + O\left(\left(\Delta T\right)^2\right)\right], \tag{16}$$

where from now on ΔT is to be interpreted as

$$\Delta T \equiv T_c - T_c^0 . \tag{17}$$

Of course, when Eq. 3 is substituted into Eq. 16 we recover the non-analytic concentration dependence proposed by Kim and Fisher [35]. However, complete scaling implies that the relationship between the intensive critical parameters should remain analytic, even for ionic fluids.

Section 3. Representative equations for the critical locus

In this section, I propose an alternative crossover equation to describe the critical locus of aqueous sodium chloride, incorporating the 3/2 power term suggested by theory, and making use of a crossover equation as suggested by the empirical formulation of Povodryev. This equation provides accuracy on par with the empirical equation of Povodryev but incorporates the non-analytic 3/2 term of Kim and Fisher as well as an absolute value crossover equation in place of the hyperbolic tangent crossover equation of Povodryev. The inclusion of the 3/2 term is not necessary to accurately represent the experimental data, even in the dilute region, however a theory-based description offers advantages over empirical descriptions of the data.

Subsection 1. Critical temperature

While Eq. 3 for the critical temperature up to a quadratic term in the concentration does yield a good description of the concentration dependence of T_c in the dilute solution limit, Figs. 8 and 9 show that deviations from the experimental data start to appear at $y \simeq 0.05$ which corresponds to a mole fraction of $x \simeq 0.001$. I prefer to express the NaCl concentration in terms of the mole fraction x, which is related to ϕ by Eq. 2. For the purpose of a theory-based fit, use of the mole fraction x is equivalent to use of the mole ratio ϕ and results in a similar form of the equation. This substitution is due to the analytic relationship between x and ϕ, and can be seen in Fig. 13, where the experimental data are compared with

$$T_c(x) = T_c^0 \left[1 + t_1 x + t_{3/2} x^{3/2} + t_2 x^2 \right], \tag{18}$$

which is mathematically equivalent to Eq. 3 and which also yields a good representation of the concentration dependence at mole fractions $x < 0.001$. Just as Kim and Fisher [31] concluded, we find that the contribution from the term proportional to $x^{3/2}$ is negative.

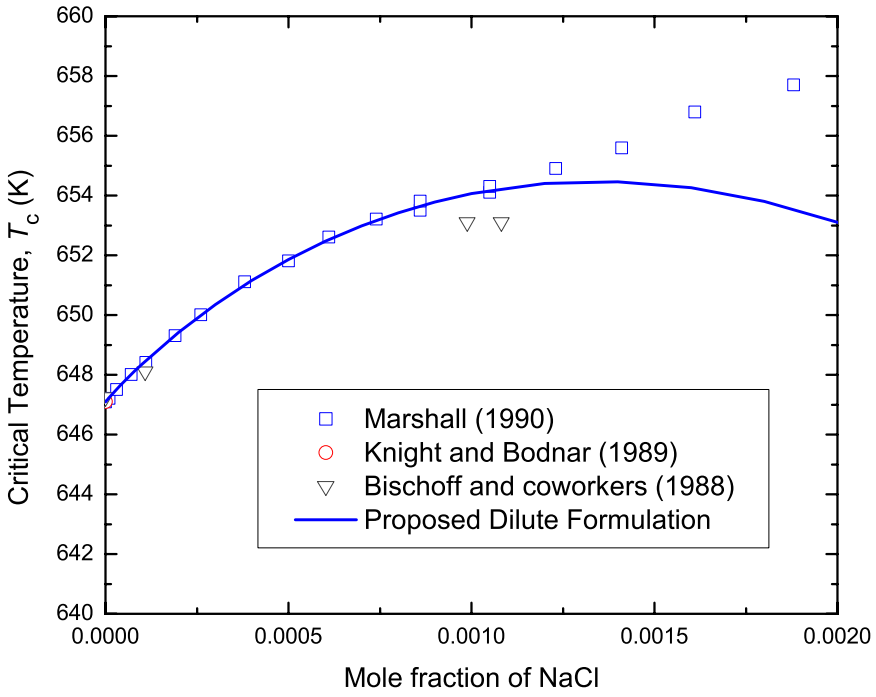

Figure 13. Critical temperature, T_c, vs. mole fraction, x, for dilute NaCl+H_2O solutions corresponding to $x < 0.001$. The symbols indicate experimental data of Marshall (1990) [31]. The curve represents Eq. 18 for low concentrations.

However, development of a more comprehensive equation for the critical temperature that reduces to Eq. 18 in the low-concentration limit is necessary in order to cover the experimental range of concentrations up to $x \simeq 0.12$. As discussed in Section 2.2 of this chapter, speculation on the phase behavior of aqueous sodium chloride critical locus, supported by the apparent dip in the experimental data of Marshall [31] provides a theoretical justification for the development of a crossover equation. Hence, following Povodyrev et al. [34], I assume that the critical locus for the temperature consists of two branches, one for the low-density concentration range

as given by Eq. 18, and another one for the high-concentration range. I thus adopt an equation of the form

$$T_c(x) = f_1(x)T_1(x) + f_2(x)T_2(x), \tag{19}$$

where $T_1(x)$ represents the branch for lower concentrations as given by Eq. 20:

$$T_1(x) = T_c^0\left[1 + t_1 x + t_{3/2}x^{3/2} + t_2 x^2\right], \tag{20}$$

and where $T_2(x)$ represents the branch for higher concentrations as given by Eq. 21:

$$T_2(x) = T_c^0\left[1 + t_1' x + t_{3/2}' x^{3/2} + t_2' x^2 + t_{5/2}' x^{5/2} + t_3' x^3 + t_{7/2}' x^{7/2} + t_4' x^4\right]. \tag{21}$$

In Eq. 19, $f_1(x)$ and $f_2(x)$ are switching functions defined by

$$f_1(x) = \frac{1}{4}\left[|Bx - C - 1| - |Bx - C + 1|\right] + \frac{1}{2}, \tag{22}$$

$$f_2(x) = \frac{1}{4}\left[|Bx - C + 1| - |Bx - C - 1|\right] + \frac{1}{2}, \tag{23}$$

with

$$B = 10\ 000, C = 10\,. \tag{24}$$

The values of B and C have been chosen so that

$$f_1(x) = 1 \text{ for } x \le 0.0009\,,\ f_1(x) = 0 \text{ for } x \ge 0.0011\,, \tag{25}$$

$$f_2(x) = 0 \text{ for } x \le 0.0009\,,\ f_2(x) = 1 \text{ for } x \ge 0.0011\,. \tag{26}$$

In Eq. 21, for the higher-concentration range we have also included non-analytic terms proportional to $x^{5/2}$ and $x^{7/2}$, since the theory of Kim and Fisher [35] implies that such non-analytic terms should also be present. The coefficients in Eqs.

20 and 21, deduced from a fit to the primary data for the critical temperature, are presented in Table 2.

Table 2. Values of t_i in the formulation for the critical temperature of NaCl+H_2O solutions as a function of mole fraction of salt.

Critical temperature T_c (K)	
Dilute	Extended, non-Dilute
$t_1 = 2.30 \times 10^1$	$t'_1 = 1.757 \times 10^1$
$t_{3/2} = -3.30 \times 10^2$	$t'_{3/2} = -3.026 \times 10^2$
$t_2 = -1.80 \times 10^3$	$t'_2 = 2.838 \times 10^3$
	$t'_{5/2} = -1.349 \times 10^4$
	$t'_3 = 3.278 \times 10^4$
	$t'_{7/2} = -3.674 \times 10^4$
	$t'_4 = 1.437 \times 10^4$
$B = 10\ 000, C = 10$	

Povodryev et al. [34] had chosen hyperbolic tangents as the form for the switching functions of the empirical formulation. The absolute value function I propose produces the same result, namely an equation that reduces to the dilute solution formulation of Eq. 20 in the dilute solution limit, and an equation that reduces to the non-dilute solution formulation of Eq. 21 in the non-dilute region. The

width of the crossover region, where the critical temperature is a function of both a weighted dilute formulation and a weighted non-dilute formulation overlaps with the area of the dip in the experimental data of Marshall [31] and can be adjusted by the parameters B and C in Eq. 22 and Eq. 23.

A comparison of Eq. 21 with the experimental data is presented in Figs. 14 and 15. Specifically, Fig. 15 shows how the two branches are connected at x ≃ 0.001, while Fig. 14 shows the comparison with the experimental data in the entire available concentration range.

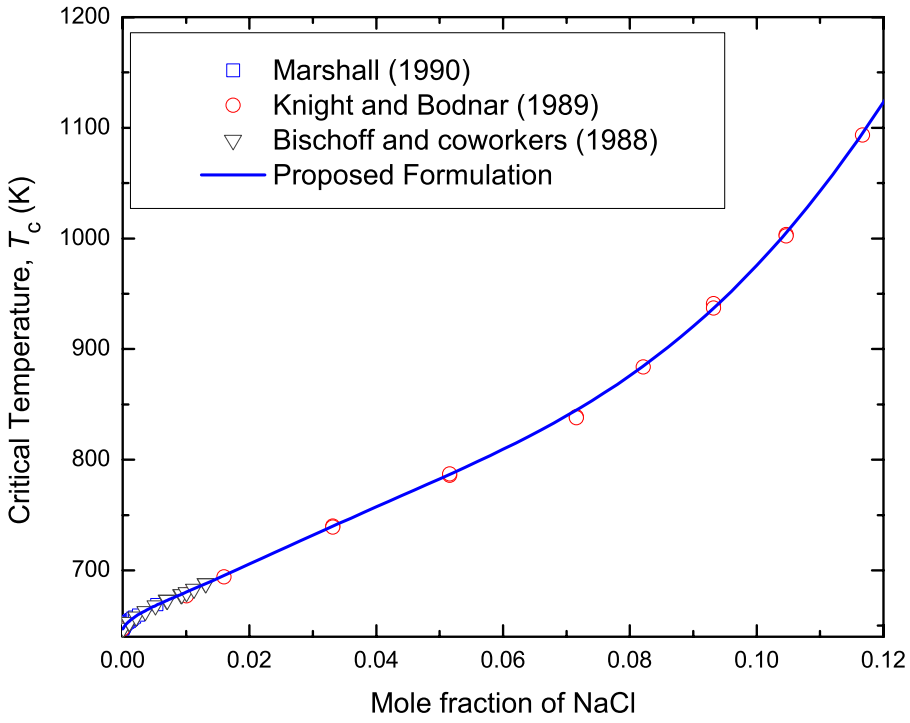

Figure 14. Critical temperature, T_c, vs. mole fraction, x, for NaCl+H_2O solutions over the entire range of available experimental data. Symbols represent the

experimental data of Marshall [31], Knight and Bodnar [32], Bischoff and coworkers [33,51-52]. The solid blue curve represents Eq. 21 for the non-dilute region.

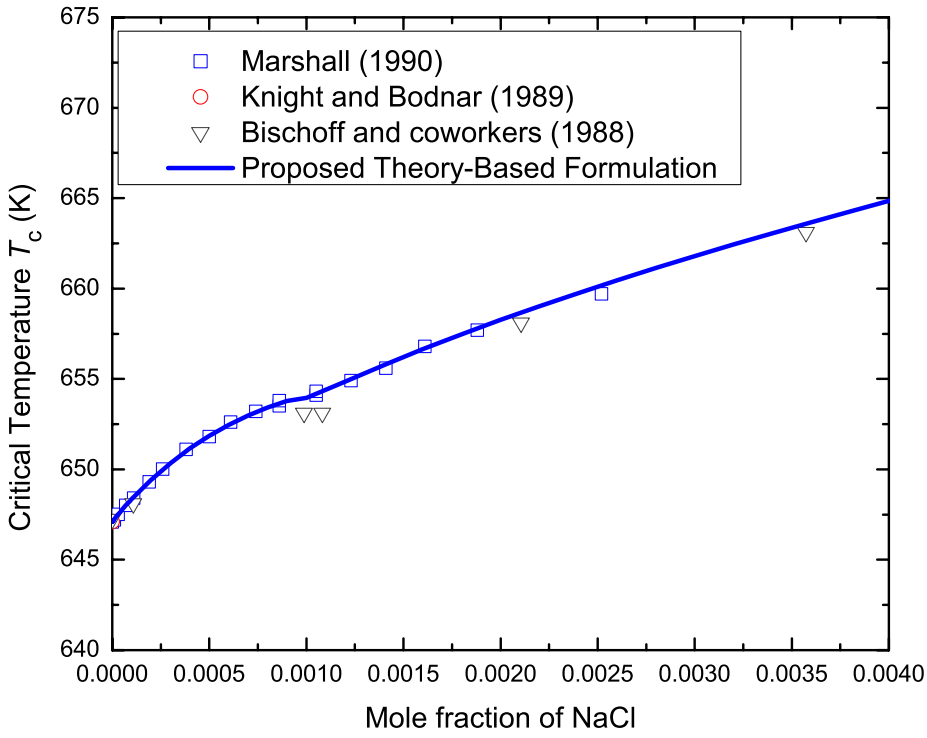

Figure 15. Critical temperature, T_c, vs. mole fraction, x, for NaCl+H_2O solutions at concentrations corresponding with $x \leq 0.004$. The symbols indicate experimental data of Marshall (1950) [31], Knight and Bodnar (1989) [32], and Bischoff and coworkers [33,51-52]. The curve represents Eq. 19 and shows the fit to experimental data in the region of the crossover between dilute and non-dilute formulations.

Subsection 2. Critical density

For a representation of the critical densities, Povodyrev et al. [34] followed Knight and Bodnar [32] by adopting a polynomial in terms of $\ln(w+1)$, where w is the weight fraction of NaCl. However, the theoretical treatment of Kim and Fisher [35] suggests that the critical density should have a non-analytic concentration expansion, shown in Eq. 5, similar to the Eqs. 20 and 21 for the critical temperature:

$$\rho_c(x) = \rho_c^0 \left[1 + r_1 x + r_{3/2} x^{3/2} + r_2 x^2 + r_{5/2} x^{5/2} + r_3 x^3 + r_{7/2} x^{7/2} + r_4 x^4 \right]. \qquad (27)$$

The values of the coefficients in Eq. 27, obtained from a fit to the experimental density data of Knight and Bodnar [32] and of those reported by Bischoff [56] are presented in Table 3. Strictly speaking, a possible dip in the critical temperature curve at $x \simeq 0.001$ could be expected to induce some irregular behavior also in the critical density at $x \simeq 0.001$. However, the effect, if any, is well within the accuracy of the experimental data and, hence, we represent the critical density by a single equation as was also done by Povodyrev et al. [34]. A comparison of Eq. 27 with the experimental data is shown in Fig. 16.

Table 3. Values of r_i in the formulation for the critical density of NaCl+H_2O solutions as a function of mole fraction of salt.

Critical density ρ_c $(\mathrm{kg \cdot m^{-3}})$
$r_1 = 1.7607 \times 10^2$
$r_{3/2} = -2.9693 \times 10^3$
$r_2 = 2.4886 \times 10^4$
$r_{5/2} = -1.1377 \times 10^5$
$r_3 = 2.8847 \times 10^5$
$r_{7/2} = -3.8195 \times 10^5$
$r_4 = 2.0633 \times 10^5$

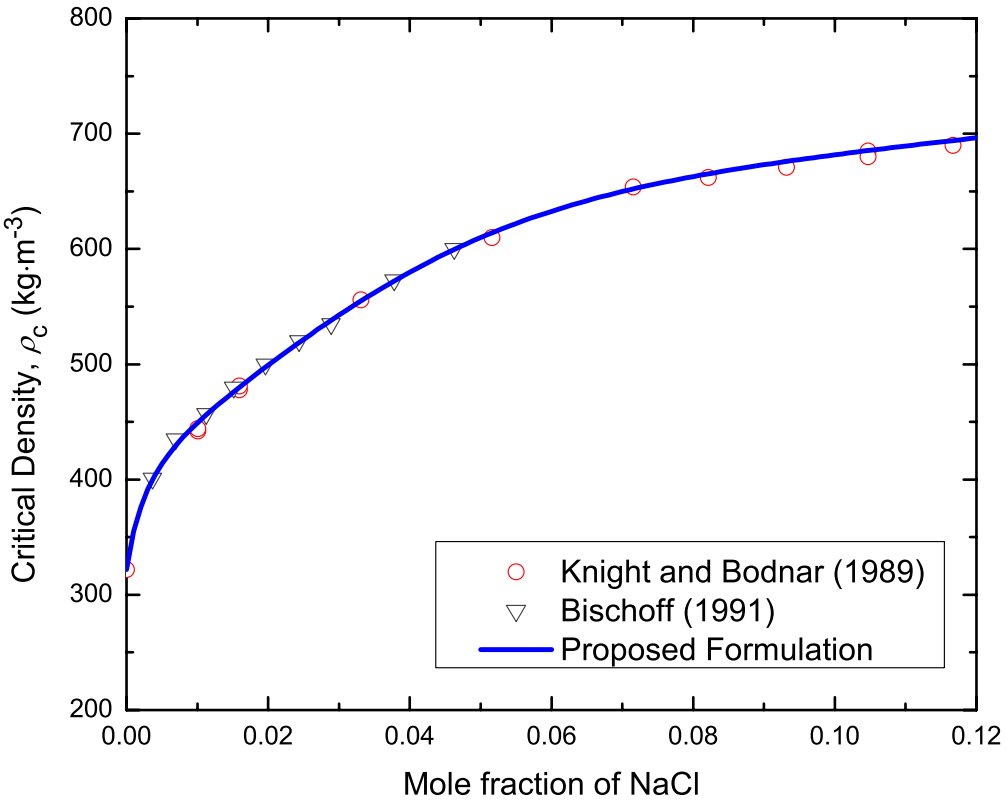

Figure 16. Critical density, ρ_c, vs. mole fraction, x, for NaCl+H_2O solutions. The symbols indicate the experimental data of Knight and Bodnar [32] and of Bischoff and coworkers [56]. The solid blue curve represents values calculated from Eq. 27.

Subsection 3. Critical pressure

Povodyrev et al. [34] noticed that it was easier to represent the critical pressure in terms of a power series of $\Delta T \equiv T_c - T_c^0$, where temperature is in K, rather than as a polynomial in terms of the salt concentration. As we now have seen in Sect. 2.1.2.3, complete scaling implies that the critical pressure is indeed an analytic

function of the temperature. Hence, we can continue to keep the truncated power series for the critical pressure in terms of the temperature earlier proposed by Povodyrev et al. [34]:

$$P_c(x) = P_c^0\left[1 + p_1\Delta T + p_2(\Delta T)^2 + p_3(\Delta T)^3 + p_4(\Delta T)^4\right] \tag{28}$$

with coefficients p_i as given in Table 4. Of course, if one substitutes Eq. 19 for the critical temperature into Eq. 28 one obtains an expansion of the critical pressure that includes a contribution proportional to $x^{3/2}$. A comparison of the values thus calculated for the critical pressure as a function of concentration is shown in Fig. 17, and for the critical pressure as a function of critical temperature in Fig. 18.

Table 4. Values of p_i in the formulation for the critical pressure of NaCl+H_2O solutions as a function of critical temperature, $T_c(x)$.

Critical pressure P_c (MPa)
$p_1 = 9.1443\times10^{-3}$ K^{-1}
$p_2 = 5.1636\times10^{-5}$ K^{-2}
$p_3 = -2.5360\times10^{-7}$ K^{-3}
$p_4 = 3.6494\times10^{-10}$ K^{-4}

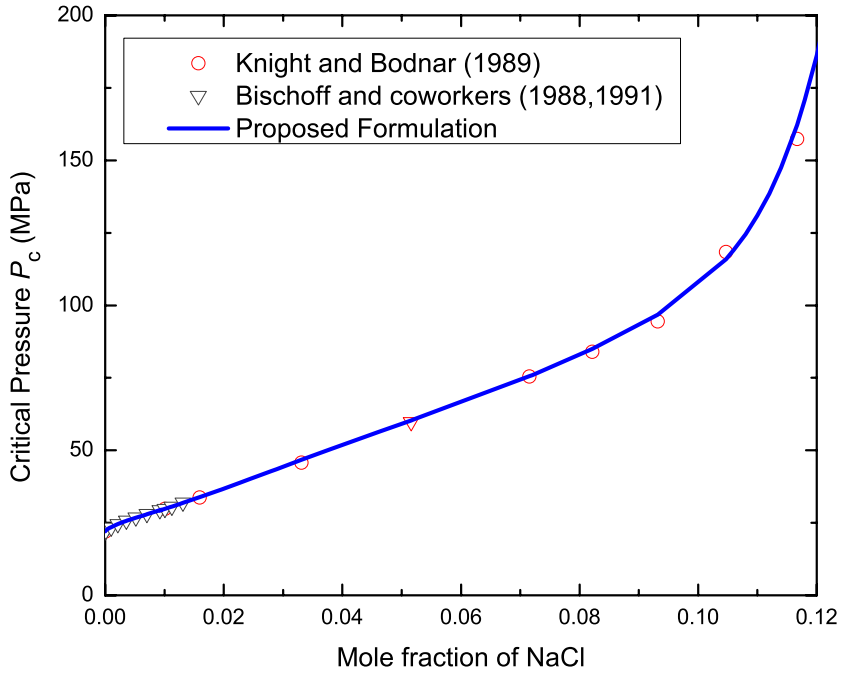

Figure 17. Critical pressure, P_c, vs. mole fraction, x, for NaCl+H_2O solutions. The symbols indicate experimental data of Knight and Bodnar [32] and of Bischoff and coworkers [33,51-52,56]. The solid curve represents values calculated from Eqs. 28 and 19.

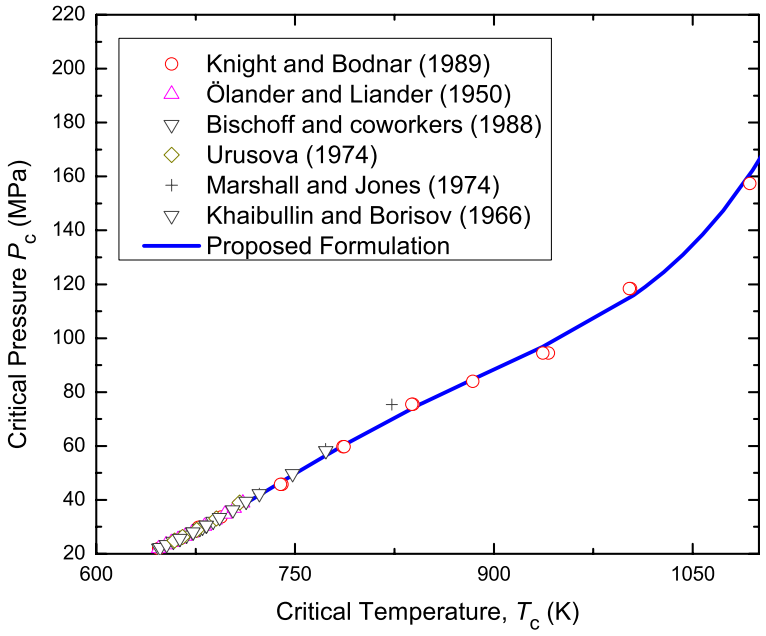

Figure 18. Critical pressure, P_c, vs. critical temperature, T_c, for NaCl+H_2O solutions. The symbols indicate experimental data of Knight and Bodnar [32], Ölander and Liander [50], Bischoff and coworkers [33,51-52,56], Urusova [53], Marshall and Jones [54], and Khaibullin and Borisov [55]. The solid curve represents values calculated from Eqs. 28 and 19.

Just as with the density, a possible dip in the critical temperature curve at $x \simeq 0.001$, corresponding to a critical temperature of $T_c = 654$ K, could be expected to also induce some irregular behavior in the critical pressure as a function of critical temperature at $x \simeq 0.001$. The proposed formulation for the critical pressure as a function of the critical temperature exhibits an irregularity due to the crossover equation used for the temperature. However, there is not sufficient experimental data for either the critical density or the critical pressure in the dilute solution limit to

determine any irregularities. For the data that does exist, the effect, if any, is well within the experimental accuracy. Fig. 19 shows the proposed formulation and experimental data for the density and the pressure in the dilute solution region.

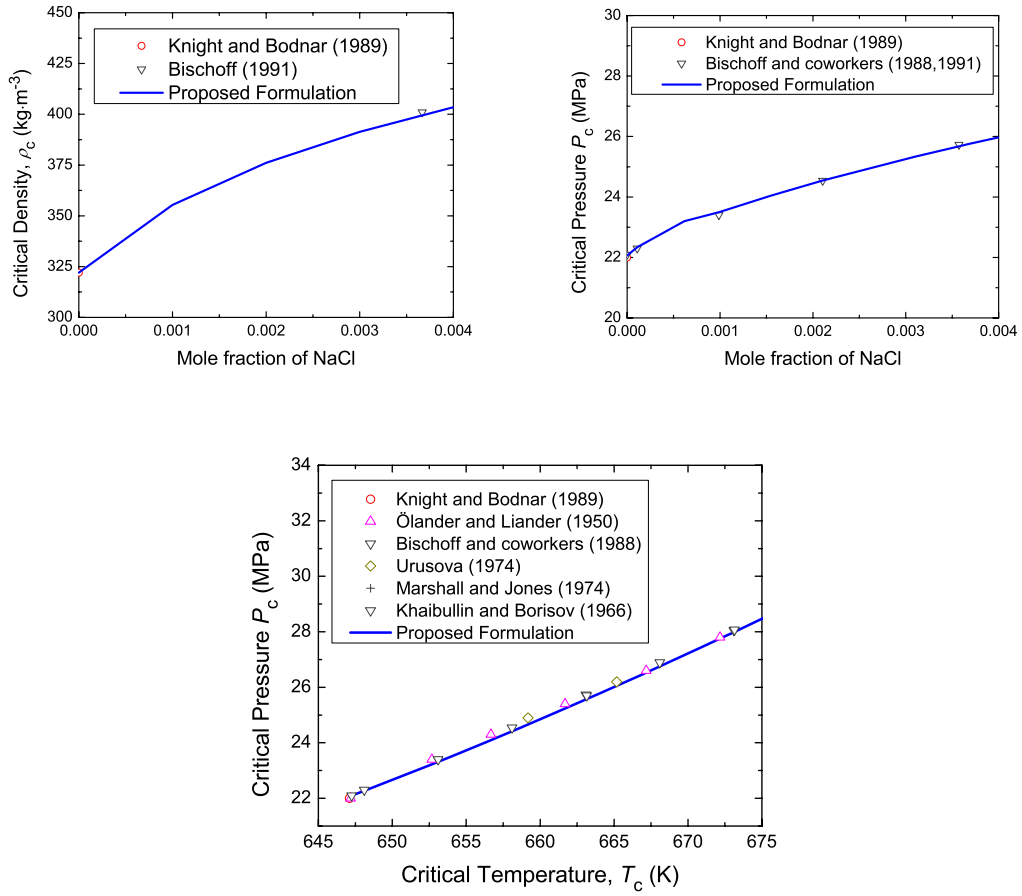

Figure 19. Critical parameters (ρ_c vs. x, P_c vs. x, and P_c vs. T_c) for NaCl+H_2O in the dilute solution region and near the apparent dip in the experimental data of the critical temperature [31] at $x \simeq 0.001$ and $T_c = 654$ K. Solid lines show the proposed formulation of Eqs. 27, 28, and 19. The symbols indicate experimental data of Knight and Bodnar [32], Ölander and Liander [50], Bischoff and coworkers [33,51-52,56], Urusova [53], Marshall and Jones [54], and Khaibullin and Borisov [55].

Section 4. Methodology and range of validity

In this chapter, I presented a formulation for the critical locus of sodium chloride solutions on the basis of an expansion of the critical parameters of H_2O that contains a non-analytic contribution in accordance with a theoretical prediction of Kim and Fisher [35,44]. Specifically, Eqs. 19, 27 and 28, with the coefficients listed in Tables 2, 3, and 4, yield a satisfactory description of the experimental data for the critical temperature, density, and pressure in the concentration range for which such experimental data are available, i.e., for concentrations such that

$$x \leq 0.12. \tag{29}$$

Experimental data was primarily fitted using the Nonlinear Curve Fitting (NLFit) functionality built into the OriginLab Data Analysis and Graphing Software, Origin 8. The NLFit function solves a system of equations designed to minimize the aggregated point-by-point differences between the experimental data and the input fitting function. These solutions are not achieved analytically, but iteratively, and use a Levenberg-Marquardt algorithm, also known as the damped least squares method, to perform the iterative computation adjusting the parameters in a chi-square minimization. Chi-square is defined as

$$\chi^2 = \sum_{i=1}^{n} w_i \left[Y_i - f\left(x_i'; \hat{\theta}\right) \right]^2 \tag{30}$$

where x_i' is the row vector for the i^{th} $\left(i = 1,2,...,n\right)$ observation; $\hat{\theta}$ are the adjustable parameters, and w_i is the i^{th} weight [76]. Using this methodology, the

parameters for the dilute solution, $T_1(x)$, in Eq. 20 were fitted to the primary data set for mole fractions of $x \le 0.0009$. The parameters for the non-dilute solution, $T_2(x)$, in Eq. 21 were fitted to the primary data set for mole fractions of $x \ge 0.0011$. The critical temperature and critical density were fitted using weighted fits based on the reported error given by the experimental data sets.

Standard deviations were calculated for each of the critical parameter formulations of aqueous sodium chloride as

$$\sigma = \sqrt{\frac{\sum (z_i - z)}{N}}, \tag{31}$$

where N is the number of experimental data points, z is an experimental critical parameter, and z_i is the critical parameter calculated from Eqs. 19, 27, and 28 for critical temperature, critical density, and critical pressure respectively. Equation 19 represents T_c with a standard deviation $\sigma = 0.019\%$ at $x \le 0.0009$, the dilute solution limit, and with a standard deviation $\sigma = 0.24\%$ at $0.0009 \le x \le 0.012$. Equation 27 represents ρ_c with a standard deviation $\sigma = 0.6\%$. Equation 28 represents P_c with a standard deviation $\sigma = 1.7\%$.

Percentage deviations of the experimental data from the formulations for critical temperature, critical pressure, and critical density are shown in Figs. 20, 21, and 22, below.

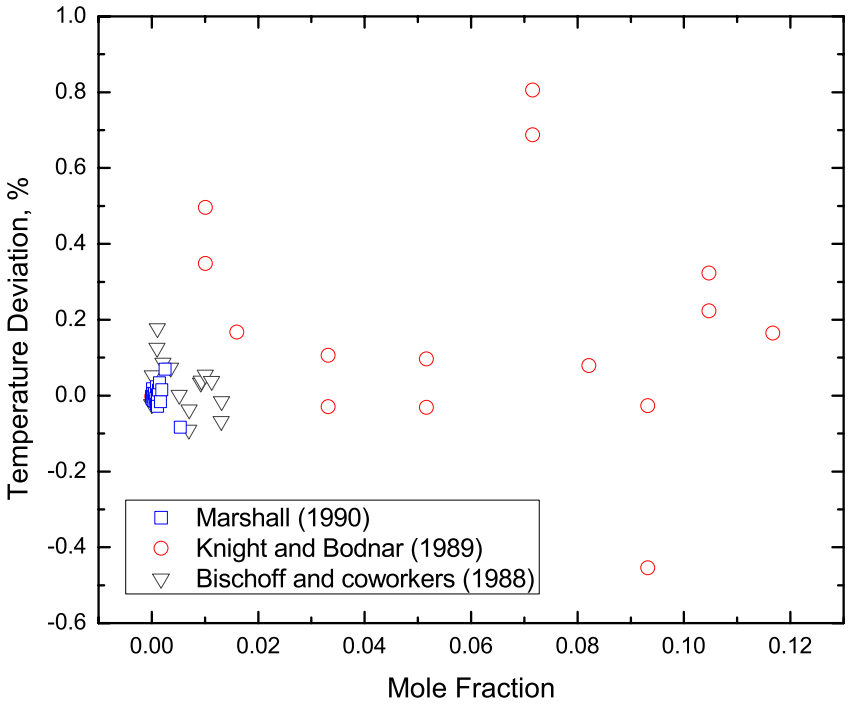

Figure 20. Percent deviation of calculated vs. experimental critical temperatures, T_c, for NaCl+H_2O solutions. Experimental critical temperatures taken from the data of Marshall [31], Knight and Bodnar [32], Bischoff and coworkers [33,51-52,56] and compared with values calculated from Eq. 19.

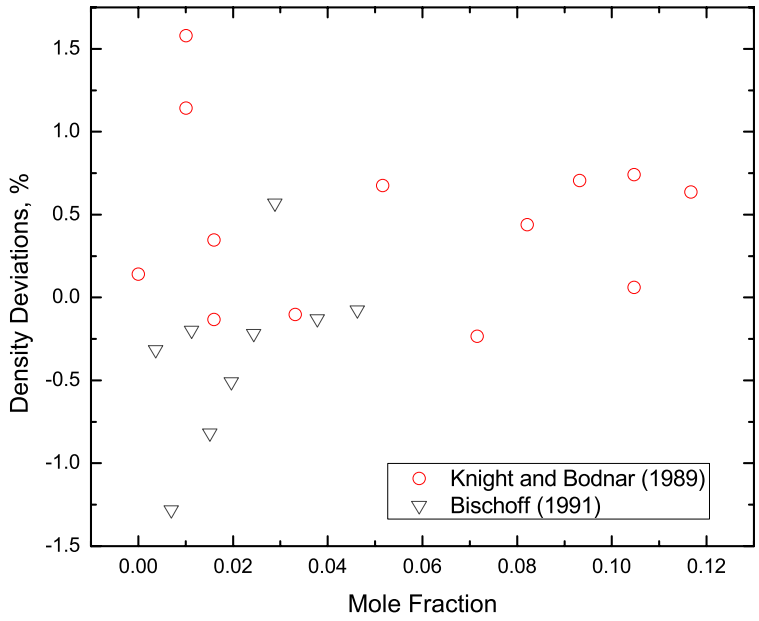

Figure 21. Percent deviation of the calculated vs. experimental critical densities, ρ_c, for NaCl+H_2O solutions. Experimental critical densities taken from the data of Knight and Bodnar [32] and of Bischoff and coworkers [56] and compared with values calculated from Eq. 27.

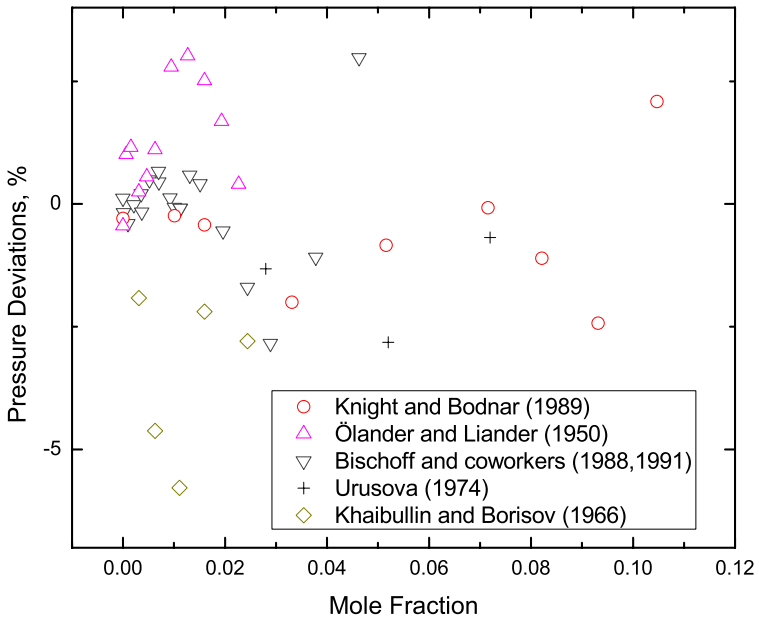

Figure 22. Percent deviation of calculated vs. experimental critical pressures, P_c, for NaCl+H_2O solutions. Experimental critical pressures taken from the data of Knight and Bodnar [32], Ölander and Liander [50], Bischoff and coworkers [33,51-52,56], Urusova [53], Marshall and Jones [54], and Khaibullin and Borisov [55] and compared with values calculated from Eq. 28.

As a cautionary note, we mention that truncated expansions in terms of concentration, whether analytic or non-analytic, will always have a finite range of validity. It is possible to describe the data equally well without the addition of a term proportional to x^4 in Eqs. 21 and 27, but at the cost of rather unphysical extrapolation behavior. However, even the equations presented here will not be reliable when extrapolated beyond the concentration range, given by Eq. 29, to which the equations were fitted.

Section 5. IAPWS guideline

Because of the practical importance of an accurate knowledge of the critical parameters for industrial, geochemical, and biological applications, the empirical equation for the critical temperature, critical pressure, and critical density of aqueous solutions of sodium chloride was adopted in 1999 by the International Association for the Properties of Water and Steam (IAPWS) as a guideline. Here, I have presented a theory-based formulation for the critical parameters of aqueous sodium chloride solutions as a proposed replacement for the empirical formulation currently in use. This formulation has been published in the International Journal of Thermophysics [1] and in September 2012 was presented at the IAPWS annual meeting in Boulder, CO [77]. At the conclusion of the meeting, the Executive Committee of IAPWS recommended my formulation for adoption as a *Revised Guideline on the Critical Locus of Aqueous Solutions of Sodium Chloride*, presented in Appendix I. Members of the working group also presented their findings confirming the proposed formulations for the critical parameters of aqueous solutions of sodium chloride, as well as comparisons to the original guideline based on the empirical formulation of Povodryev et al. [37].

Subsection 1. Comparison to empirical formulation

The most significant difference with the empirical equation of Povodyrev et al. [37] is that the proposed formulation for the critical locus of aqueous solutions of

sodium chloride takes into account the non-analytic concentration dependence of the critical parameters, as proposed by the theory of Kim and Fisher [35], and utilizes the analytic relationship between critical pressure and critical temperature justified by scaling theory and a crossover equation justified by likely phase behavior. In addition, the inclusion of a term proportional to $x^{3/2}$ leads to a more realistic representation of the critical temperatures in the low-concentration limit, as shown in Fig. 23 and more clearly in the $G(y)$ plot shown in Fig. 24, and as presented in Section 2 of this chapter, which highlights the $x^{3/2}$ concentration dependence. Otherwise, Eq. 19 yields a representation of the experimental data with an accuracy that is similar to that of the equation of Povodyrev et al. [37].

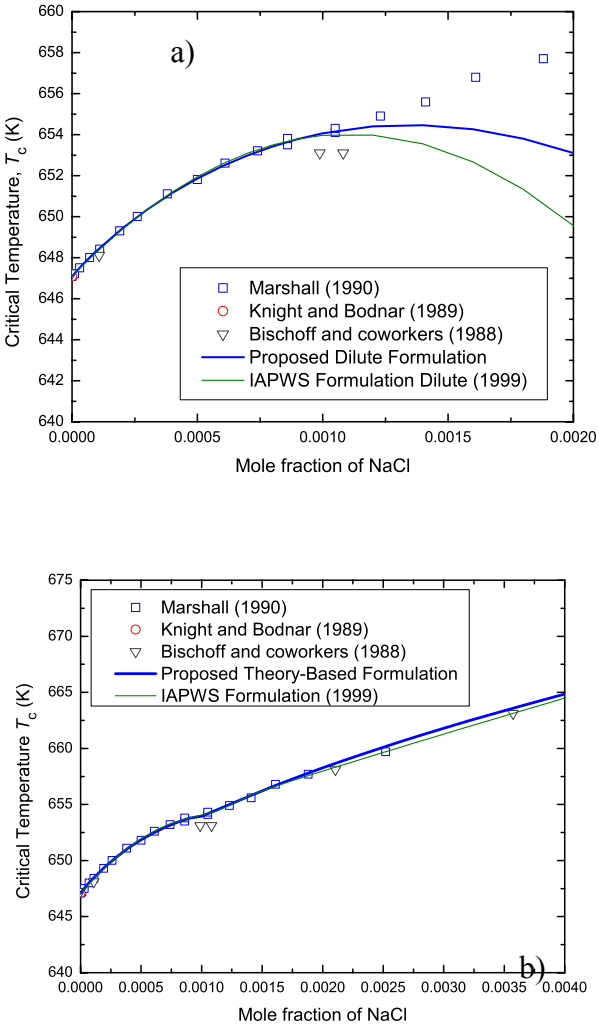

Figure 23. Comparison of proposed formulation and IAPWS for the critical temperature, T_c, vs. mole fraction, x, for NaCl+H_2O solutions at low salt concentrations. The symbols indicate the experimental data of Marshall [31], Knight and Bodnar [32], Bischoff and coworkers [33,51-52,56]. The solid, thin green curve represents values calculated from the equation of Povodyrev et al. [37]. a) The solid, thick blue curve represents the proposed dilute solution values calculated from Eq. 20. b) The solid, thick blue curve represents proposed theory-based values calculated from Eq. 19.

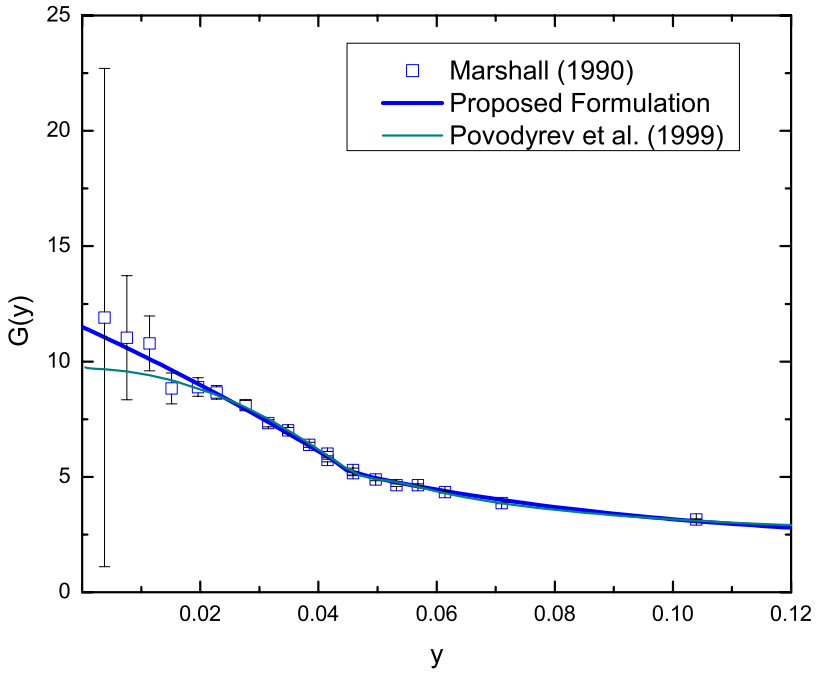

Figure 24. Comparison of proposed formulation and IAPWS for $G(y)$ vs. y for NaCl+H_2O solutions, where $G(y)=\left[T_c(\phi)-T_c^0\right]/T_c^0 y^2$ and $y=\sqrt{\phi}=\sqrt{2x/(1-x)}$. The symbols represent the experimental data of Marshall [31] with error bars corresponding to a random error of ± 0.1 K. The solid, thin green curve represents the equation of Povodyrev et al. [37], and the solid curve the proposed modified Eq. 19 presented in Section 3.1 of this chapter.

Generally, Eq. 27 represents the experimental density data with an accuracy similar to the equation of Povodyrev et. [37], as shown in Fig. 25, except that the inclusion of a term proportional to $x^{3/2}$ leads to a slightly better representation of the critical density at very low concentrations, as was the case for the critical temperature shown in Fig. 24.

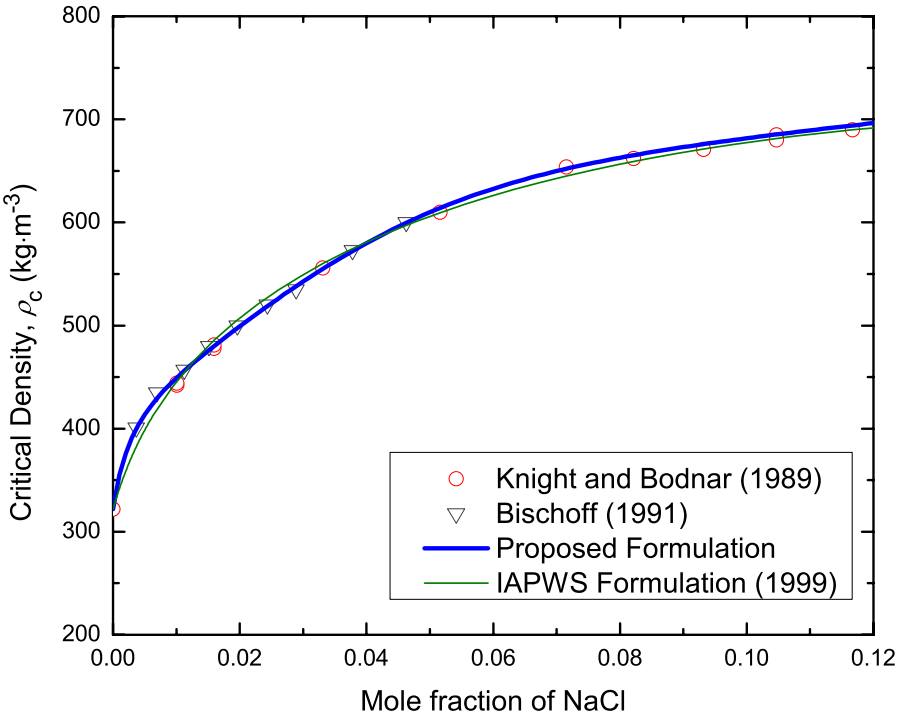

Figure 25. Compariosn of proposed formulation and IAPWS for the critical density, ρ_c, vs. mole fraction, x, for NaCl+H_2O solutions. The symbols indicate the experimental data of Knight and Bodnar [32] and of Bischoff and coworkers [56]. The solid, thick blue curve represents values calculated from Eq. 27. The solid, thin green curve represents values calculated from the equation of Povodyrev et al. [37].

A comparison between the calculated critical pressure for Eq. 28 and the IAPWS formulation as a function of temperature is shown in Fig. 26. Although the coefficients of the analytic dependence of critical pressure on critical temperature are the same for both formulations, the difference in the critical temperature formulation creates slight variances which can be seen in Fig. 27.

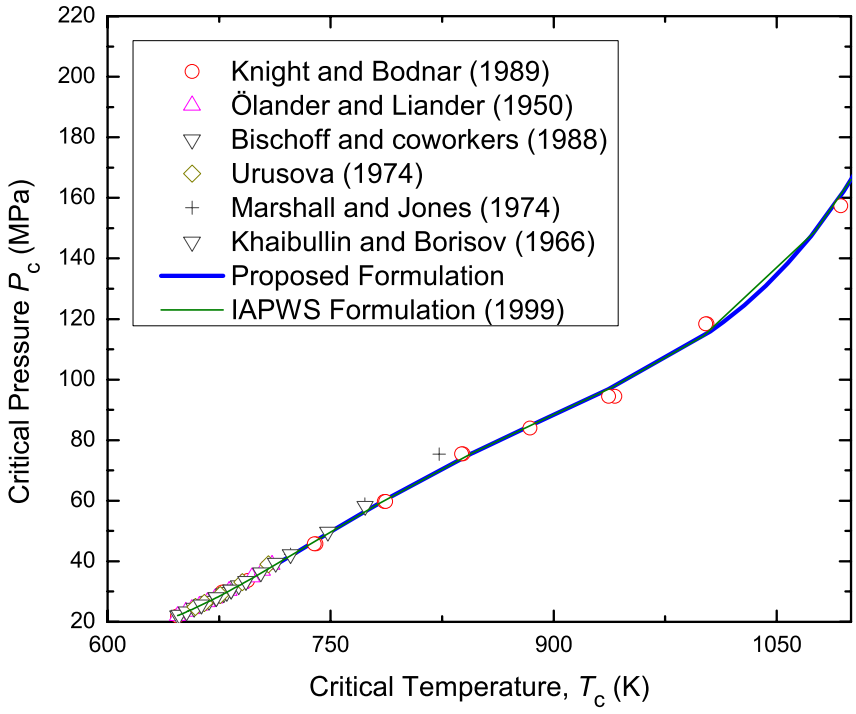

Figure 26. Comparison of proposed formulation and IAPWS for the critical pressure, P_c, vs. critical temperature, $T_c(x)$, for NaCl+H_2O solutions. The symbols indicate experimental data of Knight and Bodnar [32], Ölander and Liander [50], Bischoff and coworkers [33,51-52,56], Urusova [53], Marshall and Jones [54], and Khaibullin and Borisov [55]. The solid, thick blue curve represents values calculated from Eqs. 28 and 19. The solid, thin green curve represents values calculated from the equation of Povodyrev et al. [37].

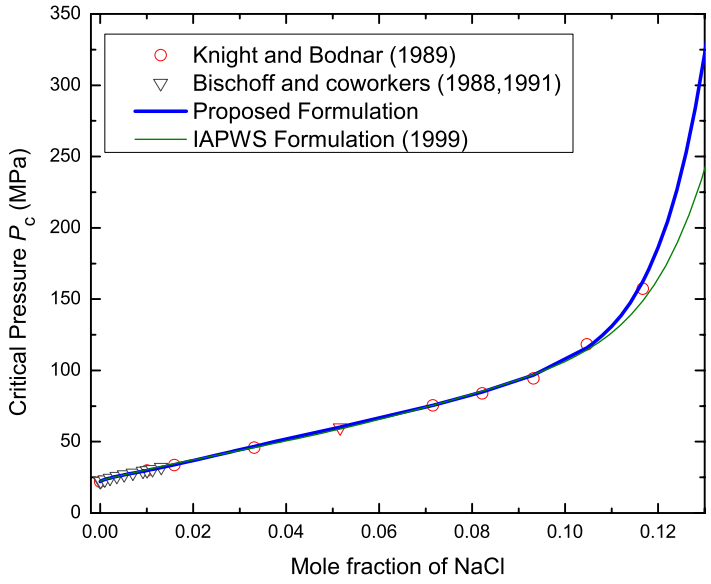

Figure 27. Comparison of proposed formulation and IAPWS for critical pressure, P_c, vs. mole fraction, x, for NaCl+H_2O solutions. The symbols indicate experimental data of Knight and Bodnar [32], and Bischoff and coworkers [33,51-52,56]. The solid, thick blue curve represents values calculated from Eqs. 28 and 19. The solid, thin green curve represents values calculated from the equation of Povodyrev et al. [37].

Section 6. Krichevskiĭ parameter for hot salty solutions

The theory based equation developed to describe the critical locus of NaCl and water can be used to calculate a new value for the Krichevskiĭ parameter. The Krichevskiĭ parameter, $\left(\frac{\partial P_c}{\partial x}\right)_{v,T}$, determines the change in pressure that occurs when

a solute is added to a solvent at its critical point. The thermodynamic relationship,

$$K_{\mathrm{Kr}} \equiv \lim_{x\to 0}\left(\frac{\partial P_{\mathrm{c}}}{\partial x}\right)_{v,T} = \left(\frac{dT_{\mathrm{c}}}{dx}\right)_{\mathrm{CL}}\left[\left(\frac{dP_{\mathrm{c}}}{dT}\right)_{\mathrm{CL}} - \left(\frac{dP}{dT}\right)_{\sigma}^{\mathrm{c}}\right], \tag{32}$$

where subscript CL denotes the critical line, relates the initial slopes of the critical line to the pure fluid vapor pressure. The term $\left(dP/dT\right)_{\sigma}^{\mathrm{c}}$ in the definition of the Krichevskiĭ parameter is the limiting slope of the vapor-pressure curve of the solvent at the critical point [78]. This parameter, K_{Kr}, is important in near-critical solution thermodynamics as it controls the difference between the behavior of the one-component fluid and that of the binary fluid mixture, controlling the shape of the dew-bubble curve and the qualitative critical behavior of the thermodynamic properties of dilute solutions in the supercritical fluids [79].

It is known that in dilute solutions the chemical potential, μ, of the solute is dominated by the logarithm of concentration as

$$\mu = k_{\mathrm{B}}T\ln x \to \lim_{x\to 0}\left(\frac{\partial \mu}{\partial x}\right)_{P,T} = \frac{k_{\mathrm{B}}T}{x} \to \infty \tag{33}$$

where x is the mole fraction of solute and k_{B} is the Boltzmann constant. However, at the mixture critical point $\left(\partial\mu/\partial x\right)_{P,T} = 0$, which in the infinitely dilute-solution limit appears to contradict to Eq. (33). This is the so-called critical-dilute-solution dilemma. This dilemma was resolved by Krichevskiĭ [79] who showed that the critical mixture condition and the dilute solution limit can be reconciled by taking into account the divergence of the isothermal compressibility at the critical point of the solvent. The thermodynamic expression for the derivative of solvent chemical potential with respect to concentration reads:

$$\left(\frac{\partial \mu}{\partial x}\right)_{P,T} = \frac{k_B T}{x} + \frac{\left(\partial P / \partial x\right)_{V,T}^2}{\left(\partial P / \partial V\right)_{T,x}} = 0 \,. \tag{34}$$

The inverse isothermal compressibility vanishes at the critical point of the pure solvent as

$$\left(\frac{\partial P}{\partial V}\right)_{T,x} \to -\frac{K_{\mathrm{Kr}}{}^2}{k_B T} x \tag{35}$$

where $K_{\mathrm{Kr}} = \left(\partial P / \partial x\right)_{V,T}^2$ at infinite dilution; thus the two conditions are never dilute if $\left(T - T_c\right)/T_c \le x$ [79,80,81].

The parameter K_{Kr} is one of the major thermodynamic quantities that control the behavior of supercritical-fluid solvents, as elucidated by Levelt Sengers [82,83]. It is commonly known as the Krichevskiĭ parameter [78]. This parameter, defined above, is largely responsible for controlling the high selectivity of the supercritical fluid solvent to fine variations of temperatures and pressures. In particular, the solute distribution between vapor (y) and liquid (x) is expressed through the Krichevskiĭ parameter as:

$$\ln \frac{y}{x} = \frac{K_{\mathrm{Kr}}}{\rho R T} \Delta \rho \tag{36}$$

with ρ as the density and R as the ideal gas constant.

Depending on the magnitude and the sign of the Krichevskiĭ parameter, the critical lines emanate from the critical point of the pure solvent into different direction as known in Fig. 28.

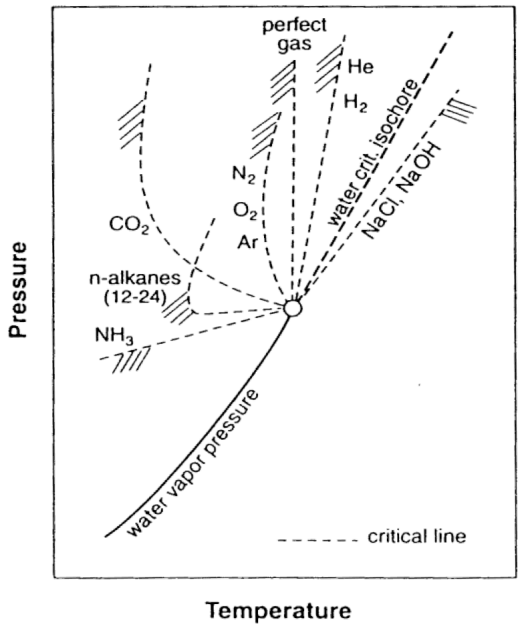

Figure 28. Critical lines emanating from the vapor-liquid critical point of water, projected on the $P - T$ phase diagram of water, reproduced from [84]. Those that move into the half plane below and to the right of the vapor pressure curve and its extension correspond to negative Krichevskiĭ parameters. Those that move into the upper half plane above and to the left of the vapor phase curve have positive Krichevskiĭ parameters.

Values reported in the literature for the Krichevskiĭ parameter of aqueous solutions have been reviewed by Anisimov et al. [85]. Because of cancellations when one evaluates the difference in slopes on the left-hand side of Eq. 32, which can also be written as

$$K_{\mathrm{Kr}} \equiv \lim_{x\to 0}\left(\frac{\partial P_{\mathrm{c}}}{\partial x}\right)_{v,T} = \lim_{x\to 0}\left[\frac{dP_{\mathrm{c}}}{dx} - \left(\frac{dP}{dT}\right)^{\mathrm{c}}_{\sigma}\frac{dT_{\mathrm{c}}}{dx}\right], \tag{37}$$

there is a considerable spread of values for K_{Kr} in the literature [78]. Moreover, we now see that the values found for the limiting slopes of the critical pressure and the critical temperature as a function of concentration may be affected by the presence of a confluent singularity proportional to $x^{3/2}$.

From the equations for the critical locus in the present paper, we find for a dilute aqueous solution of sodium chloride

$$K_{Kr} = -971 \text{ MPa} \tag{38}$$

Literature values for the Krichevskiĭ parameter of aqueous solutions are provided in Table 5 along with the calculated Krichevskiĭ parameter from our proposed crossover equation for NaCl+H_2O. Our value of $K_{Kr} = -971$ MPa is more negative than the previously reported from Kiselev or Abdulagatov [86], but more positive than that calculated from Povodryev's fit [34,37]. Nevertheless, the accuracy of the value of the Krichevskiĭ parameter given by Eq. 38, due to the cancellation between the two terms in Eq. 37, is still not better than ± 20%.

Table 5. Values of the Krichevskiĭ parameter for various aqueous solutions

Solute	K_{Kr} (MPa)
Sodium Chloride	-970 (calculated), -820 [37], -610 [86]
Heavy Water	0.43 [87]
Methane	160 [88], 150 [89], 81 [90], 100 [90]
Helium	170 [88], 167 [90], 163 [90]

The Krichevskiĭ parameter also determines the difference between the initial temperature dependence of the critical pressure of the solution and the limiting slope of the vapor-pressure curve and critical isochore of the solvent in the $P - T$ plane, as can be seen in Eq. 32, or upon multiplying Eq. 37 by $\left(dT_c / dx\right)^{-1}$. For the aqueous dilute solution of NaCl, this is shown in Fig. 29, which is a larger form of Fig. 2b. The negative value of K_{Kr} implies that the critical locus of the solution lies on the right-hand side of the critical isochore of H_2O in contrast to most non-electrolyte aqueous solutions [82,83].

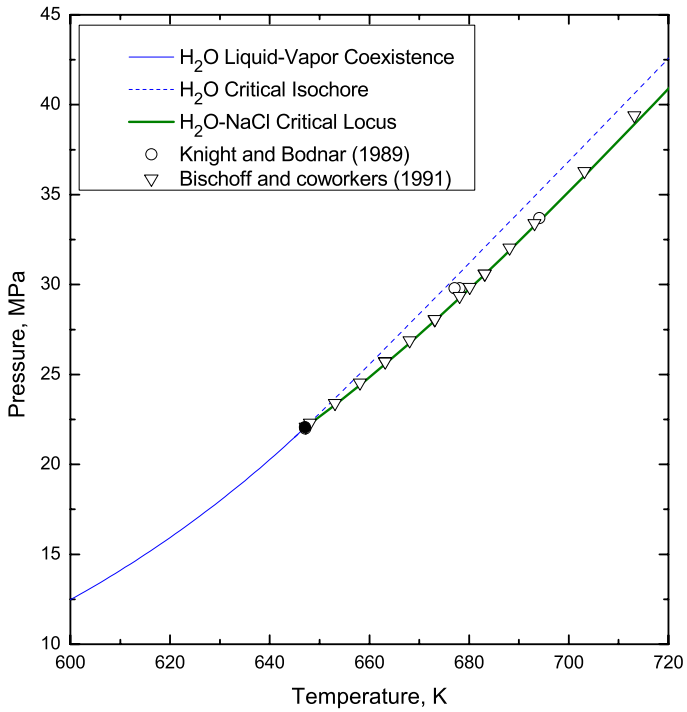

Figure 29. $P - T$ diagram of vapor pressure and critical isochore of H_2O [16,91] and critical locus of NaCl+H_2O solutions. Symbols are Knight and Bodnar [32] and Bischoff and coworkers [56].

Chapter 3: Supercooled water solutions and liquid water polyamorphism

While experimental data for liquid water behavior at stable temperatures and pressures are readily available, exhaustive experimental exploration of the behavior of supercooled liquid water is hampered by thermodynamic and kinetic limits of stability [92]. Yet, one of the most significant challenges is describing the behavior of supercooled liquid water.

Most liquids show no significant change in properties when driven into a metastable state and show no evidence of approaching a condition of impending loss of stability. In particular, the heat capacity and isothermal compressibility of most liquids do not increase anomalously below freezing temperatures. In fact, the response functions of most liquids decrease upon supercooling until freezing or vitrification occurs. Water, however, exhibits anomalous behavior with sharply increasing heat capacity, isothermal compressibility, and the magnitude of negative thermal expansivity upon supercooling [93]. The anomalous behavior of supercooled liquid water, Fig. 30, cannot be fully explained in terms of typical liquid behavior.

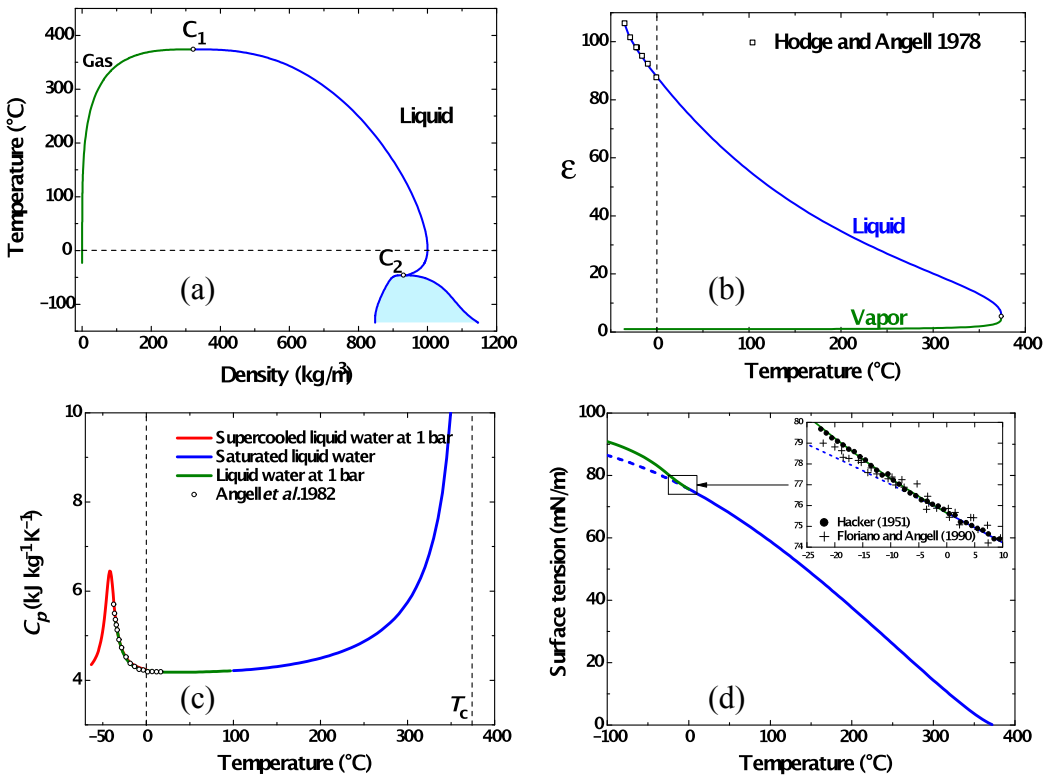

Figure 30. Thermodynamic properties of liquid water upon supercooling. Behavior of cold liquid water (a) density, (b) dielectric constant [94], (c) heat capacity [95], (d) surface tension [96,97], reproduced from [4]. (a) shows the location of the theorized second critical point in liquid water as C_2 and the liquid-vapor critical point as C_1.

The second-critical-point scenario of Poole *et al.* proposes the existence of a liquid-liquid critical point in supercooled water [98]. This scenario suggests the existence of two liquid states, characterized by high density/high entropy and low density/low entropy, and proposes that their coexistence curve terminates in a critical point. According to the second-critical-point scenario, liquid water at ambient temperature and pressure is a supercritical fluid, as the difference between two fluid phases disappears beyond the critical point and the fluid becomes homogenous.

In this chapter I present a global equation of state for supercooled water modified to account for the addition of solutes and discuss the implications of this model for the behavior of supercritical solutions. I proceed as follows. In Section 1, I discuss the role of the second critical point hypothesis in the development of a global equation of state to describe pure water in the supercooled region. In my work, published in Physical Review Letters [2] six years ago, and further developed by Bertrand et al. [3] and Holten et al. [4], I introduced the application of scaling theory to supercooled water in order to develop a scaled equation of state, based on the concept of critical point universality, and demonstrate the thermodynamic consistency of the second-critical-point scenario. This work was a starting point for further development in this field. Developing a global equation of state, our research group used a phenomenological mean-field "two-state" model and clarified the nature of the phase separation in a polyamorphic single-component liquid [3-4,99]. In Section 2, I show how this two-state model can be modified to incorporate the addition of a solute. Assuming the existence of the water liquid-liquid critical point, the addition of a solute generates critical lines emanating from the pure-water critical point. Because of the anomalous large value of change in pressure with respect to temperature for almost incompressible liquid water near the liquid-liquid critical point, the value of the Krichevskiĭ parameter, which largely determines the high selectivity of supercritical fluid solvent to fine variations of temperature and pressure, may be anomalously large even if the critical temperature weakly depends on the solute concentration. Physically, it means that even a very small addition of the solute may significantly affect the properties of cold water and aqueous solutions. Finally in

Section 3, I present different scenarios for phase behavior of supercooled aqueous solutions. Some solutes, such as glycerol, can prevent spontaneous crystallization, thus making liquid-liquid separation in supercooled water experimentally accessible. This work will help in resolving the question on liquid polyamorphism in supercooled water.

A note about liquid-liquid transitions

Liquid-liquid transitions and anomalies in the liquid state are not unique to water. Experimental or numerical support for a liquid-liquid transition exists for phosphorus, silicon, Y_2O_3-Al_2O_3, and other substances [100-106]. There is even some evidence suggesting a liquid-liquid transition in carbon [107].

Silicon, like water, forms tetrahedral structures and exhibits similar anomalous behavior, such as a liquid state with a higher density than the solid state, upon supercooling. First predicted by computer simulations and confirmed by first principle calculations, the liquid-liquid transition of silicon separates a high density liquid phase highly coordinated with metallic properties, much like normal liquid silicon, from a low density, low-coordinated and semi-metallic liquid phase, with a structure closer to that of solid silicon [108]. Liquid phosphorous also forms a tetrahedral geometry like water. While it lacks the hydrogen-bonded network of water, the tetrahedral shape of the molecular liquid phosphorous forms open spaces that can collapse with sufficient pressure, creating a higher density phase [109,110].

This “unmixing” of two liquid phases, as described above, is not typical for simple, single component fluids. The expected transition between fluid phases is that

of a vapor-liquid phase transition driven by the attractive forces between molecules, and characterized by an order parameter defined as the density difference between the two phases. However, liquid-liquid phase transitions are not prohibited by theory. Mishima and Stanley suggest a scenario for liquid-liquid phase separation based on the possibility of two minima in the intermolecular potential of a pure fluid [111]. This scenario would predict a second, liquid-liquid critical point in pure water driven by molecular interaction energy, just like the vapor-liquid critical point. Another possibility presented by Tu et al. depends on hydrogen-bond bending to drive a liquid-liquid transition [112].

In general, however, liquid-liquid transitions can be considered in the context of liquid polyamorphism. For the purpose of thermodynamic modeling, we leave the specifics of the molecular interactions to speculation, and focus instead on the phenomenology of the liquid-liquid transition in water. This allows us to make a determination of the nature of the order parameter for a hypothesized second critical point in liquid water, and explore the idea of an entropy-driven fluid phase transition in contrast to the more typical density driven transition expected for the transition from vapor to liquid. The justification for this entropy driven phase separation is discussed further in Section 2.

Section 1. Peculiar thermodynamics of the liquid-liquid critical point in supercooled water

Section 2.3 of Chapter 2 introduced the concept of complete scaling as it applied to the critical behavior of the vapor-liquid critical point of hot water. I used this theory to show the analytic dependence of critical pressure on the critical temperature for aqueous salt solutions, and to show how the non-analytic concentration dependence of the critical temperature implied a non-analytic concentration dependence of the critical pressure. In this section, I return to complete scaling, developing a model based on the universality of critical phenomena, to show how the hypothesized second critical point of liquid water is consistent with theory and can accurately predict the available experimental data. This work was the basis of further developments, and in Section 1.2 and 2.1 of this chapter I describe a two-state model, based on the insights explored here, and show how this work was an important step in the development of a phenomenological model to describe the behavior of aqueous, supercooled solutions.

Subsection 1. Scaled parametric equation of state for supercooled liquid water

It is commonly accepted that the critical behavior of all fluids, simple and complex, belongs to the universality class of the three-dimensional Ising model [74]. Water is not an exception [113]. Near the critical point the critical (fluctuation-

induced) part, h_3, of an appropriate field- dependent thermodynamic potential is a universal function of two scaling fields, ‘‘ordering,’’ h_1, and ‘‘thermal,’’ h_2 [74]:

$$h_3 = |h_2|^{2-\alpha} f^{\pm}\left(\frac{h_1}{|h_2|^{\beta+\gamma}}\right) \tag{39}$$

To apply the universal expression, Eq. (38), for describing the liquid-liquid critical point in supercooled water, we assume the scaling fields are analytical combinations of physical fields, the pressure *P*, the temperature *T*, and the chemical potential μ [98]

$$h_1 = \Delta\hat{T} + a'\Delta\hat{P}, \tag{40}$$

$$h_2 = -\Delta\hat{P} + b'\Delta\hat{T}, \tag{41}$$

$$h_3 = \Delta\hat{P} - \Delta\hat{\mu} + \Delta\hat{\mu}^r \tag{42}$$

with $\Delta\hat{T} = \frac{T - T_c}{T_c}$, $\Delta\hat{P} = \frac{(P - P_c)V_c}{RT_c}$, $\Delta\hat{\mu} = \frac{\mu - \mu_c}{RT_c}$. In Eq. (40), a' represents the slope $-d\hat{T}/d\hat{P}$ of the phase coexistence or Widom line at the critical point. In Eq. 41, b' is a so-called mixing coefficient, which accounts for the fact that the critical phase transition in supercooled water is not completely symmetric in terms of the entropy order parameter. Introduction of mixing of this type is also known in the literature as the revised-scaling approximation.

As far as the physical fields are mixed into the scaling fields, the physical properties, such as the isobaric heat capacity C_P, the isothermal compressibility κ_T, and the thermal expansivity α_P, will not exhibit universal power laws when measured along isotherms or isobars; instead, their apparent behavior will be

determined by a thermodynamic path and by the values of the mixing coefficients in Eqs. 40 and 41. As follows from Eqs. 40 and 41, the critical (fluctuation-induced) parts of the dimensionless isobaric heat capacity, isothermal compressibility, and thermal expansivity are expressed through the scaling susceptibilities [98]

$$\hat{C}_P = \hat{T}\left(\frac{\partial \hat{S}}{\partial \hat{T}}\right)_P = \hat{T}\left[\chi_1 + (b')^2 \chi_2 + 2b'\chi_{12} - \Delta\hat{\mu}^r_{\hat{T}\hat{T}}\right], \tag{43}$$

$$\hat{\kappa}_T = -\left(\frac{\partial \hat{V}}{\partial \hat{P}}\right)_T = \frac{1}{\hat{V}}\left[(a')^2 \chi_1 + \chi_2 - 2a'\chi_{12} - \Delta\hat{\mu}^r_{\hat{P}\hat{P}}\right], \tag{44}$$

$$\hat{\alpha}_V = \frac{1}{\hat{V}}\left(\frac{\partial \hat{V}}{\partial \hat{T}}\right)_P = \frac{1}{\hat{V}}\left[-a'\chi_1 + b'\chi_2 + (1 - a'b')\chi_{12} + \Delta\hat{\mu}^r_{\hat{T}\hat{P}}\right], \tag{45}$$

where the subscript $\hat{P}$ indicates a derivative with respect to $\hat{P}$ at constant $\hat{T}$, and the subscript $\hat{T}$ indicates a derivative with respect to $\hat{T}$ at constant $\hat{P}$.

Representing the scaling fields and scaling susceptibilities as functions of the "polar" variables, *r* and θ, relates the singularities in the thermodynamic functions to the variable *r*, the distance from the critical point, while the properties are analytical with respect to θ, which measures the location on a contour of constant *r*. This results in a "linear model" scaled parametric equation of state:

$$h_1 = ar^{\beta+\gamma}\theta\left(1-\theta^2\right),\ h_2 = r\left(1-b^2\theta^2\right), \tag{46}$$

$$\chi_1 = \frac{k}{a}r^{-\gamma}c_1(\theta),\ \chi_{12} = kr^{\beta-1}c_{12}(\theta),\ \chi_2 = akr^{-\alpha}c_2(\theta) \tag{47}$$

where a and k are system dependent amplitudes, while b^2 is approximated as $b^2 \simeq 1.361$ [43] in the "restricted" linear model [114]. The analytic functions $c(\theta)$ are calculated in the reference [115]. The order parameter, ϕ_1, is of the form

$\phi_1 = kr^{\beta} M(\theta)$, where $M(\theta)$, a universal analytic function of θ, can be calculated from renormalization group theory of critical phenomena [116], with the simplest approximant $M(\theta) = \theta$ [117].

This model, as shown in Fig. 31, offers a consistent scaling description of the available experimental data in supercooled water. In addition, this model identified features of the hypothesized liquid-liquid separation that would become the basis for the development of a global equation of state for supercooled water.

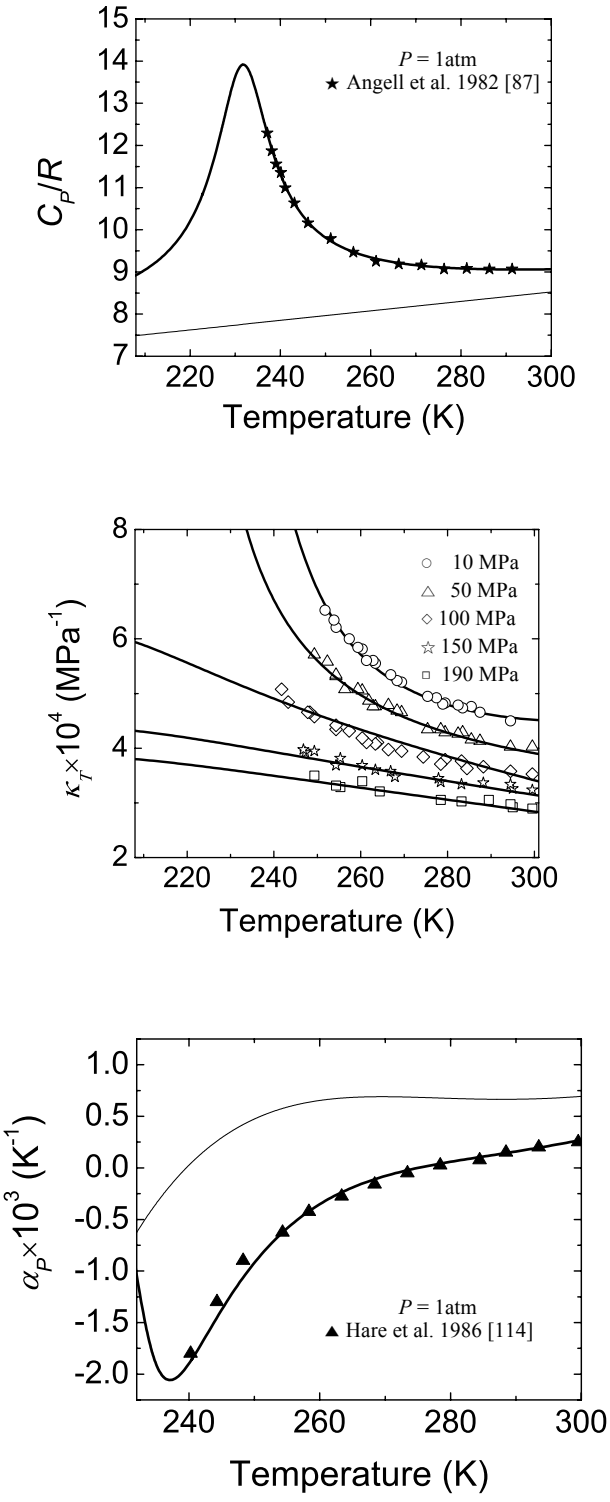

Figure 31. Head capacity, compressibility, and expansivity predicted by the scaling theory model [2]. Solid lines generated from the scaled parametric equation of state.

Data points are experimental data for heat capacity [95], compressibility [118], and expansivity [119].

Two features make the second critical point in water phenomenologically different from the well-known vapor-liquid critical point. The negative slope of the liquid-liquid phase transition line in the *P*-*T* plane means that high-density liquid water is the phase with larger entropy. The relatively large value of this slope at the critical point (about 25 times greater than for the vapor-liquid transition at the critical point) indicates the significance of the entropy change relative to the density change, and, correspondingly, the importance of the entropy fluctuations. These features suggest that liquid-liquid phase separation in water is mostly driven by entropy rather than by energy. In Fig. 32, I show the relations between theoretical scaling fields and physical fields in two physically difference cases, the vapor-liquid critical point and the liquid-liquid critical point.

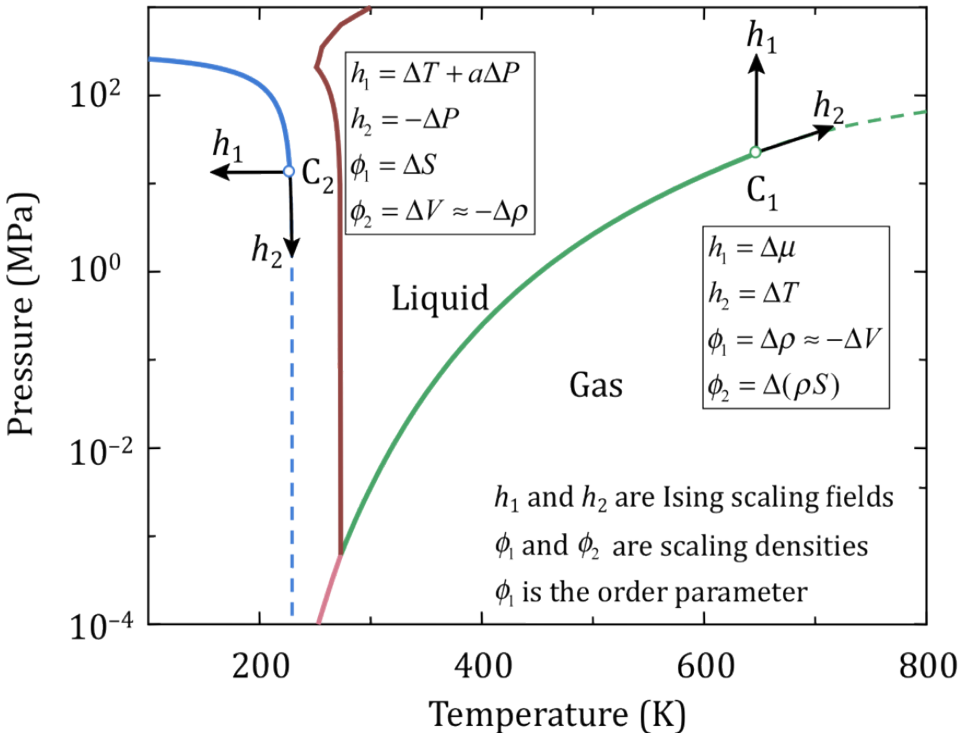

Figure 32. *P-T* phase diagram for pure water showing features suggesting the relationship between theoretical scaling fields and physical fields for the vapor-liquid critical point (discussed in Ch.2, Sec.2.3) and the liquid-liquid critical point (discussed in Ch.3, Sec.1.1)

This model has since been further developed by Bertrand et al. [3] and Holten et al. [4] and the latest description of the available experimental data is shown in Fig. 32 [99]. The location of the critical point and the system-dependent amplitudes was optimized using high-resolution experimental heat-capacity data [120-122,95], expansivity data [123-124,119], compressibility data [125-126,118], density data [123,125,127], and speed-of-sound data [128-132], as well as the most recent estimate of the liquid-liquid phase transition curve given by Kanno and Angell [118] and Mishima [125], the coefficients $\alpha = 0.1100$, $\beta = 0.3265$ [28], the molar mass of

H_2O [16], an ideal-gas constant R [133], and molar mass of D_2O [134], with $b' = 0$. The parameters for the model, defined in [4,99], correspond to a critical pressure of $P_c = 27.5$ MPa and $T_c = 224.23\,\mathrm{K}$ for H_2O, and $P_c = 32.29$ MPa and $T_c = 232.65\,\mathrm{K}$ for D_2O [4].

Subsection 2. Two-state model for supercooled water

As the first step to understand a relation between the water polyamorphism and the behavior of cold aqueous solutions, members of our research group develop and elaborate on a phenomenological mean-field "two-state" model that clarifies the nature of the phase separation in a polyamorphic single-component liquid [4,99]. Two-fluid state models trace their lineage back to a 19th century paper by Röntgen [135]. Relatively recently, Ponyatovskiĭ et al. [136] and, more quantitatively, Moynihan [137] have nicely described the emergence of a liquid-liquid critical point in supercooled water as resulting from the effects of nonideality in a mixture of two "components", the concentration of which is controlled by thermodynamic equilibrium. However, while Moynihan assumed a "regular-solution" type of nonideality, which implies an energy-driven phase separation, such as the vapor-liquid transition or the conventional liquid-liquid transition in binary solutions, I utilize a near "athermal-solution" type of nonideality. This "athermal" nonideality is mainly responsible for the entropy-driven phase separation in metastable water near the liquid-liquid critical point.

Let us assume that liquid water is a "mixture" of two states, A and B, of the

same molecular species. For instance, these two states could represent two different arrangements of the hydrogen-bond network in water and correspond to the low-density and high-density states of water. The fraction of water molecules, involved in either structure, denoted ϕ for state A and $1-\phi$ for state B, is controlled by thermodynamic equilibrium between these two structures,

$$\mathrm{A} \rightleftharpoons \mathrm{B}\,. \tag{48}$$

Unlike a binary fluid, the fraction ϕ is not an independent variable, but is determined as a function of pressure P and temperature T from the condition of thermodynamic equilibrium. The simplest "athermal solution model" [114] predicts symmetric liquid-liquid phase separation for any temperature, with the critical fraction $\phi_c = 1/2$, if the interaction parameter, which controls the excess (non-ideal) entropy of mixing, is higher than its critical value. However, unlike an athermal non-ideal binary fluid, the entropy-driven phase separation in a polyamorphic single-component liquid does not happen at any temperature. Contrarily, the critical temperature, T_c, is to be specified through the temperature dependence of the equilibrium constant K by

$$\ln K = \lambda\left(\frac{1}{T} - \frac{1}{T_c}\right), \tag{49}$$

where λ is the heat (enthalpy change) of "reaction" between A and B. A finite slope of liquid-liquid coexistence in the P-T plane can be incorporated into the two-state lattice liquid model if one assumes that the Gibbs energy change of the "reaction" also depends on pressure.

For a mixture with two states, A and B, the Gibbs energy per molecule is the sum of contributions from both states,

$$G = \left(1-\phi\right)\mu^{\mathrm{A}} + \phi\mu^{\mathrm{B}} = \mu^{\mathrm{A}} + \phi\mu^{\mathrm{BA}} \tag{50}$$

where μ^{A} and μ^{B} are chemical potentials of A and B in the mixture and $\mu^{\mathrm{BA}} \equiv \mu^{\mathrm{B}} - \mu^{\mathrm{A}}$. In an athermal, non-ideal mixture of A and B, the Gibbs energy of solution is

$$\frac{G}{k_{\mathrm{B}}T} = \frac{G^{\mathrm{A}}}{k_{\mathrm{B}}T} + \phi\frac{G^{\mathrm{BA}}}{k_{\mathrm{B}}T} + \phi\ln\phi + \left(1-\phi\right)\ln\left(1-\phi\right) + \omega\phi\left(1-\phi\right), \tag{51}$$

and the chemical potential difference is

$$\mu^{\mathrm{BA}} = G^{\mathrm{BA}} + k_{\mathrm{B}}T\left[\ln\frac{\phi}{1-\phi} + \omega\left(1-2\phi\right)\right], \tag{52}$$

where $G^{\mathrm{BA}} \equiv G^{\mathrm{B}} - G^{\mathrm{A}}$ is the difference between pure states A and B, the $\phi\ln\phi + (1-\phi)\ln(1-\phi)$ term is the ideal entropy of mixing, and $\omega\left(P\right)\phi(1-\phi)$ is the non-ideal entropy component [99]. This non-ideal term, $\omega\phi\left(1-\phi\right)$, is characterized by an interaction parameter $\omega\left(P\right)$, dependent on pressure but not temperature, and defined through $\omega = 2 + \omega_0\Delta\hat{P}$.

In this model, we can consider ϕ an extent of reaction [138] and the condition of chemical reaction equilibrium,

$$\left(\frac{\partial G}{\partial\phi}\right)_{T,P} = \mu^{\mathrm{BA}} = 0\,. \tag{53}$$

The difference between the Gibbs energy of the pure states, A and B, is related to the

equilibrium constant of reaction,

$$\frac{G^{\mathrm{BA}}}{k_{\mathrm{B}}T} = \ln \mathrm{K} \,. \tag{54}$$

Through this relationship, the finite slope of liquid-liquid coexistence in the *P*-*T* plane, defined along $\ln \mathrm{K} = 0$, can be incorporated into the two-state lattice liquid model if one assumes that the Gibbs energy change of the "reaction" also depends on pressure, and our fraction of state A becomes an extent of reaction.

The condition of chemical reaction equilibrium also determines the equilibrium fraction, ϕ_{e},

$$\ln \mathrm{K} + \ln \frac{\phi_{\mathrm{e}}}{1-\phi_{\mathrm{e}}} + \omega\left(1-2\phi_{\mathrm{e}}\right) = 0 \,. \tag{55}$$

The athermal, two-state model equation of state for supercooled water is this equilibrium fraction and the Gibbs energy expression in Eq. 51.

A regular solution model, where the interaction parameter determined the critical temperature, would take a slightly different form, namely

$$\frac{G}{k_{\mathrm{B}}T} = \frac{G^{\mathrm{A}}}{k_{\mathrm{B}}T} + \phi\frac{G^{\mathrm{BA}}}{k_{\mathrm{B}}T} + \phi\ln\phi + (1-\phi)\ln(1-\phi) + \left[\omega\phi(1-\phi)\right] / k_{\mathrm{B}}T \,. \tag{56}$$

However, the thermal field for supercooled water is not temperature, but pressure. Thus, the use of the athermal solution model shown in Eq. 51. This entropy driven phase separation, where the interaction parameter, ω, defined above, determines the critical pressure, $\omega\left(P\right) = 2$ at $P = P_{\mathrm{c}}$.

The excess entropy of mixing of the two states is given as

$$S^{\mathrm{E}} = \omega\phi\left(1-\phi\right). \tag{57}$$

The positive excess entropy of mixing means that the liquid-liquid separation is driven by the non-ideal entropy contribution to the Gibbs energy. Physically, it means that the number of possible configurations of each state is larger, when the two states are unmixed, than in the homogeneous solution of these two states. In the athermal solution, the enthalpy of mixing is zero and thus energy does not drive the phase separation.

The regular, background properties are defined through the definition of the pure state, G^{A}. The critical pressure is defined through the interaction parameter, and the critical temperature is defined through the reaction equilibrium constant. Figure 33 shows the athermal two state model representation of the experimental data for supercooled water.

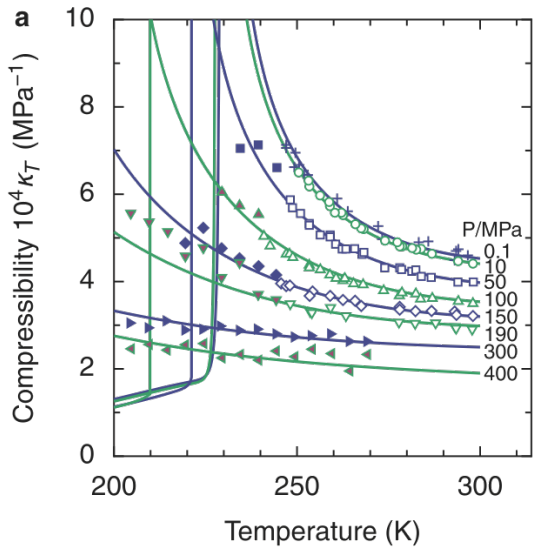
a
Compressibility $10^4 \kappa_T$ (MPa^{-1})
Temperature (K)
P/MPa
0.1
10
50
100
150
190
300
400

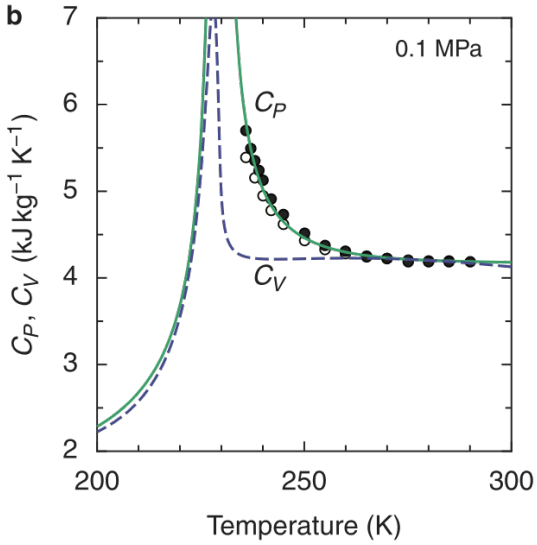
b
C_P, C_V (kJ kg^{-1} K^{-1})
Temperature (K)
0.1 MPa
C_P
C_V

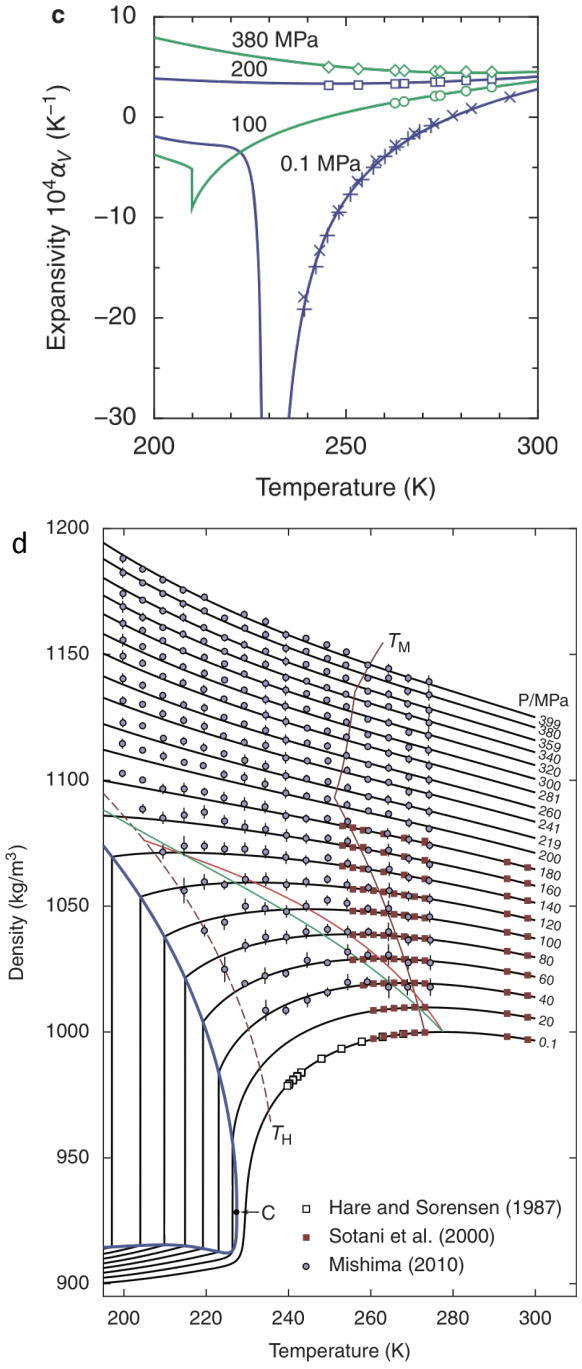

Figure 33. Response functions predicted by the athermal two-state model for liquid water shown in Eq. 51, reproduced from [99]. (a) Isothermal compressibility [125-126,118]. (b) Heat capacity at constant pressure C_P (open circles: data from Archer and Carter [122], closed circles: data from Angell et al. [95] and at constant volume

C_V (calculated) at 0.1 MPa. (c) Thermal expansivity [123-124,119]. In a, b, and c, the curves are the prediction of the crossover two-state model, and the symbols represent experimental data. (d) Density [123,127,125]

While Fig. 33 shows excellent agreement with the experimental data using this model, it is important to note that optimization of the critical point does not produce a single most likely point, but rather a narrow band in the $P - T$ diagram suggesting an area where the critical point is likely to be found. The best fit for the critical point is obtained at about 227 K and 13 MPa, with $\lambda = 2.3$ and $\omega_0 = 0.35$ [99]. The range of likely locations for the hypothesized critical temperature is shown in Fig. 34.

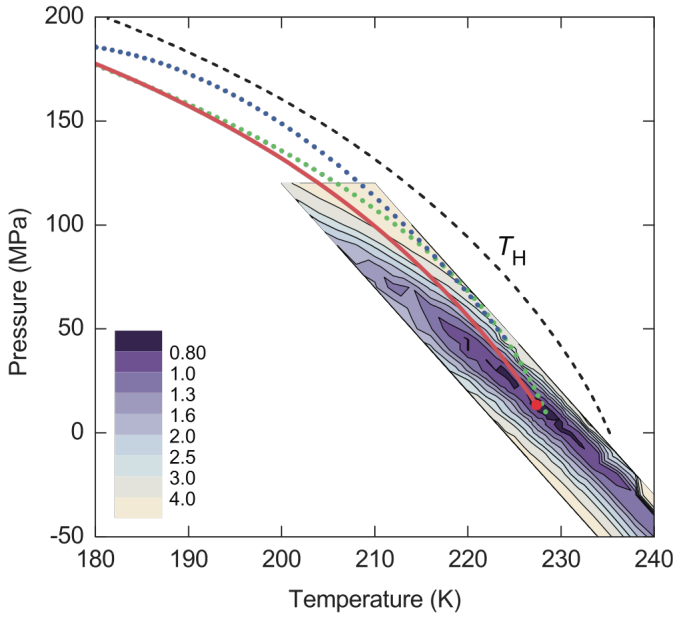

Figure 34. Optimization of the LLCP location, reproduced from [99]. The colored map shows the reduced sum of squared residuals, where dark areas correspond with

potential locations of the liquid-liquid critical point with higher optimized fits to experimental data. The solid red line is the hypothesized LLT curve. The dashed curve shows the temperature of homogeneous ice nucleation, T_H [139]. The blue dotted curve is the LLT suggestion by Mishima [125] and the green dotted curve is the 'singularity' line suggested by Kanno and Angell [118].

My work [2], shown in Section 1.1 of this chapter, was the first attempt to develop an equation of state for supercooled water, based on the assumption that the LLCP exists, and on the asymptotic theory of critical phenomena [74,75]. This work was further elaborated and clarified by Bertrand and Anisimov [3]. In particular, both works estimated the LLCP critical pressure below 30 MPa, much lower than most of simulated water-like models predicted. Holten et al. [4,99] used the same asymptotic equation of state, also in a mean-field approximation [140], but introduced the noncritical backgrounds of thermodynamic properties in a thermodynamically consistent way. The resulting correlation represents all available experimental data for supercooled water, H_2O and D_2O, within experimental accuracy.

This two state model addressed the concern regarding the application of the asymptotic theory to a broad range of temperatures and pressures including the region far away from the assumed critical point. Such an extension makes the description of experimental data inevitably semi-empirical since all non-asymptotic physical features are absorbed by the adjustable backgrounds of thermodynamic properties. This fact led to crossover formulation of the two-state model, to create a closed-form theoretically-based equation of state which would satisfy the asymptotic critical

anomalies and, at the same time, describe regular behavior far away from the critical region. Figure 35 shows the differences in density between a mean-field and a crossover formulation for the two-state model.

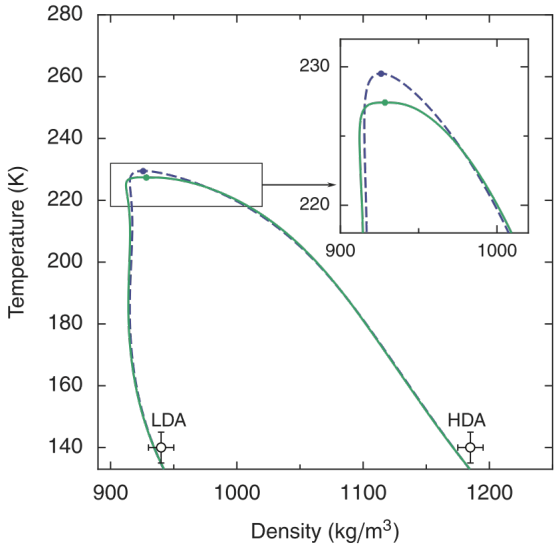

Figure 35. Density along the liquid–liquid transition curve, reproduced from [99]. The dashed line represents the mean-field two-state model; the solid line represents the crossover two-state model. The open circles are the densities of the low- density amorphous (LDA) and high-density amorphous (HDA) phases of water at 200 MPa [141]. One can notice that the crossover LLT curve is flatter than the LLT curve in the mean-field approximation and that the actual position of the critical point is shifted to a lower temperature by critical fluctuations.

Although we can speculate on the molecular basis for an entropy-driven phase transition for supercooled water, a microscopic model for water would clarify the microscopic order parameter. To explore this further, the fraction, ϕ, obtained from the two-state model, is compared with an equivalent fraction obtained in simulations of the mW model [142]. Both results show similar temperature dependence, which is in sharp contrast to the almost linear function of temperature for an ideal solution, Fig. 36.

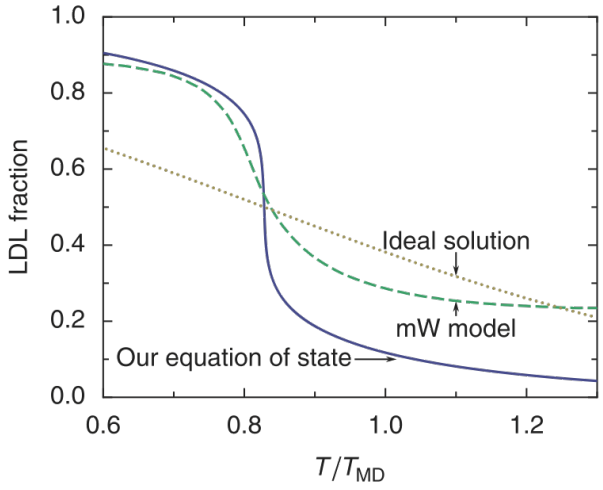

Figure 36. Fraction of molecules in a low-density state for the two-state model, for the mW model, and for an ideal solution, reproduced from [99]. The fraction ϕ is shown for the two-state model at 0.1 MPa, in the case of an athermal solution (solid) and an ideal solution (dotted). The dashed curve is the fraction of four-coordinated water molecules, i.e., the fraction of water molecules with four neighbours, for mW water simulations performed by Moore and Molinero [142]. The temperature is scaled by the temperature of maximum density (250 K for the mW model and 277 K for real water).

It is important to note that the two-state model presented here shares key features with the scaled parametric equation of state [2], namely the role of entropy in the phase separation of the two liquid phases. These features, first identified in my Physical Review Letters publication, are a first step to understanding the behavior of cold aqueous solutions.

Section 2. Cold and super-cold water as a novel supercritical-fluid solvent

Unlike ordinary substances, one can regard water near the triple point and in the supercooled region, on one side, and water near the vapor-liquid critical point, on the other side, as "the same substance – two different liquids". Highly-compressible, low-dielectric-constant near-critical water is commonly used as a supercritical-fluid solvent. On the low-temperature side of the phase diagram, water is an almost incompressible, high-dielectric-constant solvent with some anomalous properties (Fig. 30). The peculiar thermodynamics of the metastable liquid-liquid critical point have important practical consequences, in particular, for the behavior of aqueous solutions at low temperatures, because supercooled liquid water can be regarded as a specific "supercritical fluid".

Although aqueous solutions at ambient conditions have been studied extensively, a clear fundamental understanding of the properties of supercooled aqueous solutions is still not obtained. Recently a number of computational and theoretical works on aqueous supercooled solutions have been reported in the

literature. Archer and Carter [122] measured the heat capacity of pure water and aqueous NaCl solutions at ambient pressures and temperatures down to 236 K (for pure water) and down to 202 K (for NaCl solutions). They observed that for small NaCl concentrations, upon lowering the temperature, the heat capacity increases in the supercooled region. As the salt concentration is increased, this anomalous rise in heat capacity moves to lower temperatures and disappears for salt concentrations greater than 2 mol/kg. Recent molecular dynamic simulations in aqueous NaCl solutions by Corradini et al. [143] corroborate these experimental findings. Their molecular dynamic simulations also show that as the salt concentration is increased the temperature of maximum density is shifted to lower temperature values. The same effect was observed upon increasing the pressure in supercooled aqueous NaCl solutions [144-146]. In addition, Mishima [147] has concluded that the nucleation in supercooled aqueous LiCl solution occurs in two stages: the appearance of the low-density-liquid-like state and then crystallization. By studying supercooled aqueous solutions of various alcohols and sugars, Miyata and Kanno [148] showed that the homogeneous nucleation temperatures in the solutions were much lower than in supercooled water, thus enabling one to perform experiments in deeper supercooled conditions (Fig. 37).

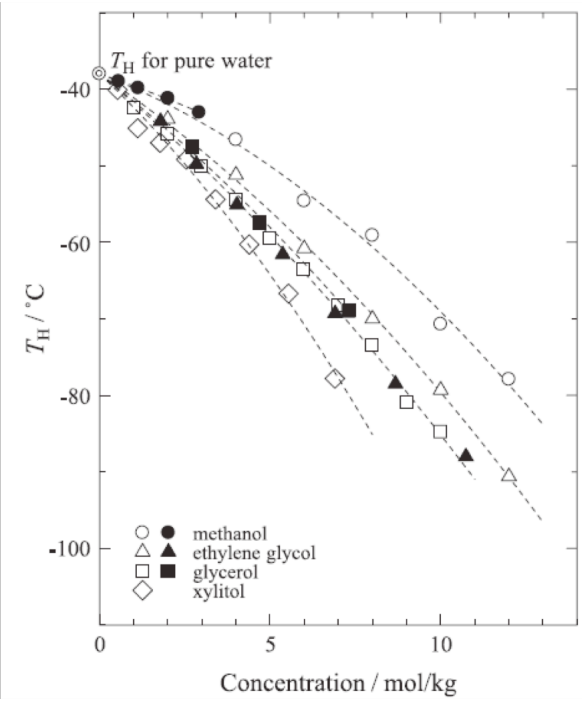

Figure 37. Depression of the homogeneous ice nucleation temperatures (T_H) in aqueous alcohol solutions at ambient pressure, reproduced from [74].

Here, I explore the anomalous behavior of supercooled water through theoretical investigation of aqueous solutions well below the freezing point of pure water. If the water liquid-liquid critical point exists, the addition of a solute will generate critical lines emanating from the pure-water critical point. The phenomenon would be conceptually similar to what is known near the vapor-liquid critical point and what is commonly exploited in supercritical-fluid science and technology. This idea has not previously been elaborated upon.

Subsection 1. Including solutes in the two-state model for supercooled water

The concept of the second critical point in water raises an intriguing possibility to consider cold water as a novel supercritical solvent. Here, we modify the two-state model developed as a global equation of state for cold water, to include the addition of solutes.

Recalling from Eq. 51, in an athermal, non-ideal mixture of A and B, the Gibbs energy of solution is

$$\frac{G}{k_{\mathrm{B}}T}=\frac{G^{\mathrm{A}}}{k_{\mathrm{B}}T}+\phi\frac{G^{\mathrm{BA}}}{k_{\mathrm{B}}T}+\phi\ln\phi+\left(1-\phi\right)\ln\left(1-\phi\right)+\omega\phi\left(1-\phi\right),$$

where the interaction parameter $\omega\left(P\right)$ determines the critical pressure, the difference between the Gibbs energy of the pure states, $\frac{G^{\mathrm{BA}}}{k_{\mathrm{B}}T}=\ln\mathrm{K}=0$ from Eqn. (54) determines the critical temperature, and the regular, background properties are defined through the pure state, G^{A}. This two-state model can incorporate the addition of solutes by taking into account the activity of the chemical species in solution.

The activity, ζ, of a chemical species in solution is a measure of effective concentration and is related to the chemical potential through

$$\zeta=\exp\left(\frac{\mu^{*}-\mu_{o}}{k_{\mathrm{B}}T}\right). \tag{58}$$

For real solutions, it takes the place of concentration in the definition of the reaction equilibrium constant, K. In order to include solvents in the two-state model for

supercooled water, we define our interaction parameter for solutions as $\omega(P,\zeta)$, and our equilibrium constant, which defines our critical temperature, becomes

$$\ln \mathrm{K} = \lambda\left(\Delta T + a\Delta P + b\Delta T\Delta P\right). \tag{59}$$

In this way both the critical temperature and critical pressure are functions of the activity, ζ, such that

$$\ln \mathrm{K}(T) = f\left[T_{\mathrm{c}}(\zeta), P_{\mathrm{c}}(\zeta)\right]. \tag{60}$$

We see from Eqn. 60 that for the two-state model for aqueous solutions there are four permutations for the effect of a solute on the critical parameters of an aqueous solution. The activity of the solute could increase both the critical temperature and critical pressure; the activity could decrease both the critical temperature and critical pressure; the activity could increase the critical temperature but decrease the critical pressure; or the activity could increase the critical pressure but decrease the critical temperature. In this way the model allows for complete flexibility for the effect of a solute on the critical parameters of the pure fluid. It should be noted that at constant ζ, we have an isomorphic equation of state, which simplifies for binary liquid solutions to the same form as for the pure solvent.

As the first step to understand a relation between the water polyamorphism and the behavior of cold aqueous solutions, this two-state model modified by the solute activity elaborates on the phenomenological mean-field two-state model for pure water. Upon the addition of a solute, a critical line emerges from the liquid-liquid critical point of the pure fluid. The shift of the critical temperature will mainly be controlled by the change in the equilibrium constant K, while the shift in the critical

pressure will mainly depend on the change in the interaction parameter which controls the non-ideality of the two-state model.

Subsection 2. Generalization of the Krichevskiĭ parameter

The concept of the Krichevskiĭ parameter can be generalized to supercooled water solutions if metastable water possesses a liquid-liquid critical point. Depending on the response of the suggested two states of metastable water to a particular solute, the critical lines would emanate from the liquid-liquid critical point of pure water toward different regions in the *P*-*T* space as shown in Fig. 38.

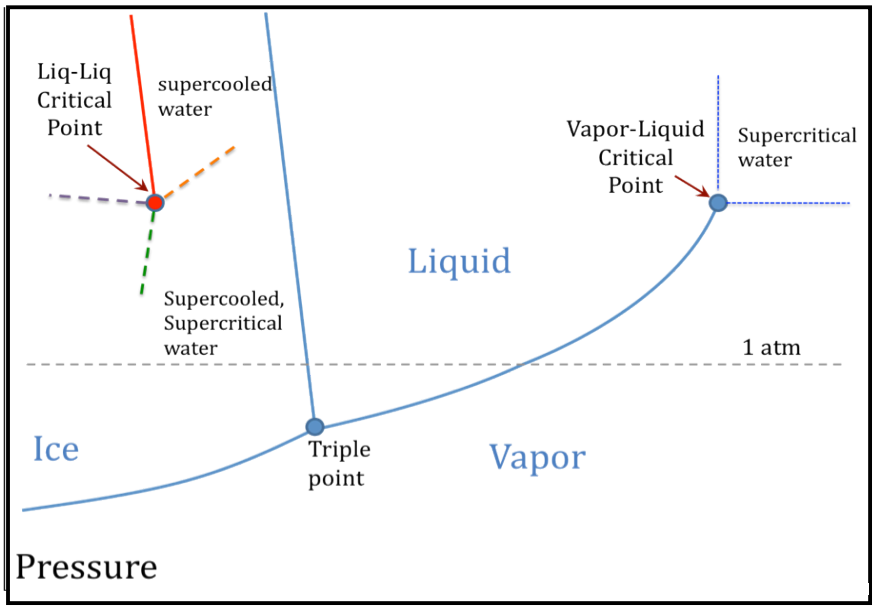

Figure 38. Hypothetical critical lines (dashed orange, green, purple) for aqueous solutions emanating from the liquid-liquid critical point of metastable water. Solid blue curves are phase transition lines for pure water.

The critical lines shown by dotted and dotted-dashed curves have particularly large values of the Krichevskiĭ parameter. Because of the anomalously large value of the derivative for almost incompressible liquid water near the liquid-liquid critical point, in accordance with Eqs. 32 and 37, the value of the Krichevskiĭ parameter may be very large even if the critical temperature weakly depends on the solute concentration. Physically, it means that even a very small addition of the solute may significantly affect the properties of cold water and aqueous solutions.

Chatterjee and Debenedetti theoretically investigated the binary fluid-phase behavior of mixtures in which one water-like component can have two critical points [149]. They considered three equal-sized non-polar solutes that differ in the strength

of their dispersive van der Waals-like interactions. They generally found five different critical lines. One of the lines always emanates from the liquid-liquid critical point of the pure solvent. Their study suggests the possibility of an experimentally accessible manifestation of the existence of a second critical point in water through investigating dilute aqueous solutions.

The proposed two-state model can be used to perform a similar analysis.

Section 3. Suggested phase diagrams for supercooled solutions

In this section, we evaluate the indirect evidence in support of a liquid-liquid critical point as it relates to solutions of supercooled water.

Some of the most promising experiments in supercooled aqueous solutions to date have been conducted by Mishima [150] with metastable ice. Along the melting line, ice is stable with respect to liquid water, Fig. 39. Upon decompression, high-pressure ice along a melting line will cool into the metastable region. Upon phase transformation, this ice, metastable with respect to liquid water, will transition to a liquid prior to freezing in the stable form of ice for that temperature and pressure [151]. Using this technique, Mishima decompressed high-pressure ice beyond the ice homogeneous nucleation limit. Since the ice homogeneous nucleation limit is a kinetic limit of stability for supercooled liquid water, it plays no role in the limits of supercooling for various phases of ice. Mishima found that at a point just past this homogeneous nucleation limit, the slope of the temperature change upon

decompression sharply altered. Since the ice was metastable with respect to the liquid phase, the one explanation for this phenomena is the phase transition line separating two distinct phases of liquid water [150].

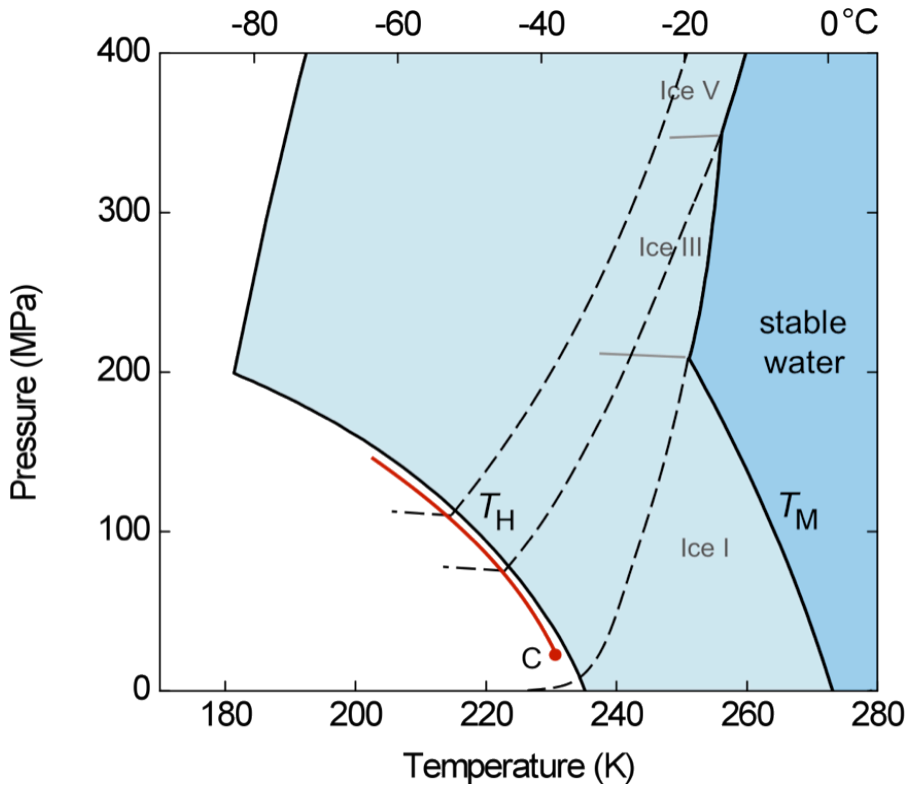

Figure 39. Decompression of ice IV, V and ice III (dashed lines) suggesting a liquid-liquid transition line in supercooled liquid water [150].

As can be seen in Fig. 39, the sharp change in slope of decompressed metastable ice IV (left-most dashed line) and that of ice V, suggests an intersection with the liquid-liquid transition line. However, the smooth change in slope seen by

decompression of metastable ice III suggests that the critical point would exist somewhere between these two lines.

Mishima also carried out similar experiments using a 4.8% solution of aqueous lithium chloride [152]. These experiments show that the addition of an ionic solute, lithium chloride (LiCl), shifts the melting line and the ice homogeneous nucleation line of pure water to lower temperatures, further from accessible ambient temperatures, as seen in Fig. 40. Although this experiment shows that Ice IV exhibits the sharp change in slope suggestive of a transition across the liquid-liquid coexistence curve, further experiments would be necessary to say whether the critical point of water will shift to higher or lower temperatures with the addition of ionic solutes such as LiCl.

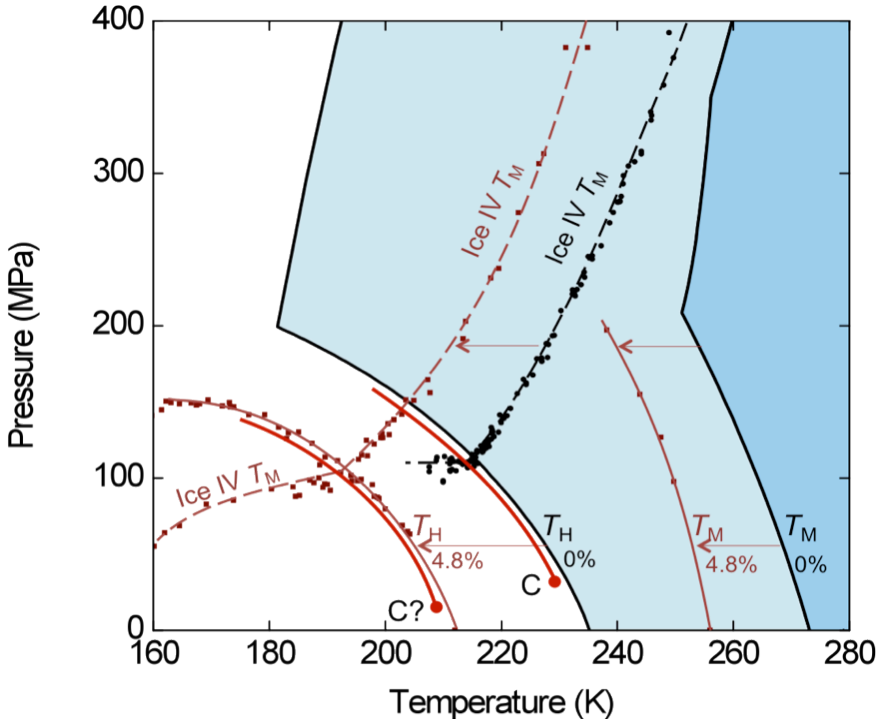

Figure 40. Decompression of pure H_2O ice IV (black dashed line) and of a 4.8% aqueous LiCl solution [151] showing the shift in the hypothesized liquid-liquid critical point for H_2O with the addition of LiCl.

Finally, I would like to address the recent experiments conducted by Murata and Tanaka with aqueous solutions of glycerol. Figure 41 is a three dimensional representation of the phase diagram for an aqueous solution of liquid water. Along the back face of the cube is the $P - T$ phase diagram for pure water. The solid blue line is the hypothesized liquid-liquid coexistence curve, terminating in a critical point for pure water denoted as $\mathrm{C}\left(\mathrm{H_2O}\right)$. Upon addition of a solute, the critical point would shift, and a critical locus would appear with increasing concentration. This critical locus can be visualized as the red line in Fig. 41, projecting forward with increasing

concentration of solute from the critical point of pure water. Murata and Tanaka conducted their experiments on supercooled glycerol-water solutions at atmospheric pressure with the understanding that if the addition of glycerol shifted the critical pressure of water down, then the surface of the liquid-liquid equilibrium curve would also curve down. As the critical point of solution crossed the plane of ambient pressure, shown in Fig. 41 in light green, a line of intersection would appear between the ambient pressure plane and the liquid-liquid coexistence curve at various concentrations of glycerol. In Fig. 42, the ice homogeneous nucleation surface is shown to help visualize how the liquid-liquid line could become experimentally accessible with the addition of solutes to pure cold water.

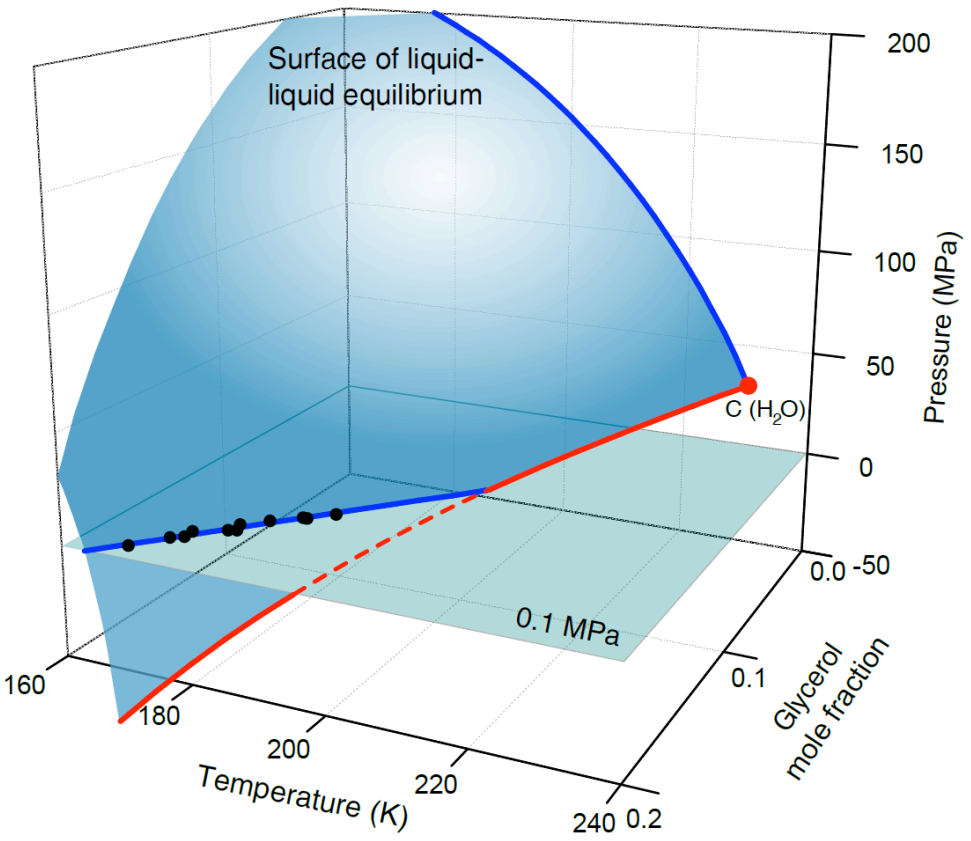

Figure 41. Three dimensional representation of the aqueous liquid-liquid equilibrium surface with increasing concentration of glycerol. Black dots indicated the experimental data of Murata and Tanaka for aqueous glycerol solutions [153].

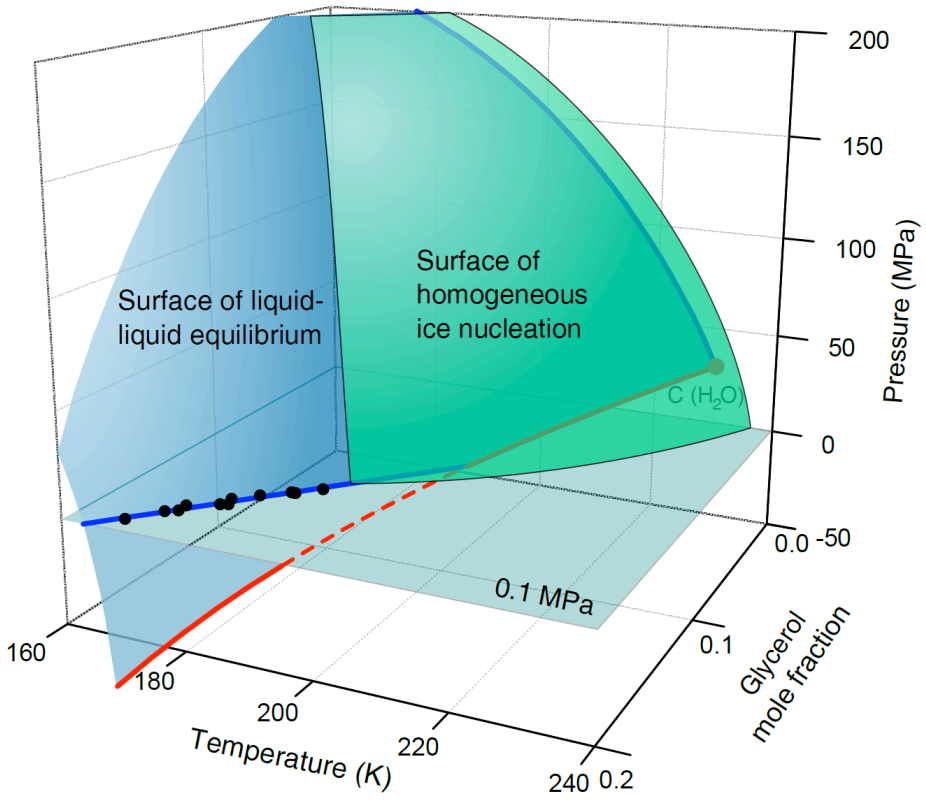

Figure 42. Three dimensional representation of the aqueous liquid-liquid equilibrium surface with increasing concentration of glycerol and the intersection with the homogeneous ice nucleation surface. Black dots indicated the experimental data of Murata and Tanaka for aqueous glycerol solutions [153].

It is important to note that, according to Tanaka [153] the solubility of glycerol in high-density and low-density liquid waters is the same. This makes the concentration of glycerol equal to the activity, ζ, introduced in Section 2.1 of this chapter. This fact significantly simplifies the application of the two-state model because we do not need a Legendre transformation to convert the activity dependent Gibbs energy, the thermodynamic potential, to the concentration dependent Gibbs energy.

The experimental measurements of Murata and Tanka [153] suggest that supercooled solutions may play an important role in the experimental investigation of the liquid water polyamorphism.

Chapter 4: Conclusions

Oil and gas exploration, seawater navigation and modeling, and the search for life on other planets are potential applications for a thermodynamic model of cold aqueous solutions.

Hydrocarbons and water are always found together in crude oil reservoirs. According to the U.S. Geological Survey, about 30% of the world's undiscovered gas and 13% of oil may be found north of the Arctic Circle. Oil exploration, treatment, and transport are affected by interactions between water and hydrocarbons. Water always contains a range of solutes, which strongly influence these interactions. In particular, oil spilt into near freezing waters takes many times longer to dissipate than oil spilt into warmer oceans.

Marine science, military technology, and the evaluation of habitable conditions on other planets all depend on understanding the properties of aqueous solutions of seawater and other cold aqueous solutions. A study of fluid systems well below the freezing temperature of pure water is indeed relevant to these issues.

This dissertation explores hot and cold water as supercritical solvents. The theory-based equation of state to describe the critical locus of aqueous sodium chloride solutions at high temperatures has been recommended for adoption as a *Revised Guideline on the Critical Locus of Aqueous Solutions of Sodium Chloride* by the International Association on the Properties of Water and Steam. My initial work on supercooled water, and the work with hot solutions of NaCl and water, served as

the stepping stone to the development of the model for aqueous solutions of supercooled water. This two-state water model, expanded to incorporate the addition of solutes, can be used to investigate the behavior of supercooled, supercritical aqueous solutions. In future work, the microscopic nature of the two-state model will be investigated.

Appendices

Appendix I. IAPWS Guideline

September 07, 2012 DRAFT

The International Association for the Properties of Water and Steam

Boulder, Colorado, USA
October 2012

Revised Guideline on the Critical Locus of Aqueous Solutions of Sodium Chloride

President:
Mr. Karol Daucik
Larok s.r.o.
SK 96263 Pliesovce, Slovakia

Executive Secretary:
Dr. R.B. Dooley
Structural Integrity Associates, Inc.
2616 Chelsea Drive
Charlotte, NC 28209, USA
Email: bdooley@structint.com

This release contains 6 pages, including this cover page

This guideline has been authorized by the International Association for the Properties of Water and Steam (IAPWS) at its meeting in Boulder, Colorado, USA, 30 September to 5 October, 2012, for issue by its Secretariat. The members of IAPWS are: Britain and Ireland, Canada, the Czech Republic, Germany, Greece, Japan, Russia, Scandinavia (Denmark, Finland, Norway, Sweden), and the United States of America. Associate members are Argentina and Brazil, Australia, France, Italy, New Zealand, and Switzerland.

This guideline replaces the "Guideline on the Critical Locus of Aqueous Solutions of Sodium Chloride", issued in 2000.

Further information concerning this guideline and other documents issued by IAPWS can be obtained from the Executive Secretary of IAPWS or from http://www.iapws.org

This guideline presents equations for the critical temperature, the critical pressure, and the critical density of aqueous solutions of sodium chloride as a function of mole fraction x of NaCl. The proposed equations yield an accurate description of the experimental data for the critical parameters from the pure-water limit to the highest salt concentration ($x = 0.12$) for which data are available.

The supporting document for this Guideline is: D.A. Fuentevilla, J.V. Sengers, and M.A. Anisimov, "Critical Locus of Aqueous Solutions of Sodium Chloride Revisited", Int. J. Thermophys. **33**, 943-958 (2012); *ibid.* in press.

DEFINITION OF SYMBOLS

B, C: coefficients in Eqs. (4) and (5)

$f_1(x)$, $f_2(x)$: functions in Eq. (1)

P_c: critical pressure (MPa)

P_c^0 : critical pressure of pure water (MPa)

p_1, p_2, p_3, p_4: coefficients in Eq. (8)

r_1, $r_{3/2}$, r_2, $r_{5/2}$, r_3, $r_{7/2}$, r_4: coefficients in Eq. (7)

T_c: critical temperature (K)

T_c^0 : critical temperature of pure water (K)

$T_1(x)$, $T_2(x)$: functions in Eq. (1)

t_1, $t_{3/2}$, t_2: coefficients in Eq. (2)

$t_1', t_{3/2}', t_2', t_{5/2}', t_3', t_{7/2}', t_4'$: coefficients in Eq. (3)

x: mole fraction of NaCl

$\Delta T = T_c - T_c^0$

ρ_c: critical density ($kg \cdot m^{-3}$)

ρ_c^0 : critical density of pure water ($kg \cdot m^{-3}$)

Critical parameters of pure water*:
$T_c^0 = 647.096\,\mathrm{K}, \quad \rho_c^0 = 322.0\,\mathrm{kg\cdot m^{-3}}, \quad P_c^0 = 22.064\,\mathrm{MPa}$.

Equation for the critical temperature:

$$T_c(x) = f_1(x)T_1(x) + f_2(x)T_2(x), \tag{1}$$

with

$$T_1(x) = T_c^0\left(1 + t_1 x + t_{3/2}x^{3/2} + t_2 x^2\right), \tag{2}$$

$$T_2(x) = T_c^0\left(1 + t_1' x + t_{3/2}' x^{3/2} + t_2' x^2 + t_{5/2}' x^{5/2} + t_3' x^3 + t_{7/2}' x^{7/2} + t_4' x^4\right), \tag{3}$$

$$f_1(x) = \frac{1}{4}\left[\,|Bx - C - 1| - |Bx - C + 1|\,\right] + \frac{1}{2}, \tag{4}$$

$$f_2(x) = \frac{1}{4}\left[\,|Bx - C + 1| - |Bx - C - 1|\,\right] + \frac{1}{2}, \tag{5}$$

with

$$B = 10\,000, \quad C = 10. \tag{6}$$

Equation for the critical density:

$$\rho_c(x) = \rho_c^0\left[1 + r_1 x + r_{3/2}x^{3/2} + r_2 x^2 + r_{5/2}x^{5/2} + r_3 x^3 + r_{7/2}x^{7/2} + r_4 x^4\right]. \tag{7}$$

Equation for the critical pressure:

$$P_c(x) = P_c^0\left[1 + p_1(\Delta T/\mathrm{K}) + p_2(\Delta T/\mathrm{K})^2 + p_3(\Delta T/\mathrm{K})^3 + p_4(\Delta T/\mathrm{K})^4\right]. \tag{8}$$

Equation (1) represents T_c with a standard deviation $\sigma = 0.019\%$ at $x \leqslant 0.0009$

and with a standard deviation $\sigma = 0.24\%$ at $0.0009 \leqslant x \leqslant 0.012$

Equation (7) represents ρ_c with a standard deviation $\sigma = 0.6\%$

Equation (8) represents P_c with a standard deviation $\sigma = 1.7\%$

---

*Release: *Values of Temperature, Pressure and Density of Ordinary and Heavy Water Substance at their Respective Critical Points* (IAPWS, September, 1992).

Table I. Coefficients in Eqs. (1) – (8) for the critical locus of aqueous solutions of NaCl up to a NaCl mole fraction of 0.12

Critical temperature, T_c (K)

$T_1(x)$	$T_2(x)$
$t_1 = 2.30 \times 10^1$	$t'_1 = 1.757 \times 10^1$
$t_{3/2} = -3.30 \times 10^2$	$t'_{3/2} = -3.026 \times 10^2$
$t_2 = -1.80 \times 10^3$	$t'_2 = 2.838 \times 10^3$
	$t'_{5/2} = -1.349 \times 10^4$
	$t'_3 = 3.278 \times 10^4$
	$t'_{7/2} = -3.674 \times 10^4$
	$t'_4 = 1.437 \times 10^4$

Critical pressure P_c (MPa)

$$p_1 = 9.1443 \times 10^{-3}$$
$$p_2 = 5.1636 \times 10^{-5}$$
$$p_3 = -2.5360 \times 10^{-7}$$
$$p_4 = 3.6494 \times 10^{-10}$$

Critical density ρ_c (kg·m^{-3})

$$r_1 = 1.7607 \times 10^2$$
$$r_{3/2} = -2.9693 \times 10^3$$
$$r_2 = 2.4886 \times 10^4$$
$$r_{5/2} = -1.1377 \times 10^5$$
$$r_3 = 2.8847 \times 10^5$$
$$r_{7/2} = -3.8195 \times 10^5$$
$$r_4 = 2.0633 \times 10^5$$

Table II. Critical temperature, density, and pressure calculated from Eqs. (1) – (8) at selected mole fractions of NaCl[†]

x	T_c (K)	P_c (MPa)	ρ_c (kg·m^{-3})
0	647.096000	22.0640000	322.000000
0.0005	651.858942	23.0502156	341.467388
0.001	653.957959	23.5003231	355.403431
0.0015	656.214478	23.9942848	366.631874
0.002	658.266685	24.4522876	376.071640
0.003	661.792675	25.2578916	391.370335
0.004	664.850727	25.9748152	403.503882
0.005	667.640852	26.6429248	413.572545
0.006	670.274404	27.2851928	422.220364
0.007	672.818265	27.9158160	429.857769
0.008	675.314254	28.5438775	436.760441
0.009	677.789002	29.1752574	443.120149
0.01	680.259476	29.8137278	449.073533
0.02	705.710570	36.7725468	499.162456
0.03	731.830060	44.3508666	542.631406
0.04	757.383936	51.8585660	579.897786
0.05	782.719671	59.1490976	609.816085
0.06	809.415999	66.4909864	632.701609
0.07	839.687528	74.2862762	649.832063
0.08	875.954487	82.9284097	662.792131
0.09	920.557281	93.0389707	673.036769
0.1	975.571016	106.692174	681.662669
0.11	1042.68691	130.966478	689.331958
0.12	1123.13874	186.176548	696.300163

[†] The number of decimals quoted does not correspond to the estimated uncertainties, but is given for program verification.

Appendix II. IAPWS Report

September 8, 2012
K. Miyagawa

Test of the proposed equations in the draft of "Revised Guideline on the Critical Locus of Aqueous Solutions of Sodium Chloride"

1. Introduction

Dr. Harvey asked me to check a draft of IAPWS guideline "Revised Guideline on the Critical Locus of Aqueous Solutions of Sodium Chloride" dated August 07, 2012. It is a revision of the previous IAPWS guideline. I reviewed the draft and performed some numerical tests.

I suggested some minor changes, and the proposer revised the draft. This report is based on the revised draft dated September 07, 2012.

2. Proposed Draft and Background Paper

The draft contains 6 pages. It includes information on the proposed equations, a list of coefficients, and a table for program verification.

Dr. Harvey gave me a copy of a paper "Critical Locus of Aqueous Solutions of Sodium Chloride Revisited" by Fuentevilla et al., which is the background paper for the proposed equations.

3. Test Results

3.1. Information given in the draft to implement the equation

I developed Fortran program codes for the proposed equation. It was confirmed that the draft contains sufficient information to implement the equation.

3.2General behavior of the equation

I tested the behavior of the proposed equation and confirmed that the equation behaves reasonable in the range of validity defined in page 2 of the proposed document.

3.3 Table II for computer-program verification

Table II was examined. It was confirmed that the values with 9 effective figures in the table were exactly reproduced.

Dr. Harvey examined the table using Excel working sheet. He confirmed that the values were successfully reproduced.

3.4 Comparison with the old equations

I compared the new equations with the old ones.

Figures 1 to 3 are plots of values calculated from the new and old equations.

Figures 4 to 6 are plots of difference between the new and old equations defined as:

$$\Delta T_c = T_{c\,old} - T_{c\,new} \quad (K)$$

$$\Delta \rho_c = (\rho_{c\,old} - \rho_{c\,new}) / \rho_{c\,new} \times 100 \quad (\%)$$

$$\Delta \rho_c = (\rho_{c\,old} - \rho_{c\,new}) / \rho_{c\,new} \times 100 \quad (\%).$$

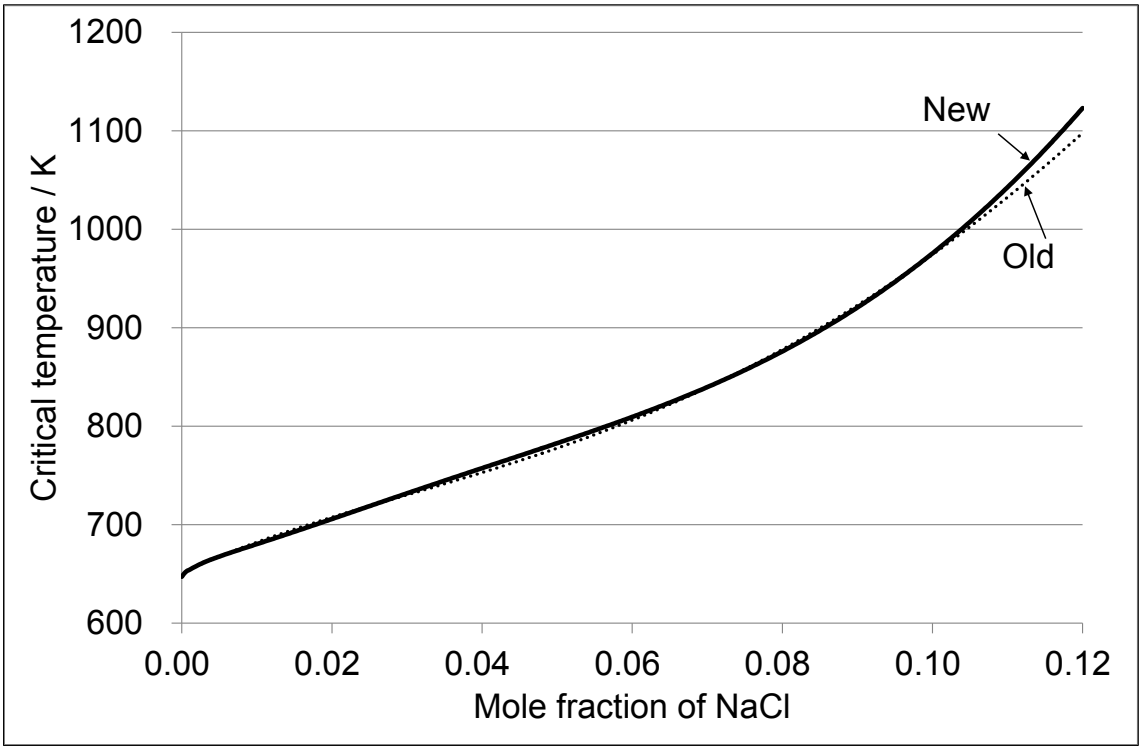

Figure 1 Critical temperature T_c

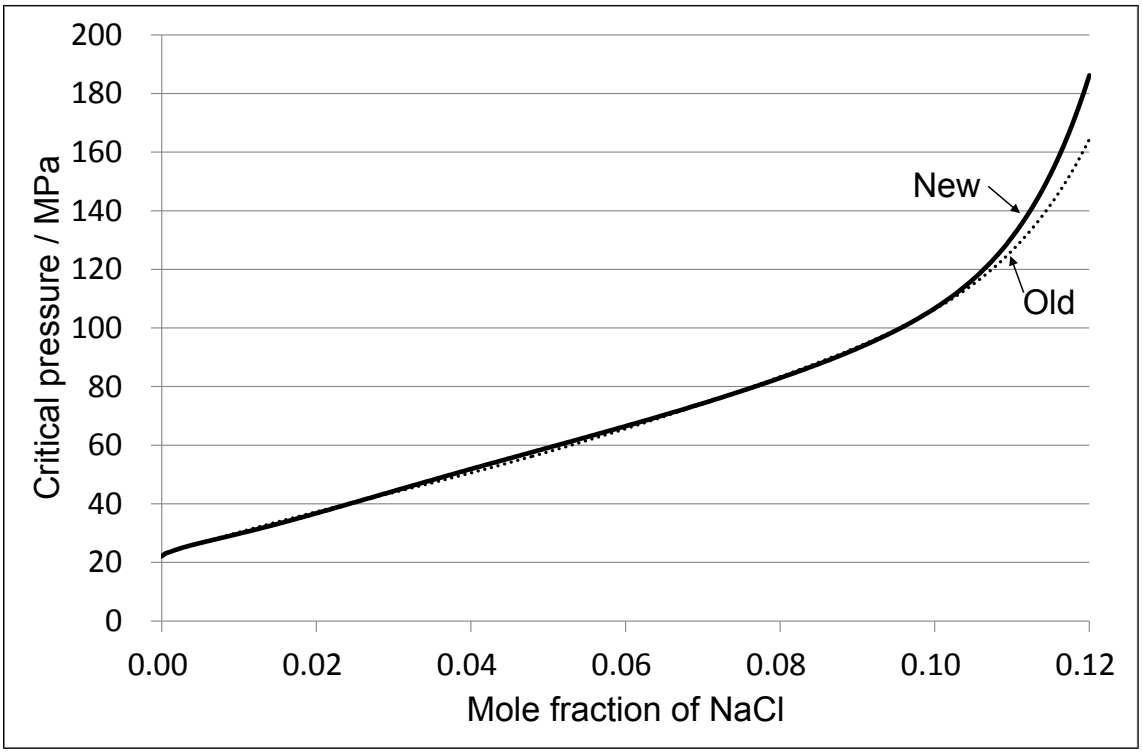

Figure 2 Critical pressure p_c

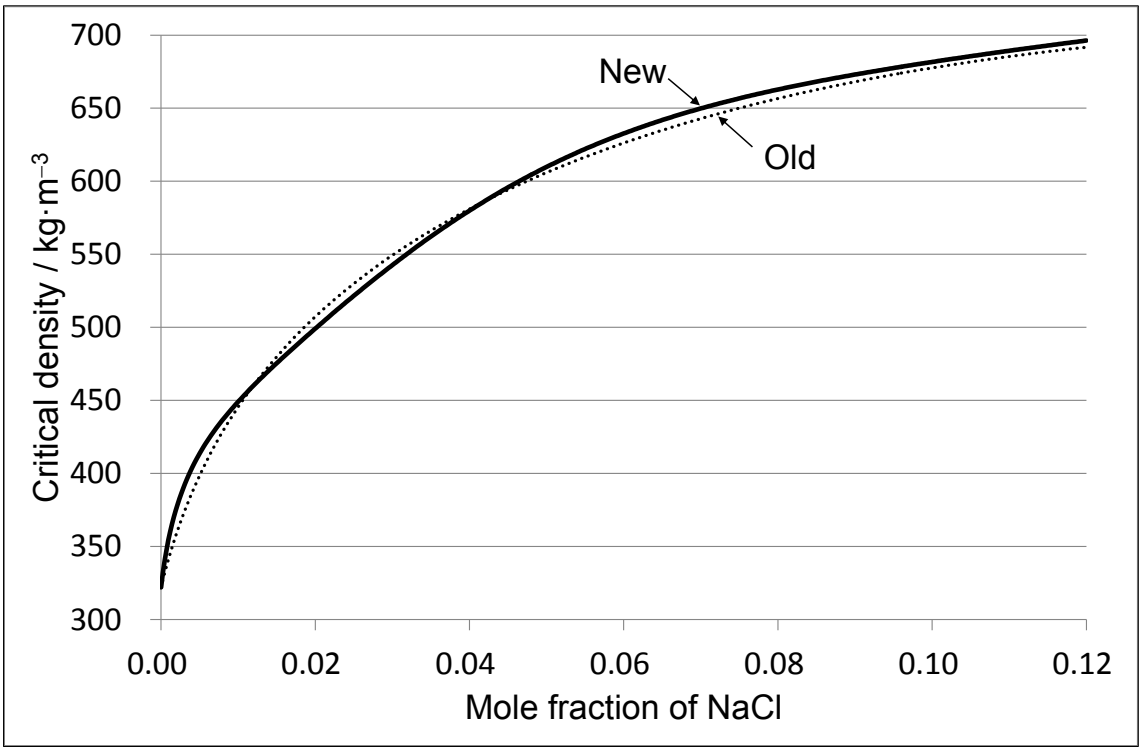

Figure 3 Critical density ρ_c

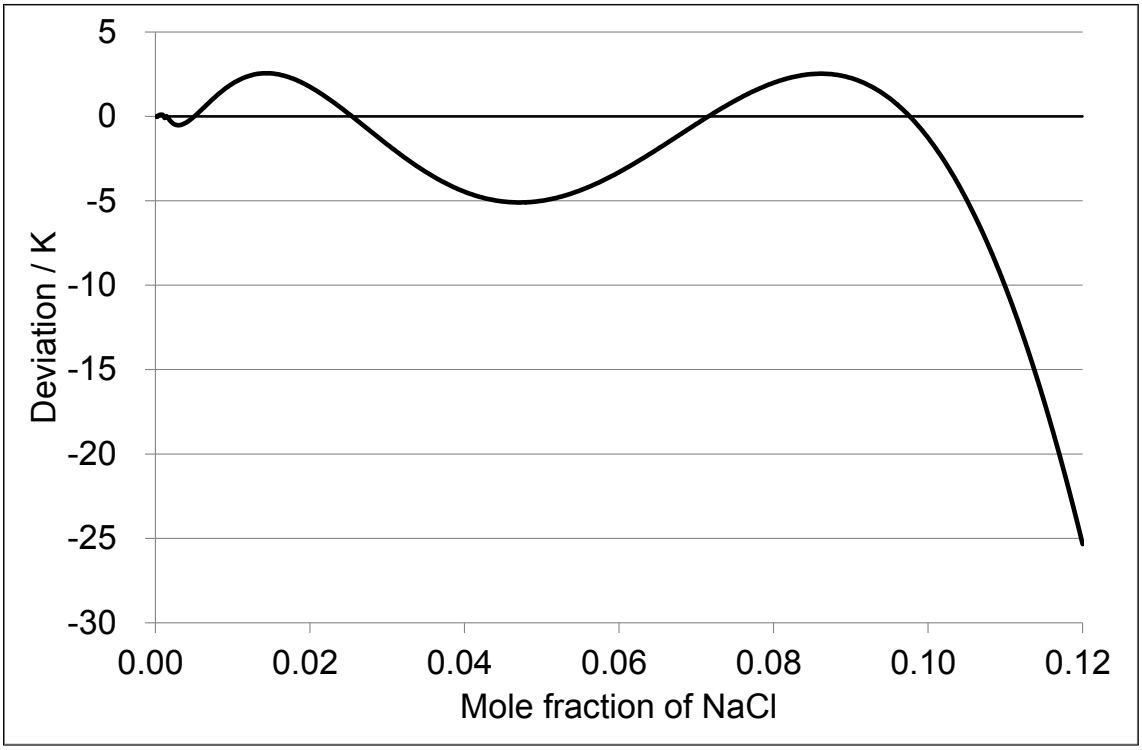

Figure 4 Difference in critical temperature ΔT_c

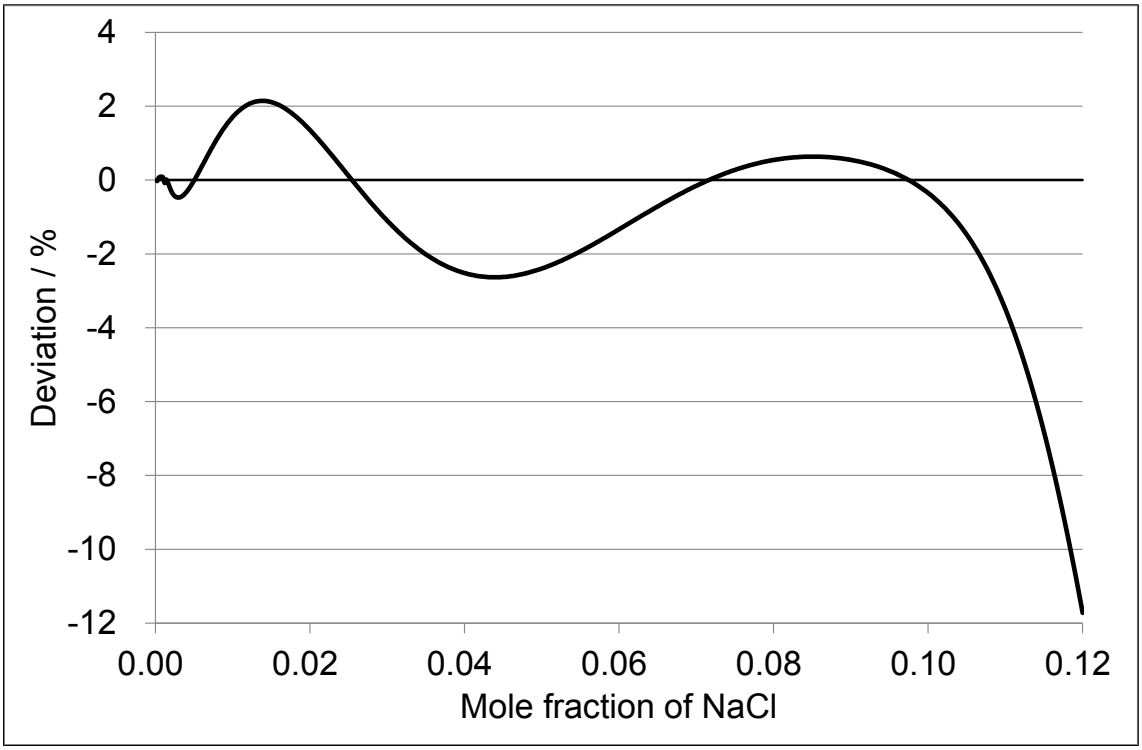

Figure 5 Difference in critical pressure Δp_c

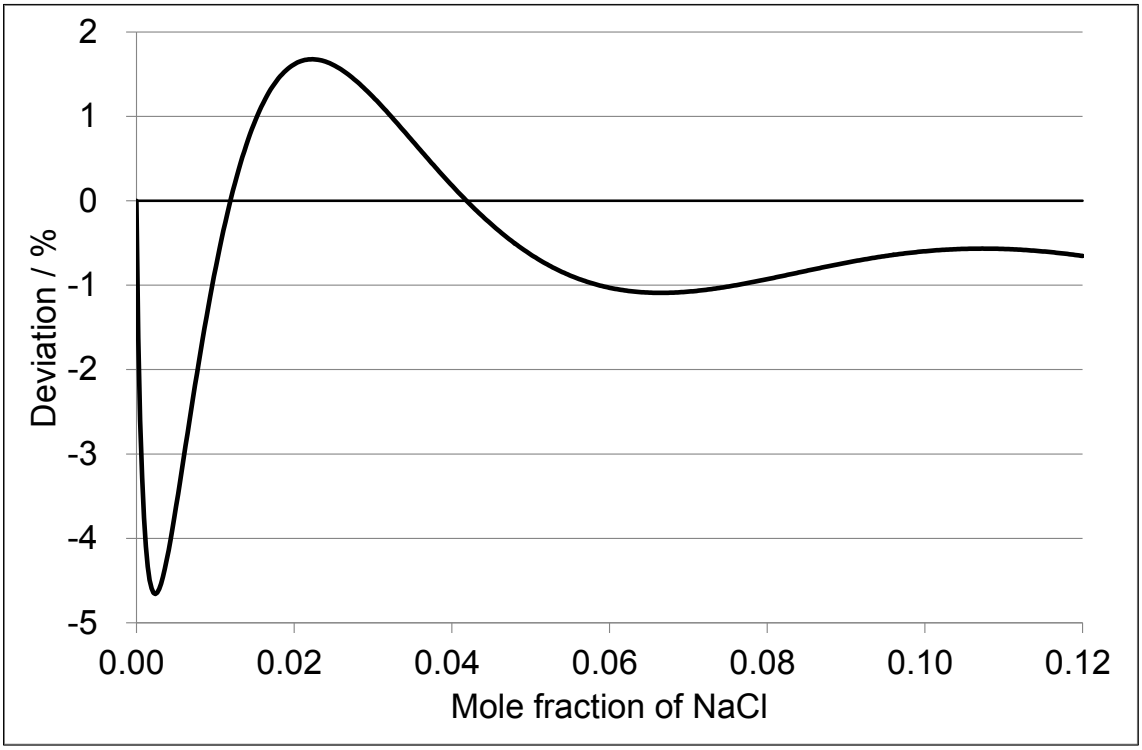

Figure 6 Difference in critical density $\Delta\rho_c$

3.8 Agreement with the experimental data

I didn't compare the results with the experimental data referred in the background paper. Instead, I plotted my results overlapping with Figs. 1 to 3 in the background paper. The plots are seen in Figures 7 to 9 below.

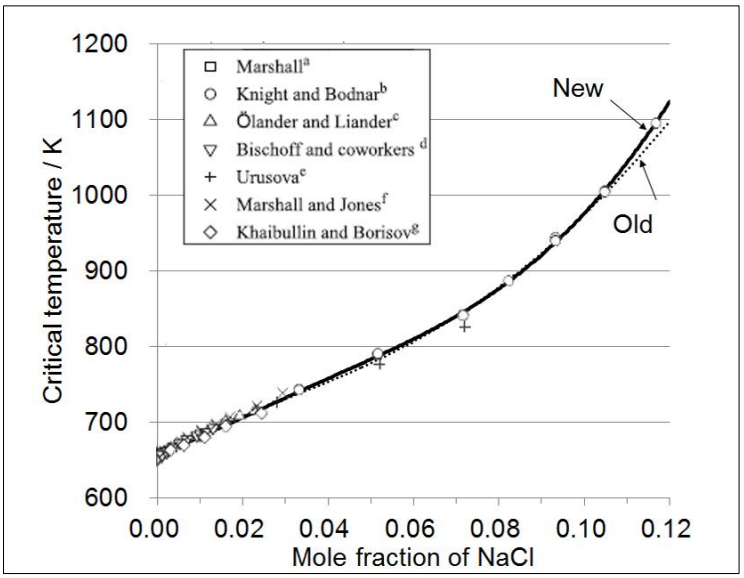

Figure 7 Experimental data and calculation results for T_c

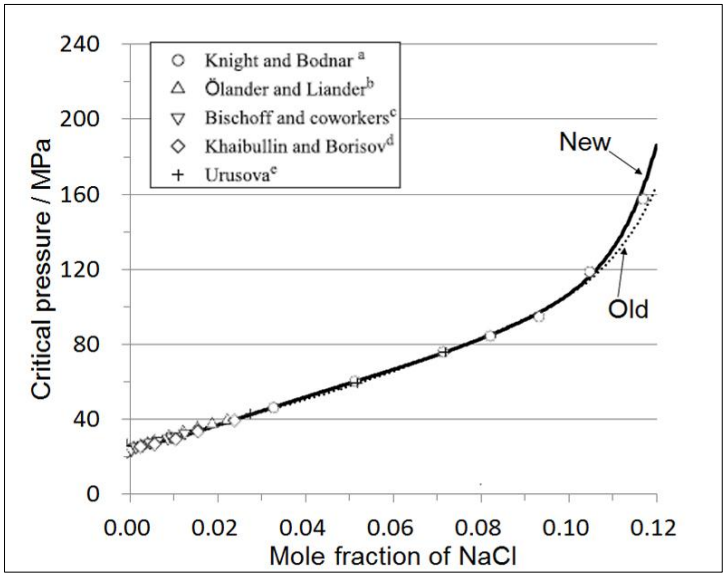

Figure 8 Experimental data and calculation results for ρ_c

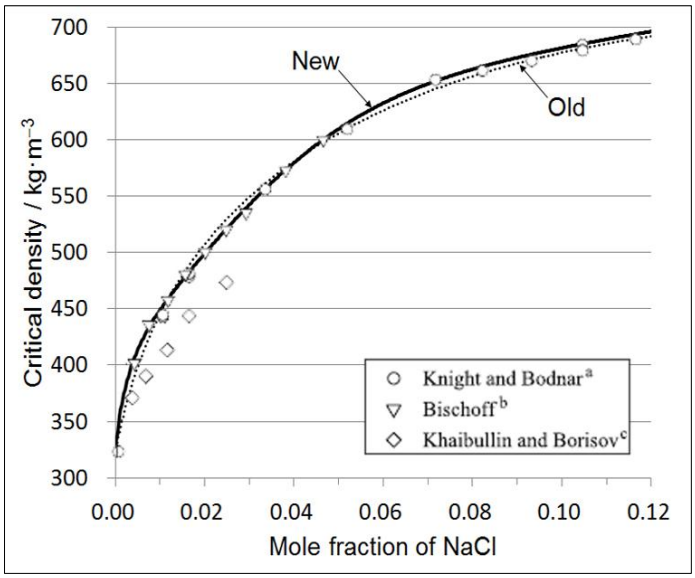

Figure 9 Experimental data and calculation results for ρ_c

4. Conclusions

It is my recommendation that the draft should be adopted as an IAPWS guideline.

Appendix III. List of Publications and Presentations

List of Publications

1. IAPWS *Revised Guideline on the Critical Locus of Aqueous Solutions of Sodium Chloride* http://www.iapws.org, *pending publication*
2. D.A. Fuentevilla, J.V. Sengers, and M.A. Anisimov, *Int. J. Thermophys*. **33**, 943 (2012); *ibid.* in press.
3. D.A. Fuentevilla and M. A. Anisimov, *Phys. Rev. Lett.* **97**, 195702 (2006); **98**, 149904 (2007)

Presentations and Conference Participation

1. D.A. Fuentevilla, V. Holten, M.A. Anisimov, "Supercooled Liquid Water as a Novel Supercritical Solvent: A Two-State Model," *AICHE Annual Meeting 2012*, Pittsburg, PA. Oct 2012
2. D.A. Fuentevilla, J.V. Sengers, M.A. Anisimov, "Revisiting the IAPWS Guideline on the Critical Locus of Aqueous Solutions of Sodium Chloride," *IAPWS Annual Meeting 2012*, Boulder, CO. Oct 2012
3. D.A. Fuentevilla, J.V. Sengers, M.A. Anisimov, "Vapor-Liquid Critical Locus of Aqueous Electrolyte Solutions at High Temperatures," *IAPWS Annual Meeting 2009*, Doorwerth, Netherlands. Sept 2009

4. D.A. Fuentevilla, M.A. Anisimov, "Thermodynamics of the Critical Behavior of Supercooled Water,"*15th International Conference on the Properties of Water and Steam*, Berlin, Germany. Sept 2008 (student award, outstanding presentation)
5. D.A. Fuentevilla, M.A. Anisimov, J.V. Sengers, "A Vapor-Liquid Critical Locus for Aqueous Solutions of Sodium Chloride," *AICHE Meeting*, Philadelphia, PA Mar 2008
6. D.A. Fuentevilla, M.A. Anisimov, "Thermodynamics of the Liquid-Liquid Critical Point in Supercooled Water," *XVI International Conference on Chemical Thermodynamics*, Suzdal, Russia, Jul 2007
7. D.A. Fuentevilla, M.A. Anisimov, "Thermodynamics of the Liquid-Liquid Critical Point in Supercooled Water" *11th International Conference on Properties and Phase Equilibria for Product and Process Design (PPEPPD)*, Crete, Greece May 2007. Poster presentation
8. IPST Statistical Physics Seminar at University of Maryland, College Park, MD Dec 2006
9. D.A. Fuentevilla, M.A. Anisimov, "Parametric Equation of State Near the Liquid-Liquid Critical Point in Supercooled Water," *AICHE Annual Meeting 2006*, San Francisco, Nov 2006
10. D.A. Fuentevilla, M.A. Anisimov, "Scaling Fields and Equation of State Near Liquid-Liquid Critical Point in Supercooled Water," APS Meeting, Baltimore, MD, Mar 2006

** Presenter indicated by underline*

Glossary

T_c	critical temperature
P_c	critical pressure
ρ_c	critical density
x	mole fraction of solute
K	Kelvin, unit of temperature
MPa	megapascal, unit of pressure
mg	milligram
m	meter
mm	millimeter
$^\circ$C	degree Celcius, unit of temperature
g	gram
kg	kilogram
cm	centimeter
mol	mole
J	Joule
s	second
IAPWS	International Association on the Properties of Water and Steam
h_1	independent theoretical scaling field, “ordering”
h_2	independent theoretical scaling field, “thermal”
h_3	critical part of field-dependent theoretical thermodynamic potential
N	# of independent physical fields; or # of experimental data points

ϕ	salt concentration, $\phi = 2x/(1-x)$; or fraction of state A for supercooled water solutions
$G(y)$	$G(y) \equiv \left(T_c(\phi) - T_c^0\right)/T_c^0 y^2$
y	$y = \sqrt{\phi} = \sqrt{2x/(1-x)}$; or mole fraction of liquid
ΔT	$\Delta T \equiv T - T_c$
ΔP	$\Delta P \equiv P - P_c$
μ	chemical potential
$\Delta\mu$	$\Delta\mu \equiv \mu_1 - \mu_{1,c}$
μ_{21}	$\mu_{21} \equiv \mu_{21} - \mu_{21,c}$
c	subscript, refers to property at critical point
0	superscript, refers to parameters of pure substance
s_i	fitting parameter for critical temperature of NaCl+H_2O solution [31]
t_i	fitting parameter for critical temperature of NaCl+H_2O solution
p_i	fitting parameter for critical pressure of NaCl+H_2O solution
r_i	fitting parameter for critical density of NaCl+H_2O solution
B, C	fitting parameters for T_c switching function of NaCl+H_2O solution
σ	standard deviation, $\sigma = \sqrt{\sum(z_i - z)/N}$
z	critical parameter (temperature, pressure, density)
LLCP	liquid-liquid critical point
UCEP	upper critical end point
LCEP	lower critical end point

K_{Kr}	Krichevskiĭ parameter
$k_{\mathbf{B}}$	Boltzman constant, $1.3806503\times10^{-23}\ \mathrm{m}^2\cdot\mathrm{kg}\cdot\mathrm{s}^{-2}\cdot\mathrm{K}^{-1}$
R	ideal gas constant, $8.3144621\ \mathrm{J}\cdot\ \mathrm{mol}^{-1}\cdot\mathrm{K}^{-1}$
C_P	heat capacity at constant pressure
κ_T	isothermal compressibility
α_P	thermal expansivity
$\Delta\hat{T}$	$\Delta\hat{T}=\dfrac{T-T_c}{T_c}$
$\Delta\hat{P}$	$\Delta\hat{P}=\dfrac{(P-P_c)V_c}{RT_c}$
$\Delta\hat{\mu}$	$\Delta\hat{\mu}=\dfrac{\mu-\mu_c}{RT_c}$
a'	variable representing slops of phase coexistence at the critical point
b'	variable , mixing coefficient, to account for non-symmetry in the order parameter
S	entropy
S^{E}	excess entropy
V	volume
G	Gibbs energy of solution
χ	susceptibility; parameter for iterative curve fitting
$r,\ \theta$	polar coordinates
a, k	system dependent amplitudes
T_{H}	homogeneous ice nucleation temperature

λ	heat of reaction, enthalpy change between two states
ω	interaction parameter
K	equilibrium constant

Bibliography

1. D.A. Fuentevilla, J.V. Sengers, and M.A. Anisimov, *Int. J. Thermophys*. **33**, 943 (2012); *ibid.* in press.
2. D.A. Fuentevilla and M. A. Anisimov, *Phys. Rev. Lett.* **97**, 195702 (2006); **98**, 149904 (2007)
3. C.E. Bertrand and M. A. Anisimov, *J. Phys. Chem. B* **115**, 14099 (2011)
4. V. Holten, C.E. Bertrand, M.A. Anisimov, J.V. Sengers. arXiv:1111.5587v2 [physics.chem-ph] 7 Dec 2011
5. J.M.H.L. Sengers, *Supercritical fluids: Their properties and applications. Supercritical fluids: Fundamentals and applications,* Series E, Applied Sciences, Vol. 336, Eds. Kiran, E.; Debenedetti, P.G.; Peters, C. J. 1998
6. L.T. Taylor. *Supercritical Fluid Extraction.* John Wiley & Sons, Inc.; New York, 1996
7. G. Brunner. *Gas Extraction: An Introduction to Fundamentals of Supercritical fluids and the Application to Separation Processes.* Topics in Physical Chemistry, Vol. 4, Eds. Baumgärtel, H.; Franck, E. U.; Grünbein, W. Steinkopff, Darmstadt/Springer, New York, (1994)
8. G. Brunner. *Annu. Rev. Chem. Biomol. Eng*. **1**, 321-342 (2010)
9. M. Blunt. F.J. Fayers. F.M. Orr Jr. *Energy Convers. Manag.* **34**, 1197-1204 (1993)
10. S. Peper, M. Johannsen, G. Brunner, *J. Chromatogr. A*, **1176**, 246-53 (2007)
11. L.T. Taylor. *J. Supercrit. Fluids*, **47**, 566-73 (2009)

12. E. Reverchon, G.D. Porta, *Pure Appl. Chem.* **73**, 1293-1297 (2001)

13. S-D. Yeo, E. Kiran, *J. Supercrit. Fluids*, **34**, 287-308 (2005)

14. ACS Symposium Series 860, *Supercritical Carbon Dioxide: Separations and Processes*, A.S. Gopalan, C.M. Wai, H.K. Jacobs (Oxford University Press, 2003)

15. T.M. Jonin, L.P. Adjadj, S.S. Rizvi, *Food engineering: Encyclopedia of life support systems.* Vol. III, 529, 2005.

16. W. Wagner and A. Pruß, *J. Phys. Chem. Ref. Data* **31**, 387 (2002)

17. H. Weingartner, E.U. Franck. *Angew. Chem. Int. Ed.*, **44**, 2672-2692 (2005)

18. A. Shanableh, N. Crain, *Water (Artarmon, Australia)*, **1**, 26-31 (2000)

19. R.W. Shaw, T.B. Brill, A.A. Clifford, C.A. Eckert, E.U. Franck, *Chemical & Engineering News*, 69, (51), 26-39 (1991)

20. Nuclear's Next Generation. *The Economist*. **393**, 15-18 (2009)

21. I. Svishchev. *J. of Supercritical Fluids*. **60**, 121-126 (2011)

22. M. Antal, S. Allen, D. Schulman, S. Xu. *Ind. Eng. Chem. Res.* **39**, 4040-4053 (2000)

23. Y. Matsumura, T. Minowa, B. Potic, S. Kersten, W. Prins, W. van Swaaij, B. van de Beld, D. Elliott, G. Neuenschwander, A. Kruse, M. Antal. *Biomass and Bioenergy* **29**, 269-292 (2005)

24. A. Koschinsky, *Geology*, **36**, 615 (2008)

25. D. Rosenfeld, W.L. Woodley, *Nature*, **405**, 440 (2000)

26. A. Devasthale, M.A. Thomas, *J. Climate*, **25**, 7297 (2012)

27. P.H. Van Konynenburg and R.L. Scott. *Philos. Trans. Roy. Soc. London A*, **298**, 495- 540 (1980)

28. J. S. Rowlinson and F. L. Swinton, *Liquids and Liquid Mixtures*, 3rd ed. (Butterworth, London, 1982)

29. C. Reed, *Nature* **439**, 905-907 (2006)

30. M.C. Hicks, U.G. Hegde, and J.W. Fisher. *Proc. of ISSF 2012: 10th Symp. Supercrit. Fluids.* (2012)

31. W.L. Marshall, *J. Chem. Soc. Faraday Trans*. **86**, 1807 (1990)

32. C.L. Knight and R.J. Bodnar, *Geochim. Cosmochim. Acta* **53**,3 (1989)

33. J.L. Bischoff and R.J. Rosenbauer, *Geochim. Cosmochim. Acta* **52**, 2121 (1988)

34. A.A. Povodyrev, M.A. Anisimov, J.V. Sengers, Marshall, Levelt Sengers, *Intl J. Thermophysics*, **20**, 1529 (1999)

35. Y.C. Kim and M.E. Fisher, *J. Phys. Chem. B*, **105**, 11791 (2001)

36. IAPWS homepage. < http://www.iapws.org/> visited 4 Nov 2012

37. IAPWS. *Guideline on the Critical Locus of Aqueous Solutions of Sodium Chloride*, 2000. <http://www.iapws.org/> visited 4 Nov 2012

38. J.V. Sengers, J.G. Shanks, *J. Stat. Phys*. **137**, 857 (2009)

39. W. Schröer, *Contrib. Plasma Phys*. **52**, 78 (2012)

40. M. Ley-Koo, M.S. Green, *Phys. Rev. A* **23**, 2650 (1981)

41. M.A. Anisimov, E.E. Gorodetskii, V.D. Kulikov, J.V. Sengers, *Phys. Rev. E* **51**, 1199 (1995)

42. M.E. Fisher, G. Orkoulas, *Phys. Rev. Lett.* **85**, 696 (2000)

43. G. Orkoulas, M.E. Fisher, C. Üstün, *J. Chem. Phys.* **113**, 7530 (2000)

44. Y.C. Kim, M.E. Fisher, G. Orkoulas, *Phys. Rev. E* **67**, 061506 (2003)

45. J.T. Wang, M.A. Anisimov, *Phys. Rev. E* **75**, 051107 (2006)

46. C.A. Cerdeiriña, M.A. Anisimov, J.V. Sengers, *Chem. Phys. Lett*. **424**, 414 (2006)

47. J.T. Wang, C.A. Cerdeiriña, M.A. Anisimov, J.V. Sengers, *Phys. Rev. E* **77**, 0311127 (2008)

48. G. Pérez-Sánchez, P. Losada-Pérez, C.A. Cerdeiriña, J.V. Sengers, M.A. Anisimov, *J. Chem. Phys.* **132**, 154502 (2010)

49. P. Losada- Pérez, C.S.P. Tripathy, J. Leys, C.A. Cerdeiriña, G. Glorieux, J. Thoen,

Chem. Phys. Lett. **523**, 69 (2012)

50. A. Ölander, H. Liander, *Acta Chem. Scand*. **4**, 1437 (1950)

51. J.L. Bischoff, R.J. Rosenbauer, K.S. Pitzer, *Geochim. Cosmochim. Acta* **50**, 1437 (1986)

52. R.J. Rosenbauer, J.L. Bischoff, *Geochim. Cosmochim. Acta* 51, 2349 (1987)

53. M.A. Urusova, *Russ. J. Inorg. Chem*. **19**, 450 (1974)

54. W.L. Marshall, E.V. Jones, *J. Inorg. Nuclear Chem.* **36**, 2319 (1974)

55. I.Kh. Khaibullin, N.M. Borisov, *High Temp*. **4**, 489 (1966)

56. J.L. Bischoff, *Am. J. Sci.* **291**, 309 (1991)

57. E. Schroer, *Z. Physik. Chem.* **129**, 79 (1927)

58. S. Sourirajan, G.C. Kennedy, *Am. J. Sci*. **260**, 115 (1962)

59. M.M. Bochkov, Ph.D. thesis (Makhachkala, USSR Academy of Sciences, 1989)

60. D.A. Palmer, R. Fernández-Prini, A.H. Harvey (eds.), *Aqueous Systems at Elevated Temperatures and Pressures* (Elsevier, Amsterdam, 2004)

61. J.M.H. Levelt Sengers, J. Straub, K. Watanabe, P.G. Hill, *J. Phys. Chem. Ref. Data* **14**, 193 (1985)

62. IAPWS, *Release on the Values of Temperature, Pressure, and Density of Ordinary and Heavy Water Substance at their Respective Critical Points* (1994) <www.iapws.org>

63. H. Preston-Thomas, *Metrologia* **27**, 3-10 (1990)

64. R.L. Rusby, *J. Chem. Thermodynamics* **23**, 1153 (1991)

65. R.L. Rusby, R.P. Hudson, M. Durieux, *Metrologia* **31**, 149 (1994)

66. J.L. Bischoff, K.S. Pitzer, *Am. J. Sci*. **289**, 217 (1989)

67. S.B. Kiselev, I.G. Kostyukova, A.A. Povodyrev, *Int. J. Thermophys.* **12**, 877 (1991)

68. A.H. Harvey, *J. Chem. Phys*. **95**, 479 (1991)

69. R. Thiéry, S.N. Lvov, J. Dubessy, *J. Chem. Phys.* **109**, 214 (1998)

70. K.S. Pitzer, *Int. J. Thermophys*. **19**, 355 (1998)

71. R.L. Scott, P.H. van Konynenburg, *Discus. Faraday Soc*. **49**, 98 (1970)

72. F.H. Barr-David, *J. AIChE* **2**, 426, 1956; reproduced with permission in *Introduction to Chemical Engineering Thermodynamics* 7th Ed., J.M. Smith, H.C. Van Ness, M.M. Abbott (ed.) 2005

73. R.J.J. Chen, P.S. Chappelear, R. Kobayashi, *J. Chem Eng. Data*. **21**, 213 (1976)

74. M. E. Fisher, in *Critical Phenomena*, edited by F. J. W. Hahne, Lecture notes in Physics Vol. 186 (Springer, Berlin, 1982) p. 1.

75. H. Behnejad, J.V. Sengers, M.A. Anisimov, in *Applied Thermodynamics*, A.H.Goodwin, J.V. Sengers, C.J. Peters (eds.), (RSC Publishing, Cambridge, 2010), p. 321

76. OriginLab Corp. *Origin 8 User Guide*, (Northampton, MA 2007)

77. D.A. Fuentevilla, V. Holten, M.A. Anisimov. *Proc. 2012 IAPWS Annual Meeting*, Boulder, CO. Sept. 2012.

78. J.M.H. Levelt Sengers, *J. Supercrtical Fluids* **4**, 215 (1991)

79. I.R. Krichevskiĭ, *Russ. J. Phys. Chem*. **41**, 1332 (1967)

80. M.A. Anisimov, *Russ. J. Phys. Chem*. **45**, 877 (1971)

81. M.A. Anisimov, *Russ. J. Phys. Chem*. **45**, 439 (1971)

82. J.M.H. Levelt Sengers, in *Supercritical Fluid Technology*, T.J. Bruno, J.F. Ely (eds.) (CRC Press, Boca Raton, 1991), p. 1

83. J.M.H. Levelt Sengers, in *Supercritical Fluids: Fundamentals for Application*, E. Kiran, J.M.H. Levelt Sengers (eds.) (Kluwer, Dordrecht, 1994), p. 3

84. J.M.H.L. Sengers, *Supercritical fluids: Their properties and applications. Supercritical fluids: Fundamentals and applications,* Series E, Applied Sciences, Vol. 336, Eds. E, Kiran; P.G. Debenedetti; C.J. Peters (1998)

85. M.A. Anisimov, J.V. Sengers, J.M.H. Levelt Sengers, in Ref.[56], p. 29

86. A.I. Abdulagatov, I.M. Abdulagatov, G.V. Stepanov, *J. Struct. Chem.*, **42**, 412-422 (2001)

87. Kh.S. Abdulkadirova, Kostrowicka A. Wyczalkowska, M.A. Anisimov, J.V. Sengers, *J. Chem. Phys.*, **116**, 4202-4211 (2002)

88. R. Fernandez-Prini, J.L. Alvarez, A.H. Harvey, A.H. as Chapter 4 in *The Physical Properties of Aqueous Systems at Elevated Temperatures and pressures: Water,Steam and Hydrothermal Solutions*, D. A. Palmer, R. Fernandez-Prini, and A. H. Harvey, eds., pp. 29- 72, Academic Press, (2004)

89. A.V. Plyasunov, E.L. Shock, *J. Supercrit. Fluids*, **20**, 91-103 (2001)

90. A.V. Plyasunov, *J. Phys. Chem. Ref. Data*, **41**, 033104-1, (2012)

91. A.H. Harvey, A.P. Peskin, S.A. Klein, NIST/ASME Steam Properties, NIST Standard Reference Database 10, Version 2.22 (National Institute for Standards and Technology, Gaithersburg, MD, 2008)

92. P.G. Debenedetti, *Metastable Liquids. Concepts and Principles* (Princeton University Press, 1996)

93. P.F. Debenedetti, *J. Phys.: Condens. Matter* **15**, R1669 (2003)

94. I.M. Hodge, C.A. Angell, *J. Chem. Phys.* **68** 1363 (1978)

95. C. A. Angell, M. Oguni, and W. J. Sichina, *J. Phys. Chem*. **86**, 998 (1982)

96. P. T. Hacker, Technical Note 2510 (National Advisory Committee for Aeronautics, 1951), <http://naca.larc.nasa.gov/reports/1951/naca-tn-2510/naca-tn-2510.pdf>

97. M. A. Floriano and C. A. Angell, J. Phys. Chem. 94, 4199 (1990)

98. P.H. Poole, F. Sciortino, U. Essmann, and H.E. Stanley, *Nature* **360**, 324 (1992)

99. V. Holten, M.A. Anisimov, *Scientific Reports*, **2**:713 (2012)

100. P.H. Poole, T. Grande, C.A. Angell, P.F. McMillam, Science 275, 322 (1997)

101. H. Tanaka *Phys. Rev. E* **62**, 6968-6976 (2000)

102. Y. Katayama, T. Mizutani, W. Utsumi, O. Shimomura, M. Yamakata, *Nature* **403**, 170-173 (2000)

103. S. Sastry, C.A. Angell, *Nature Mater.* **2**, 739-743 (2003)

104. V.V. Vasisht, S. Saw, S. Sastry, *Nature Phys.* **7**, 549-553 (2011)

105. S. Aasland, P.F. McMillam, *Nature* **369**, 633-639 (1994)

106. G.N. Greaves et al. *Science* **322**, 566-570 (2008)

107. C.J. Wu, J.N. Glosli, G. Galli, F.H. Ree, *Phys Rev Lett* **89**, 135701 (2002)

108. P. Ganesh, M. Widom, *Phys. Rev. Lett.* 102, 075701 (2009)

109. Y. Katayama, T. Mizutani, W. Utsumi, O. Shimomura, M. Yamakata, K. Funakoshi, *Nature* **403**, 170 (2000)

110. L.M. Ghiringhelli, E.J. Meljer, *J. Chem. Phys.* **122**, 184510 (2005)

111. O. Mishima, H.E. Stanley, *Nature* **396**, 329–335 (1998)

112. Y. Tu, S.V. Buldyrev, Z. Liu, H. Fang, H.E. Stanley, *EPL* **97**, 56005 (2012)

113. M. A. Anisimov, J. V. Sengers, and J. M. H. Sengers, in *Near-Critical Behavior of Aqueous Systems*, edited by D.A. Palmer, R. Fernandez-Prini, and A.H. Harvey, The Physical Properties of Aqueous Systems at Elevated Temperatures and Pressures: Water, Steam and Hydrothermal Solutions (Academic Press, New York, 2004)

114. J. V. Sengers and J. M. H. Levelt Sengers, in *Progress in Liquid Physics*, edited by C. A. Croxton (Wiley, New York, 1978) Chap. 4, pp. 103–174.

115. M. A. Anisimov, V. A. Agayan, and P. J. Collings, *Phys. Rev. E* **57**, 582 81 (1998)

116. E. Brézin, D. J. Wallace, and K. G. Wilson, *Phys. Rev. Lett.* **29**, 591 83 (1972)

117. P. Schofield, J. D. Litster, and J. T. Ho, *Phys. Rev. Lett.* **23**, 1098 (1969)

118. H. Kanno and C. A. Angell, *J. Chem. Phys.* **70**, 4008 (1979)

119. D. E. Hare and C. M. Sorensen, *J. Chem. Phys*. **84**, 5085 (1986)

120. C. A. Angell, J. Shuppert, and J. C. Tucker, J. *Phys. Chem*. **77**, 3092 (1973)

121. D. H. Rasmussen, A. P. MacKenzie, C. A. Angell, and J. C. Tucker, *Science* **181**, 342 (1973)

122. D. G. Archer and R. W. Carter, *J. Phys. Chem. B* **104**, 8563 (2000)

123. D. E. Hare and C. M. Sorensen, *J. Chem. Phys*. **87**, 4840 (1987)

124. L. Ter Minassian, P. Pruzan, and A. Soulard, *J. Chem. Phys*. **75**, 3064 (1981)

125. O. Mishima, *J. Chem. Phys*. **133**, 144503 (2010)

126. R. J. Speedy and C. A. Angell, *J. Chem. Phys.* **65**, 851 (1976)

127. T. Sotani, J. Arabas, H. Kubota, and M. Kijima, *High Temp. High Pressures* **32**, 433 (2000)

128. A. Taschin, R. Cucini, P. Bartolini, and R. Torre, *Phil. Mag*. **91**, 1796 48 (2011)

129. E. Trinh and R. E. Apfel, *J. Chem. Phys.* **72**, 6731 (1980)

130. J.-C. Bacri and R. Rajaonarison, *J. Physique Lett.* **40**, L403 (1979)

131. E. Trinh and R. E. Apfel, *J. Acoust. Soc. Am.* **63**, 777 (1978)

132. E. Trinh and R. E. Apfel, *J. Chem. Phys.* **69**, 4245 (1978)

133. P. J. Mohr, B. N. Taylor, and D. B. Newell, "The 2010 CO-DATA recommended values of the fundamental physical constants," http://physics.nist.gov/constants (2011)

134. Guideline on the Use of Fundamental Physical Constants and Basic Constants of Water, IAPWS (2008), <http://www.iapws.org/relguide/fundam.pdf>

135. W.C. Röntgen, *Ann. Phys. (Leipzig)* **281**, 91 (1892)

136. E.G. Ponyatovskiĭ, V.V. Sinand, T.A. Pozdnyakova. *JETP Lett.* **60**, 360 (1994)

137. C.T. Moynihan, *Res. Soc. Symp. Proc.*, **455**, 411 (1997)

138. I. Prigogine, R. Defay, Chemical Thermodynamics (Longmans, Green & Co., London, 1954)

139. H. Kanno, K. Miyata, *Chem. Phys. Lett.* **422**, 507–512 (2006)

140. V. Holten, J. Kalova´, M.A. Anisimov, J.V. Sengers, *Int. J. Thermophys.* **33**, 758 (2012)

141. Loerting, T. et al. How many amorphous ices are there? Phys. Chem. Chem. Phys. 13, 8783 (2011)

142. E.B. Moore, V. Molinero, *J. Chem. Phys.* **130**, 244505 (2009)

143. D. Corradini, D.; Rovere, M.; Gallo, P. 2011, arXiv: 1101.5311v1 [cond-mat.soft]

144. D. Corradini, P. Gallo, M. Rovere. *J. Phys.: Condens. Matt.* **22**, 284104/1-284104/7 (2010)

145. J. Holzmann, R. Ludwig, A. Geiger, D. Paschek. *Angew. Chem. Int. Ed.* **46**, 8907-8911 (2007)

146. D. Corradini, P. Gallo, *J. of Phys. Chem. B* **115**, 14161-14166 (2011)

147. O. Mishima, *J. Chem. Phys.* **23**, 154506/1 -154506 /4 (2005)

148. K. Miyata, H. Kanno, *J. Mol. Liq*. **119**, 189-193. (2005)

149. S. Chaterjee, P.G. Debenedetti. *J. Chem. Phys.* **124**, 154503/1-154503/10 (2006)

150. O. Mishima, *Phys. Rev. Lett.* **85**, 334 (2000)

151. O. Mishima, *Nature*, **384**, 546 (1996)

152. O. Mishima, *J. Phys. Chem. B* **115**, 14064 (2011)

153. K. Murata, H. Tanaka, *Nature Mat.* **11**, 436 (2012)